Pontificia Universidad
Católica del Perú

Escuela de Posgrado

State estimation for coupled PDE systems using Modulation Functions

Tesis para obtener el grado académico de Magíster en Ingeniería de Control y Automatización que presenta:

David Raúl Pumaricra Rojas

Profesor Responsable (PUCP):   *Dr. Ing. Carlos Gustavo Pérez Zúñiga*

Profesor Responsable (TU Ilmenau):   *Univ.-Prof. Dr.-Ing. Johann Reger*

Supervisor (TU Ilmenau):   *M.Sc. Matti Noack*

Lima, 2022

Abstract

This master thesis is devoted to the state estimation of a particular form of PDE systems, coupled parabolic PDEs with spatial dependent coefficients. This form of PDEs represent some dynamic systems such as Tubular Reactors, Diffusion in lithium-ion cells and Diffusive Gradient in Thin Films sensor. Other methods for this problem use "Backstepping" observers, in which the estimation error system is transformed into another system that is stable, reducing the problem to calculate the Kernel functions making the transformation possible. In some cases this calculation is not simple, also the simulation in real time of the observer system, that is also a PDE, can be difficult. The method presented in this thesis uses the properties of the so-called Modulating Functions in order to estimate the states. The procedure consists of generating an orthonormal basis of functions that can represent the state as a combination of them. Then auxiliary systems are formed from the original systems with boundary conditions that help in the simplification of the problem. Resolving these auxiliary systems, result in the calculation of the Modulating kernels. All of these steps can be made offline and do not have to be repeated. The functions are used together with the orthonormal basis in the online part, that consists of an integration of a combination of the kernel functions, inputs and outputs of the system in a time window. Finally, with a matrix multiplication the coefficients for the basis expansion of the state can be obtained, resulting in the desired state estimation. The present method is tested in systems that resemble the forms of the dynamics of Tubular Reactors and the performance is compared to other methods.

Kurzfassung

Diese Masterarbeit widmet sich der Zustandsschätzung einer bestimmten Art von Systemen, gekoppelten partiellen Differenzialgleichungen mit raumabhängigen Koeffizienten. Diese besondere Form von PDEs repräsentiert einige dynamische Systeme wie Röhrenreaktoren, Diffusion in Lithium-Ionen-Batterien und Gradienten in dünnen Schichten. Andere Methoden für dieses Problem benutzen "Backstepping" Beobachter, bei denen das Schätzfehlersystem in ein anderes stabiles System transformiert wird, wodurch das Problem reduziert wird, um die Kernfunktionen zu berechnen, die die Transformation ermöglichen. In manchen Fällen ist diese Berechnung nicht einfach. Auch die Simulation in Echtzeit des Beobachters System, das auch eine PDE ist, kann sehr schwierig sein. Die in dieser Arbeit vorgestellte Methode verwendet die Eigenschaften der sogenannten Modulationsfunktionen, um die Zustände zu schätzen. Das Verfahren besteht darin, eine Orthonormalbasis von Funktionen zu erzeugen können, die den Zustand als Kombination von ihnen repräsentieren, dann werden Hilfssysteme gebildet von dem ursprünglichen Systemen mit Randbedingungen, die bei der Vereinfachung helfen, von dem Problem. Das Auflösen dieser Hilfssysteme ergibt die Berechnung der modulierende Kerne. Alle diese Schritte können offline durchgeführt und müssen nicht wiederholt werden. Die Funktionen werden zusammen mit der Orthonormalbasis im Online-Teil verwendet. Dieser Teil besteht aus einer Integration einer Kombination der Kernfunktionen, Eingaben und Ausgaben des Systems in einem Zeitfenster. Schließlich können die Koeffizienten zur Basiserweiterung mit einer Matrixmultiplikation berechnet werden, was zu der gewünschte Zustandsschätzung führt. Das Verfahren wird am Beispiel der Dynamik eines Rohreaktors getestet und die Ergebnisse werden mit anderen Methoden verglichen.

Acknowledgements

iv

Contents

List of Figures

List of Tables

List of Abbreviations

PDE	**P**artial **D**ifferential **E**quation
MF	**M**odulation **F**unction
SNR	**S**ignal to **N**oise **R**atio
ISE	**I**ntegral **S**quared **E**rror
DGT	**D**iffusive **G**radient in **T**hin Films
ODE	**O**rdinary **D**ifferential **E**quation
SMC	**S**ignal **M**odel **C**ontrol

Chapter 1

Introduction

1.1 Motivation

Many systems are modelled by Partial Differential Equations(PDEs). For example, solar collector systems[19], drilling systems [23] [6], chemical reaction systems [14], medical imaging, seismic imaging, oil exploration and computer tomography [15]. A particular type of this kind of systems are Coupled Reaction-Diffusion PDEs. This type of systems are characterized for a coupling between the system states in the PDEs. Every equation has the form of a Reaction-Diffusion PDE and are dependant on the other ones making the system more complex in comparison to a normal PDE.

Example of this kind of systems are Chemical Tubular Reactors [25] where the state variables: temperature and concentration, are coupled by the PDE related to each one of this states. [27] Develops a novel tubular reactor-enhanced ecological floating bed to enhance nitrogen removal of secondary effluents. Excessive nitrogen emission is a common problem in the secondary effluents of rural waste-water treatment facilities. From both of the systems it is evident a coupling between states and a diffusion-reaction dynamic.

Other example are Diffusive Gradients in Thin Films(DGT), [5] an in situ passive sampling techniques commonly used in environmental chemistry, which has been applied to the detection of elements and compounds in natural environments, including water, sediment and soil. Based on Fick's first law of diffusion, the time-weighted average concentration of labile species during the deployment time can be obtained using DGT. [28] Shows that DGT can be used to get measurements of antibiotics in urban waste-waters. This is crucial to map the impact of antibiotic pollution and to provide the basis for designing water quality and environmental risk in regular water monitoring programs. Another example is the diffusion of lithium ions in the porous electrodes of lithium-ion that comprise multiple active materials. Manufacturers are using multiple active materials in the positive electrode of lithium-ion cells to combine power and energy characteristics or reduce degradation [16] [20]. The recent interest to use electrochemical models for online state-of-charge estimation motivates the design of observers for the PDEs appearing in these models.

For the control of this kind of systems, a measurement of the whole spatial domain is often required and this requisite is nearly impossible with physical sensors. Because of this, observers are devolped in order to estimate the whole state only with boundary measurements. An observer in combination with a control strategy can enable a feedback output control to achieve its goal with only boundary measurements that can be done with a sensor collocated at the boundary. Different kinds of observers, such as adaptive and iterative observers have been proposed by [24], recursive observers based methods have been introduced in [17]. Different other types of observers have been proposed for coupled dynamical cascade systems including Ordinary Differential Equations (ODE) and PDEs for example in [22].

Most of the work related to state estimation for coupled diffusion-reaction PDEs uses the backstepping approach to solve the problem. This method uses an observer system, very similar in form to the original system with an output feedback in order to correct the estimation. The idea of the backstepping method is to stabilize the estimation error system transforming it with Volterra integral transformations to a stable system. The main task in the method is the calculation of the Kernels thorough the solution of non-trivial PDEs and can be made offline, but the simulation of the observer system that is also a Coupled Reaction-Diffusion PDE has to be made online and requires the solution of the PDEs that can be a heavy computational task. The approach of this thesis is based on the so-called modulating function (MF), introduced in the early 1950s by Shinbrot [30] [31], to be used for parameters identication of ODEs. In this case, modulating functions are used for the state estimation. This method reduces the original problem to a calculation of the coefficients that are used in the basis representation of the actual state through the solution of a linear system of equations, making the process of estimation much simpler to calculate and also less computational intensive.

The problem of state estimation for coupled Reaction Diffusion with the use of Modulating functions implies different aspects of the whole observer. The filter characteristics of the observer are very important to the solution of the problem. Here, numerics issues are crucial in the solving since the basis approximation and the integration required in the modulation process can be a source of error on the estimation and it has to be addressed. The signal model control is another area to be explored, since the use of the modulating function requires some conditions imposed on each modulating function used and together with the auxiliary models obtained, requires a controller to fulfill these requirements. Another topic of interest is the system class that the current work can be applied to. In our case we are dealing with Linear Coupled PDE systems with Reaction and Advection terms that also have spatially dependent coefficients with main applications on Chemical Tubular Reactors and DGT that are described previously. All of these related topics are resumed in the Figure 1.1. where this overview is shown.
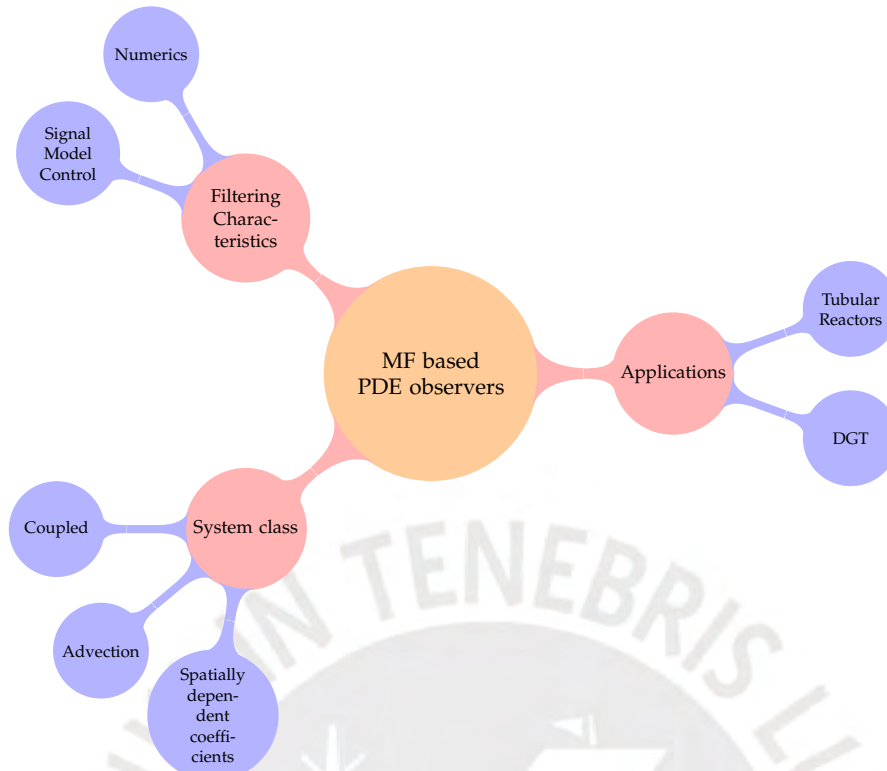
FIGURE 1.1: Overview of the related topics in the thesis

1.2 State of the art

The problem of state estimation for coupled linear parabolic equations is strongly related to the stabilization problem. The estimation problem, commonly requires the design of an observer that has stability properties for the origin of the estimation error system. Thus, this stability implies the convergence of the state estimate and finally implying a successful state estimation. With this relation, the following section also includes investigation related to the stabilization problem. Most of the investigation realized for both stabilization and estimation problem have been addressed using the backstepping method for PDEs. The backstepping method uses an invertible Volterra integral transformation mapping, that transforms the system into a exponentially stable target system. In the case of the state estimation, it transforms the observer error dynamics to achieve a stabilization of the estimation error and in consequence a convergence in the state estimate to the actual state. The main problem is to find the Kernels in the integral transformation that ensures the actual transformation. That requires to solve other PDE in order to find the Kernel needed.

One of the early attempts on the solution of the problem was done in [3]. The work was devoted to the solution of the stabilization problem for reaction-diffusion PDEs with the same diffusitivity parameters. The restriction of same diffusitivity

parameters is established because in the Kernel equation, a different diffusivity parameter sets an overdetermined PDE with no solution without other specific constrains on the form of the Kernel matrix. The paper uses the method of successive approximations to have a solution for the kernel matrix.

In [2] using a similar approach to [3], the problem of state estimation for reaction-diffusion PDEs with the same diffusivity parameters is done. The observer is designed in order to have a convergence in the estimation error system, transforming the original system through the use of the Kernel matrix. Similar to [3], a very similar PDE has to be solved in order to obtain the Kernel Matrix and using the same approach of [3], a solution is obtained.

In [1] the extension is done for reaction-advection-diffusion equations also with the same restriction of the same diffusivity parameters through the backstepping method. The next step in reducing the system restrictions for the stabilization problem is done in [2], where the problem is resolved for a reaction-diffusion system with constant parameters, not requiring to have the same diffusivity parameters as the previous works. This is done by imposing some constraints on the kernel matrix.

In [26] some of the results from [2] are used to design an observer for a reaction-diffusion system with constant parameters that is used for an Output feedback stabilization of the same system.

Then, in [18] and [10] a next step in generalizing the type of systems approached is done by solving the stabilization and estimation for coupled reaction-diffusion systems with spatially-varying reaction terms. In [10] the estimation is done for a 2-Coupled reaction-diffusion PDE with spatially varying coefficients, which can be used to model the diffusion phenomena in lithium-ion batteries with electrodes that comprise multiple active materials. and in [11] the approach is generalized for a n-Coupled reaction-diffusion PDE with spatially varying coefficients.

The Modulating Function Based method is different in conception from the PDE backstepping approach because it involves approximate the signals as a function basis representation and using some properties of the modulating function and applying a modulation operation in the original system, transform the original system into a series of algebraic relations. Often this process also involves some restrictions in the modulating functions that can be understood as an auxiliary system(also called signal modelling) that can be resolved before the estimation.

The method has been used for parameters and source estimation for one dimensional PDEs [21]. In this work Modulation Function methods are used to estimate the source function and velocity for the wave equation and . It is also explore the influence of different parameters in the method, such as the length of the Basis, the size of the Time window and the type of basis functions chosen. The results also show the behavior of the estimation with respect to noise on the output of the system, showing a good performance and robustness of the method.

[7] develops fault detection and isolation for a parabolic PDE system using Modulation functions, applying the method for a faulty heat conducting rod. This method traces back the fault detection problem to a trajectory planning problem using Modulating functions obtained by the realization of a set-point change for their signal models, and using previous results on motion planning for distributed parameter systems the fault detection and isolation can be achieved.

The most recent result [12] is related to the state estimation for reaction diffusion PDE with constant parameters. In this work the whole state is estimated from a measurement in the boundary. Through the use of Modulating functions the estimation problem is transformed in a linear system of equations for the coefficients of the basis expansion that represents the whole state. The resulting auxiliary system has a very similar form of the original system. This work makes the foundation for the present work, since it demonstrates that the Modulation Function approach is possible for Reaction Diffusion PDE systems and how the state estimation can be achieved. In the present thesis, this results are very inspiring for the formulation of the same problem but for Coupled Reaction Diffusion PDE systems.

So far no work has been made in relation of state estimation using Modulating Functions for Coupled Reaction-Diffusion PDE.

1.3   Objectives

The problem to solve is the state estimation for linearly coupled Reaction-Diffusion with spatially varying coefficients PDE systems. In this kind of problem the usually solution is the use of backstepping observers, that similar to their controller counterpart involves founding a kernel and also solving a PDE due to the observer equation, a computing intensive task. The modulation function as in [12] is an alternative since only involve simple matrix multiplication and an integral that can be done numerically. Main limitations here involve the basis expansion approximation to the state that can cause an error on the estimation. Also the signal model control(SMC) problem is crucial to the convergence time since the modulation function requisites has to be solved in a time window. All of these aspects have to be taken into account for the solution of the state estimation using modulation functions. With this background the general objective of this thesis is the development and implementation of a MFs based state estimation for coupled PDE systems.

The specific objectives of this thesis are:

- Development of a theoretical framework for the use of Modulating Functions in coupled PDE systems.

- Implementation and simulation on a specific application(Tubular chemical reactors)

- Check and compare performance of the MF based observer with other observers

1.4   Outline

The thesis is organized in a way that the reader can follow the natural development of the framework and the generalization of the method. It is structured as follows:

Chapter 2 presents some fundamentals about the main topics that are related to the thesis, such as Coupled Parabolic PDEs, Modulating Function, the control of this type of PDEs. This theoretical framework will allow the reader to have a better understanding of the thesis and also will familiarize with some of the concepts presented throughout the next chapters.

Chapter 3 presents the use of Modulating functions for the state estimation of a n-Coupled Reaction-Advection-Diffusion PDE with spatially varying coefficients. In this chapter, the problem is stated and then using Modulating Functions an Auxiliary System is derived. After solving this system, a reconstruction of the state through the solution of a linear system of equations can be done.

Chapter 4 presents an implementation of the method developed in the last chapter. Different parameters of the observer are tested in order to analyze their influence on the estimation. Finally, simulation results are presented and compared with other works results.

Chapter 5 finalizes the manuscript showing the main conclusions and future work to be done.

Chapter 2

Theoretical Fundamentals

This chapter will explain some fundamentals that are needed for the understanding of the modulating function method applied and also will be referred in the application of the method in the next chapter since it provides some results that are fundamental on the developing of the method for the present thesis.

2.1 Coupled Parabolic Reaction-Advection-Diffusion PDE with spatially varying coefficients

This thesis is devoted to a class of linear systems modelled by the following n coupled reaction-advection-diffusion equations with spatially-varying coefficients:

$$\frac{\partial U}{\partial t}(x,t) = \Sigma(x)\frac{\partial^2 U}{\partial x^2}(x,t) + \Phi(x)U_x(x,t) + \Lambda(x)U(x,t) \tag{2.1}$$

With the Dirichlet-type left actuation and the Neumann-type right boundary condition:

$$U(0,t) = U_c(t), U_x(L,t) = 0 \tag{2.2}$$

where

$$U(x,t) = \begin{bmatrix} u_1(x,t) & \dots & u_n(x,t) \end{bmatrix}^T$$

is the state vector and

$$U_c(t) = \begin{bmatrix} u_{c_1}(t) & \dots & u_{c_n}(t) \end{bmatrix}^T$$

is the input vector. $\Sigma(x)$ is the nxn matrix, whose components $\epsilon_{ij}(x), \phi_{ij}(x), \lambda_{ij}(x)$ for $i = 1,...,n$, are the diffusion term coefficients, advection term coefficients and diffusion term coefficients respectively.

$$\Sigma(x) = \begin{bmatrix} \epsilon_{11}(x) & \dots & \epsilon_{1n}(x) \\ \vdots & \ddots & \vdots \\ \epsilon_{n1}(x) & \dots & \epsilon_{nn}(x) \end{bmatrix}, \Phi(x) = \begin{bmatrix} \phi_{11}(x) & \dots & \phi_{1n}(x) \\ \vdots & \ddots & \vdots \\ \phi_{n1}(x) & \dots & \phi_{nn}(x) \end{bmatrix}$$

$$\Lambda(x) = \begin{bmatrix} \lambda_{11}(x) & \dots & \lambda_{1n}(x) \\ \vdots & \ddots & \vdots \\ \lambda_{n1}(x) & \dots & \lambda_{nn}(x) \end{bmatrix} \tag{2.3}$$

The state estimation of this kind of systems are explored in the Chapter 5.

If $\Phi(x) = 0$, the system becomes a reaction-diffusion PDE with spatially varying coefficients and has the following form:

$$\frac{\partial U}{\partial t}(x,t) = \Sigma(x)\frac{\partial^2 U}{\partial x^2}(x,t) + \Lambda(x)U(x,t) \tag{2.4}$$

The state estimation of this kind of systems are explored in the Chapter 4.

Also if $\Sigma(x)$ and $\Lambda(x)$ are not dependant on x, then the system becomes a reaction-diffusion PDE with constant coefficients with the following form:

$$\frac{\partial U}{\partial t}(x,t) = \Sigma\frac{\partial^2 U}{\partial x^2}(x,t) + \Lambda U(x,t) \tag{2.5}$$

Definition 2.1.1. *[29] Let $u_i(x,t)$ and $u_j(x,t)$ be two different states of a system modelled by (3.1)-(3.3). If $\lambda_{ij} \neq 0$ or $\lambda_{ji} \neq 0$, $u_i(x,t)$ and $u_j(x,t)$ are said to be directly coupled.*

Definition 2.1.2. *[29] A system modelled by (3.1)-(3.3) is said fully coupled, if for any two different states $u_i(x,t)$ and $u_j(x,t)$, there exists a series of other states $u_i, u_{r_1}, u_{r_2}, ..., u_{r_m}$ with $m \geq n - 2$, such that the states $u_{r_1}, u_{r_2}, ..., u_{r_m}, u_j$ are directly coupled in turn, which means that the system cannot be decomposed into any number of independent subsystems.*

These definitions are important because the focus of the thesis is the state estimation for Coupled Reaction-Advection-Diffusion PDE systems that are fully coupled.

2.2   Modulating Function

Definition 2.2.1. *(Modulating Function) A function $\varphi \in C^k([a,b], \mathbb{R})$ is called a modulating function of order k with $k \in \mathbb{N}^*$ if and only if:*

$$\varphi^{(i)}(a) = \varphi^{(i)}(b) = 0, i = 0, 1, ..., k-1 \tag{2.6}$$

An extension to distributed systems can be obtained by defining the kernel function in the time and spatial domain [8] [7].

Definition 2.2.2. *(Modulation Functional) The state modulation functional is defined by*

$$M[h] = \int_{t-T}^{t} \int_{0}^{L} m(x, \tau - t + T)h(x,\tau)dxd\tau \tag{2.7}$$

where $h : [0, L] \times \mathbb{R}_0^+ -> \mathbb{R}$ and $m : [0, L] \times [0, T] -> \mathbb{R}$ is the modulating function to be constructed.

For simplicity the following notation is used:

$$\langle m, h \rangle_{\Omega, I} := M[h]$$

where $\Omega := [0, L]$ and $I := [t - T, t]$ with receding horizon length $T > 0$. If the integration only concerns the temporal or spatial variable, $\langle m, h \rangle_I$ and $\langle m, h \rangle_\Omega$ are used.

Here, some properties of the modulation functional with respect to the time derivative and spatial derivative are stated:

Shift of time derivative

Using derivation by parts, the following is stated:

$$
\begin{aligned}
\langle \varphi, u_t \rangle_{\Omega,I} &= \int_{t-T}^{t} \int_0^L \varphi(x, \tau - t + T) u_t(x, \tau) dx d\tau \\
&= \int_0^L (\varphi u - \int_{t-T}^{t} \varphi_t(x, \tau - t + T) u(x, \tau) d\tau) dx \\
&= \int_0^L \varphi u \Big|_{t-T}^{t} - \langle \varphi_t, u \rangle_{\Omega,I}
\end{aligned}
\tag{2.8}
$$

In general:

Theorem 2.2.3. *Given φ, a modulation function, and u, one of the states of the system represented in 2.1, then the following is true:*

$$
\langle \varphi, \frac{\partial^n u}{\partial t^n} \rangle_{\Omega,I} = \int_0^L (\sum_{i=0}^{n-1} (-1)^i \frac{\partial^i \varphi}{\partial t^i} \frac{\partial^{(n-1)-i} u}{\partial t^{(n-1)-i}}) \Big|_{t-T}^{t} dx + (-1)^n \langle \frac{\partial^n \varphi}{\partial t^n}, u \rangle_{\Omega,I}
\tag{2.9}
$$

Proof. The base case($n = 1$) has been demonstrated in 2.8 Then we will proceed to demonstrate the general case using the inductive step. Inductive Step($n \to n + 1$):

$$
\begin{aligned}
\langle \varphi, \frac{\partial^{n+1} u}{\partial t^{n+1}} \rangle_{\Omega,I} &= \int_{t-T}^{t} \int_0^L \varphi(x, \tau - t + T) \frac{\partial^{n+1} u}{\partial t^{n+1}} dx d\tau \\
&= \int_0^L (\varphi \frac{\partial^n u}{\partial t^n} \Big|_{t-T}^{t} - \int_{t-T}^{t} \varphi_t(x, \tau - t + T) \frac{\partial^n u}{\partial t^n} d\tau) dx \\
&= \int_0^L \varphi \frac{\partial^n u}{\partial t^n} \Big|_{t-T}^{t} dx - \langle \varphi_t, \frac{\partial^n u}{\partial t^n} \rangle_{\Omega,I}
\end{aligned}
\tag{2.10}
$$

Using 2.9, then

$$
\langle \varphi, \frac{\partial^{n+1} u}{\partial t^{n+1}} \rangle_{\Omega,I} = \int_0^L \varphi \frac{\partial^n u}{\partial t^n} \Big|_{t-T}^{t} - \langle \varphi_t, \frac{\partial^n u}{\partial t^n} \rangle_{\Omega,I}
$$

$$
= \int_0^L \varphi \frac{\partial^n u}{\partial t^n} \Big|_{t-T}^{t} - (\int_0^L (\sum_{i=0}^{n-1} (-1)^i \frac{\partial^i \varphi_t}{\partial t^i} \frac{\partial^{(n-1)-i} u}{\partial t^{(n-1)-i}}) \Big|_{t-T}^{t} + (-1)^n \langle \frac{\partial^n \varphi_t}{\partial t^n}, u \rangle_{\Omega,I})
$$

$$
= \int_0^L \varphi \frac{\partial^n u}{\partial t^n} \Big|_{t-T}^{t} + \int_0^L (\sum_{i=0}^{n-1} (-1)^{i+1} \frac{\partial^{i+1} \varphi}{\partial t^{i+1}} \frac{\partial^{(n-(i+1))} u}{\partial t^{(n-(i+1))}}) \Big|_{t-T}^{t} + (-1)^{n+1} \langle \frac{\partial^{n+1} \varphi}{\partial t^{n+1}}, u \rangle_{\Omega,I}
$$

$$
= \int_0^L (\varphi \frac{\partial^n u}{\partial t^n} + \sum_{i=1}^{n} (-1)^i \frac{\partial^i \varphi}{\partial t^i} \frac{\partial^{(n-i)} u}{\partial t^{(n-i)}}) \Big|_{t-T}^{t} + (-1)^{n+1} \langle \frac{\partial^{n+1} \varphi}{\partial t^{n+1}}, u \rangle_{\Omega,I}
$$

$$
\langle \varphi, \frac{\partial^{n+1} u}{\partial t^{n+1}} \rangle_{\Omega,I} = \int_0^L (\sum_{i=0}^{n} (-1)^i \frac{\partial^i \varphi}{\partial t^i} \frac{\partial^{(n-i)} u}{\partial t^{(n-i)}}) \Big|_{t-T}^{t} + (-1)^{n+1} \langle \frac{\partial^{n+1} \varphi}{\partial t^{n+1}}, u \rangle_{\Omega,I}
$$

$$
\tag{2.11}
$$

$\square$

Shift of space derivative Using derivation by parts, the following is stated:

$$\langle \varphi, u_x \rangle_{\Omega,I} = \int_{t-T}^{t} \int_{0}^{L} \varphi(x, \tau - t + T) u_x(x, \tau) dx d\tau$$

$$= \int_{t-T}^{t} (\varphi u - \int_{0}^{L} \varphi_x(x, \tau - t + T) u(x, \tau) dx) d\tau \tag{2.12}$$

$$= \int_{t-T}^{t} \varphi u \Big|_{0}^{L} d\tau - \langle \varphi_x, u \rangle_{\Omega,I}$$

In general:

Theorem 2.2.4. *Given φ a modulation function and u one of the states of the system represented in 2.1, then the following is true:*

$$\langle \varphi, \frac{\partial^n u}{\partial x^n} \rangle_{\Omega,I} = \int_{t-T}^{t} \left(\sum_{i=0}^{n-1} (-1)^i \frac{\partial^i \varphi}{\partial x^i} \frac{\partial^{(n-1)-i} u}{\partial x^{(n-1)-i}} \right) \Big|_{0}^{L} + (-1)^n \langle \frac{\partial^n \varphi}{\partial x^n}, u \rangle_{\Omega,I} \tag{2.13}$$

Proof. The base case($n = 1$) has been demonstrated in 2.12 Then we will proceed to demonstrate the general case using the inductive step. Inductive Step($n \to n + 1$):

$$\langle \varphi, \frac{\partial^{n+1} u}{\partial x^{n+1}} \rangle_{\Omega,I} = \int_{t-T}^{t} \int_{0}^{L} \varphi(x, \tau - t + T) \frac{\partial^{n+1} u}{\partial t^{n+1}} dx d\tau$$

$$= \int_{t-T}^{t} (\varphi \frac{\partial^n u}{\partial x^n} - \int_{0}^{L} \varphi_x(x, \tau - t + T) \frac{\partial^n u}{\partial x^n} dx) d\tau \tag{2.14}$$

$$= \int_{t-T}^{t} \varphi \frac{\partial^n u}{\partial x^n} \Big|_{0}^{L} - \langle \varphi_x, \frac{\partial^n u}{\partial x^n} \rangle_{\Omega,I}$$

Assuming 2.13 for n, then

$$\langle \varphi, \frac{\partial^{n+1} u}{\partial x^{n+1}} \rangle_{\Omega,I} = \int_{t-T}^{t} \varphi \frac{\partial^n u}{\partial x^n} \Big|_{0}^{L} - \langle \varphi_x, \frac{\partial^n u}{\partial x^n} \rangle_{\Omega,I}$$

$$= \int_{t-T}^{t} \varphi \frac{\partial^n u}{\partial x^n} \Big|_{0}^{L} - \left(\int_{t-T}^{t} \left(\sum_{i=0}^{n-1} (-1)^i \frac{\partial^i \varphi_x}{\partial x^i} \frac{\partial^{(n-1)-i} u}{\partial x^{(n-1)-i}} \right) \Big|_{0}^{L} + (-1)^n \langle \frac{\partial^n \varphi_x}{\partial x^n}, u \rangle_{\Omega,I} \right)$$

$$= \int_{t-T}^{t} \varphi \frac{\partial^n u}{\partial x^n} \Big|_{0}^{L} + \int_{t-T}^{t} \left(\sum_{i=0}^{n-1} (-1)^{i+1} \frac{\partial^{i+1} \varphi}{\partial x^{i+1}} \frac{\partial^{(n-(i+1))} u}{\partial x^{(n-(i+1))}} \right) \Big|_{t-T}^{t} + (-1)^{n+1} \langle \frac{\partial^{n+1} \varphi}{\partial x^{n+1}}, u \rangle_{\Omega,I}$$

$$= \int_{t-T}^{t} \left(\varphi \frac{\partial^n u}{\partial x^n} + \sum_{i=1}^{n} (-1)^i \frac{\partial^i \varphi}{\partial x^i} \frac{\partial^{(n-i)} u}{\partial x^{(n-i)}} \right) \Big|_{0}^{L} + (-1)^{n+1} \langle \frac{\partial^{n+1} \varphi}{\partial x^{n+1}}, u \rangle_{\Omega,I}$$

$$\langle \varphi, \frac{\partial^{n+1} u}{\partial x^{n+1}} \rangle_{\Omega,I} = \int_{t-T}^{t} \left(\sum_{i=0}^{n} (-1)^i \frac{\partial^i \varphi}{\partial x^i} \frac{\partial^{(n-i)} u}{\partial x^{(n-i)}} \right) \Big|_{0}^{L} + (-1)^{n+1} \langle \frac{\partial^{n+1} \varphi}{\partial x^{n+1}}, u \rangle_{\Omega,I}$$

$$\tag{2.15}$$

$$\square$$

These properties of the Modulation functional are very useful in the state estimation, since they enable to shift the derivatives applied to the state, to the modulating function. The other terms in the summatory can be eliminated with more restrictions on the modulating function and others can be known with the boundary sensing and

the actuation. The propierties are used in the Chapters 3,4 and 5 for the derivation of the auxiliary systems.

2.3 Orthonormal Basis of Functions

An orthonormal basis for an inner product space V is a basis for V whose vectors are orthonormal, that is, they are all unit vectors and orthogonal to each other. In the case related to this thesis, the goal is to approximate the state, a function dependant on time and space, as a linear combination of an orthonormal basis of functions. In order to obtain more insight on the system behaviour, a certain solution structure of the desired state is proposed using the following function expansion representation[12]:

$$u(x,t) = \sum_{k=0}^{\infty} c_k(t)\psi_k(x) \tag{2.16}$$

The precise task will then be to estimate the time dependent coefficients c_k for every time instance given an approximation order $N \in \mathbb{N}$ and an appropriate spatial orthonormal function basis ψ_k. Let us denote the respective function space with $X := \{f : \Omega \rightarrow \mathbb{R}, ||f||_v^2 < \infty\} = \text{span}\{\psi^k, k \in \mathbb{N}_0\}$ where the related scalar product is defined as $\langle f,g \rangle_v = \int_\Omega v(x)f(x)g(x)dx$ with the weighting function v. The right choice of a proper description for the solution structure of w has to be made as part of the estimator design process. The orthonormal basis $\Psi = \{\psi_k, ||\psi^k||_v = 1 \wedge \langle \psi^k, \psi_j \rangle_v = 0 \text{ for } k \neq j\}$ with respect to the weighted inner product can be constructed by applying the Gram-Schmidt procedure.

For an example of how precise this function expansion representation can be, the state of a 2-Coupled Reaction-Diffusion system that represents a temperature-concentration system of Chemical Tubular reactors given by [2] and simplified by [4]. In Figure 2.1, the original states are shown in the first row and the function expansion represented with the hat in the row below, illustrating the similitude between the original and approximated states, important for the estimation using modulation functions, since the modulation function observer will estimate this function expansion. The integral squared error of this approximation is presented in Figure 2.2, showing better results with $N = 5$. Also the absolute error of this approximation is shown in the Figure 2.3 where the maximum errors are located in the boundaries of x and t. The error caused by the approximation is significantly important in the estimation process because the method is estimating a basis expansion of the state and the best scenario possible is when the estimation is equal to the basis expansion and if the basis expansion already has an error in the projection, then the estimation will also have this error, making this projection error important to take into account.
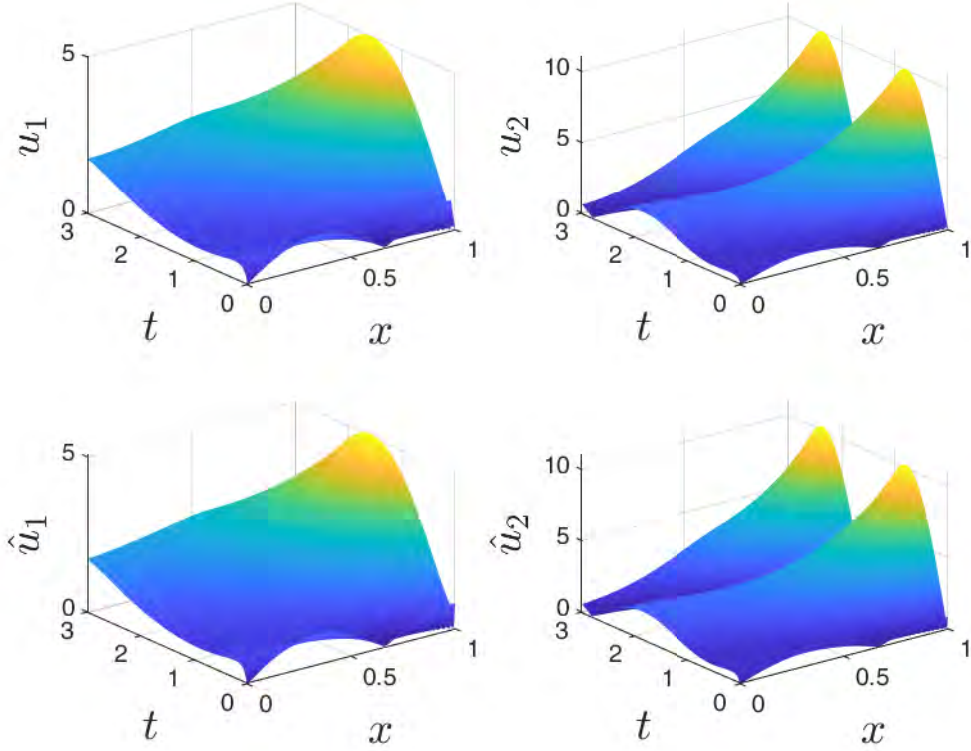
FIGURE 2.1: Original states (above) and projected states (below)

2.4   Backstepping Control of coupled parabolic reaction-diffusion PDE

The backstepping method for PDE systems [9] uses an invertible Volterra integral transformation mapping, that transforms the system into a exponentially stable target system. The main problem is to find the Kernels in the integral transformation that ensures the actual transformation. That requires to solve other PDEs in order to find the Kernel needed.

For this purpose, in [29] the kernel function $H(x, y)$ is computed such that the following backstepping transformation:

$$W(x,t) = U(x,t) - \int_0^x K(x,y)U(y,t)dy \tag{2.17}$$

can transform the system defined in 2.5 into the following target system:

$$\frac{\partial W}{\partial t}(x,t) = \Sigma(x)\frac{\partial^2 W}{\partial x^2}(x,t) - \tilde{C}W(x,t)$$
$$\frac{\partial W}{\partial x}(x,t) = 0 \tag{2.18}$$
$$W(1,t) = 0$$
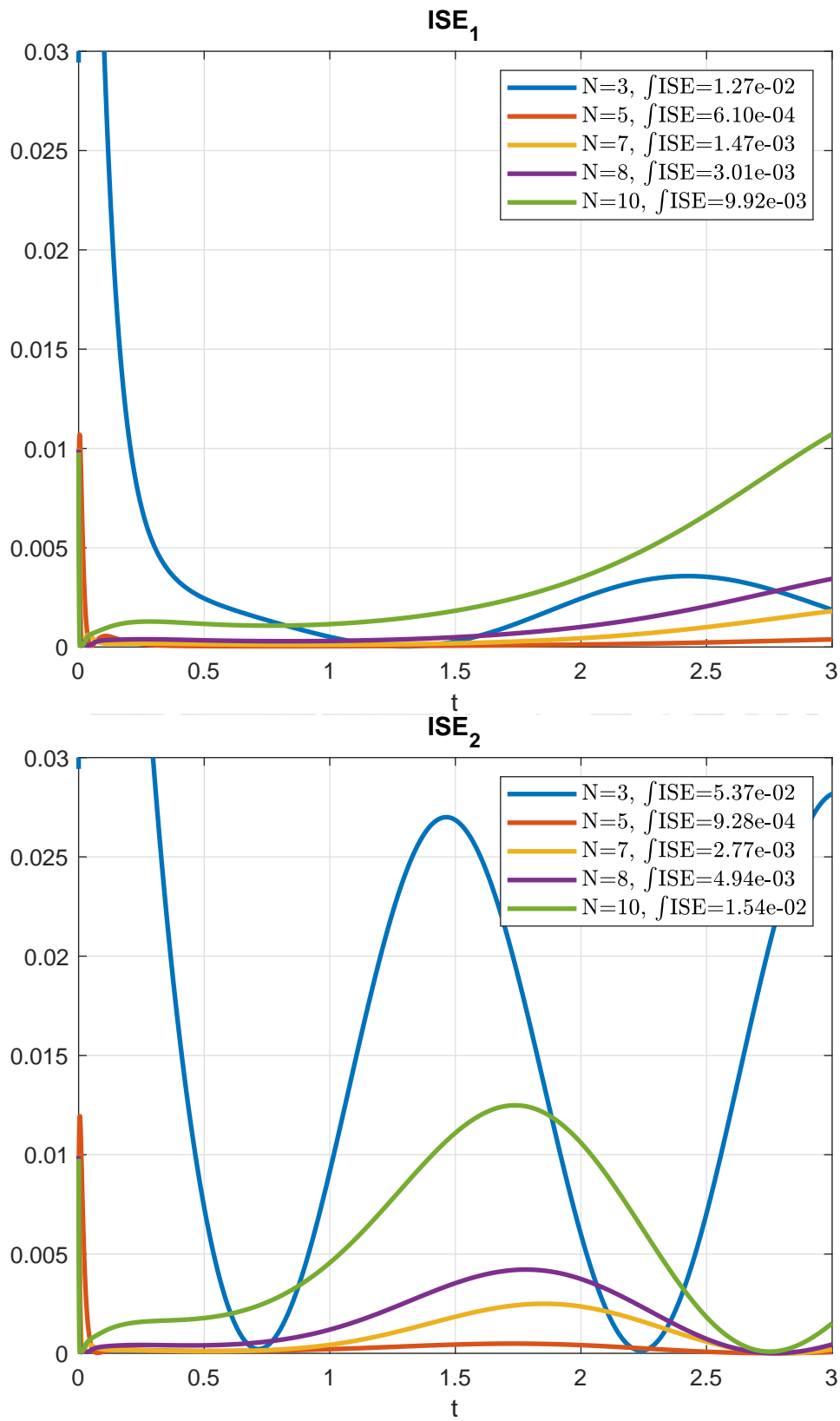
FIGURE 2.2: Integral squared error of the basis projection of the state
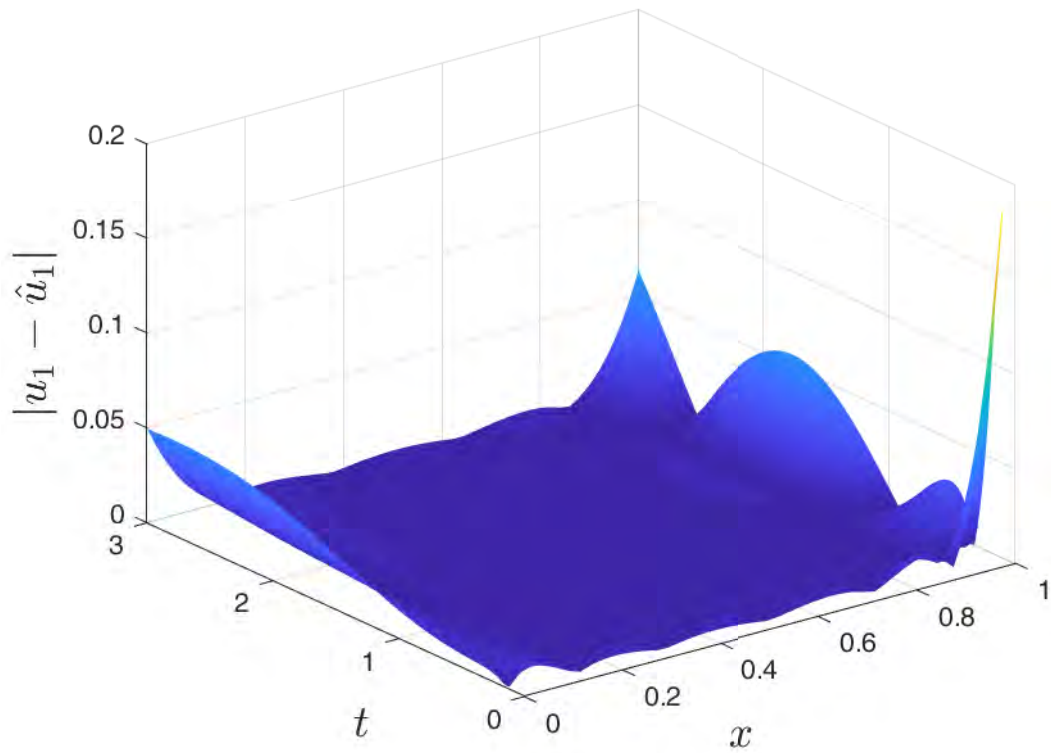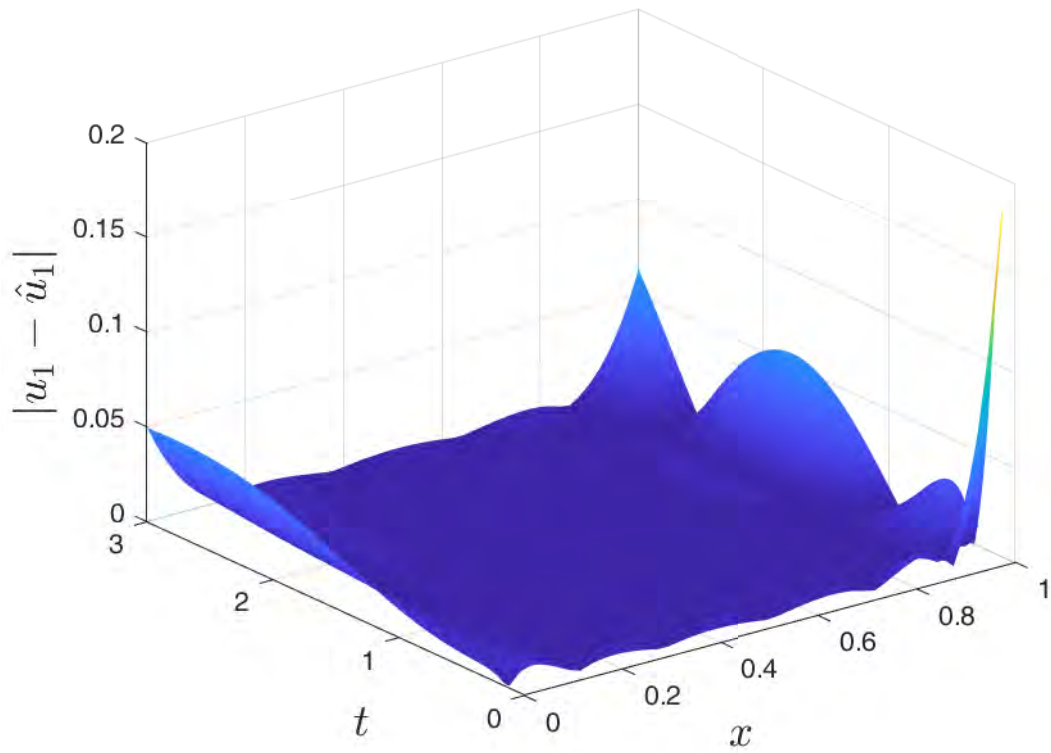
FIGURE 2.3: Absolute error of the approximation for N=5

where $\tilde{C}$ is a $n \times n$ matrix with the components c_{ij} for $i, j = 1, 2, ..., n$, $K(x, y)$ is the kernel matrix with the form: $K(x, y) = k(x, y)I_{nxn}$ and $k(x, y)$ is the kernel function given by:

$$k(x, y) = -\tilde{k}x \frac{I_1(\sqrt{\tilde{k}(x^2 - y^2)})}{\tilde{k}(x^2 - y^2)} \tag{2.19}$$

where I_1 is the modified Bessel function of the first kind and the parameter $\tilde{k}$ is defined by the following equation:

$$\tilde{k}I_{nxn} = (\tilde{C} + \Lambda)\Sigma^{-1} \tag{2.20}$$

If the parameter $\tilde{k}$ is chosen such that $S[\tilde{C}] = (C + C^T)/2$ is positive definite, then the target system (2.18) is exponentially stable with the following convergence rate:

$$||W(x, t)||_{2,n} \leq ||W(x, 0)||_{2,n}e^{-\sigma_{min}(S[\tilde{C}])t} \tag{2.21}$$

In order to fulfil this condition, the next inequality has to be fulfilled:

$$-S[\Lambda] + \frac{\Sigma_{min}}{4}I_{nxn} + \tilde{k}\Sigma > 0 \tag{2.22}$$

Thus, the controller defined by:

$$U_c(x, t) = -\int_0^1 \tilde{k}\frac{I_1(\sqrt{\tilde{k}(x^2 - y^2)})}{\tilde{k}(x^2 - y^2)}U(y, t)dy \tag{2.23}$$

stabilizes the system defined by 2.5. With these requirements, the control can be done. This method is useful for solving the problem of the signal modelling control when the auxiliary system that is also a Coupled Reaction-Diffusion system.

2.5 Backstepping Control of coupled parabolic reaction-diffusion with spatially varying coefficients PDE

Considering the system defined in 2.4 with the following boundary conditions:

$$\begin{aligned} U(0, t) &= 0 \\ U(1, t) &= U_c(t) \end{aligned} \tag{2.24}$$

In [18] the following feedback control law:

$$U(t) = \int_0^1 K(1, \xi)u(\xi, t)d\xi \tag{2.25}$$

where the kernel matrix $K(x, \xi)$ is a solution from the following matrix system of PDEs:

$$\Sigma K_{xx}(x, \xi) - K_{\xi\xi}(x, \xi)\Sigma = K(x, \xi)\Lambda(\xi) + CK(x, \xi) \tag{2.26}$$

in the domain $T = (x, \xi) : 0 \leq \xi \leq x \leq 1$, with the boundary conditions

$$\Sigma K_\xi(x, x) - \Sigma K_x(x, x) + \Sigma \frac{d}{dx} K(x, x) = -\Lambda(x) - C$$
$$\Sigma K(x, x) = K(x, x)\Sigma \qquad (2.27)$$
$$K_{ij} = 0, i \leq j$$

In order to obtain the kernel K, it is necessary to define first:

$$L(x, \xi) = \sqrt{\Sigma} K_x(x, \xi) + K_\xi(x, \xi)\sqrt{\Sigma} \qquad (2.28)$$

Then the original nxn system in 2.27 is replaced by a $n^2 \times n^2$ system of first-order hyperbolic equation on the same domain

$$\sqrt{\Sigma} K_x + K_\xi \sqrt{\Sigma} = L$$
$$\sqrt{\Sigma} L_x - L_\xi \sqrt{\Sigma} = K\Lambda(\xi) + CK \qquad (2.29)$$

with the following boundary conditions:

- If $i = j$, then

$$L_{ii}(x, x) = -\frac{\lambda_{ii}(x) + c_i}{2\sqrt{\epsilon_i}}$$
$$K_{ii}(x, 0) = 0 \qquad (2.30)$$

- If $i < j$, then

$$L_{ij}(x, x) = -\frac{\lambda_{ij}(x) + c_i}{\sqrt{\epsilon_i} + \sqrt{\epsilon_j}}$$
$$K_{ij}(x, x) = K_{ij}(x, 0) = 0 \qquad (2.31)$$

- If $i > j$ and $\epsilon_i \neq \epsilon_j$ then

$$L_{ij}(x, x) = -\frac{\lambda_{ij}(x) + c_i}{\sqrt{\epsilon_i} + \sqrt{\epsilon_j}}$$
$$K_{ij}(x, x) = 0 \qquad (2.32)$$
$$K_{ij}(1, \xi) = l_{ij}(\xi)$$

Then, similar to [13] the kernels can be calculated using the successive approximation method and the control problem solved. With these requirements, the control can be done. This method is useful for solving the problem of the signal modelling control with relation to the auxiliary system(see Chapter 3) that when it is a Coupled Reaction-Diffusion with spatially varying coefficients system.

Finally, all of these fundamentals are very important in the state estimation problem that the present thesis deals with. The properties of the modulation function and the orthornormal basis of functions are essential in deriving the modulation kernel equations that implies solving an auxiliary system, where the backstepping control

is an approach that can solve the requirement imposed on the modulation function and thus, achieving the state estimation required.

Chapter 3

State estimation of n-Coupled Reaction-Advection-Diffusion PDE

The following chapter will explore the state estimation of n-Coupled Reaction-Advection-Diffusion PDEs using modulating functions. First, the problem statement is explained and then with the use of modulation functionals, auxiliary systems are obtained. These auxiliary systems are closely related to the original system and their solution are the modulating functions. Then, a linear combination of the coefficients from the basis expansion can be obtained with the calculation of the modulation kernel that is dependent on the input, output and the modulating functions obtained previously. Finally, the decoupling of the coefficients can be made by generating more linear combinations and establishing a linear system of equations to solve and obtain the coefficients. With the coefficients, the state can be reconstructed using the function expansion representation.

3.1 Problem Statement

The system which states are going to be estimated is a n-Coupled Reaction-Diffusion PDE with spatially varying coefficients described by the following equations:

$$
\begin{cases}
U = \Sigma(x)U_{xx} + \Phi(x)U_x + \Lambda(x)U \\[2mm]
\Sigma(x) = \begin{bmatrix} \epsilon_{11}(x) & \dots & \epsilon_{1n}(x) \\ \vdots & \ddots & \vdots \\ \epsilon_{n1}(x) & \dots & \epsilon_{nn}(x) \end{bmatrix}, \Phi(x) = \begin{bmatrix} \phi_{11}(x) & \dots & \phi_{1n}(x) \\ \vdots & \ddots & \vdots \\ \phi_{n1}(x) & \dots & \phi_{nn}(x) \end{bmatrix} \\[6mm]
\Lambda(x) = \begin{bmatrix} \lambda_{11}(x) & \dots & \lambda_{1n}(x) \\ \vdots & \ddots & \vdots \\ \lambda_{n1}(x) & \dots & \lambda_{nn}(x) \end{bmatrix} \\[6mm]
U(x,t) = \begin{bmatrix} u_1(x,t) & \dots & u_n(x,t) \end{bmatrix}^T
\end{cases}
\tag{3.1}
$$

With a mixed type boundary condition:

$$
P_1 U_x(0,t) + P_0 U(0,t) = F(t)
\tag{3.2}
$$

That can be a Dirichlet or Neumann type boundary condition choosing either $P_1 = 0$ or $P_0 = 0$ respectively.

A known actuation at the boundary:

$$Q_1 U_x(L, t) + Q_0 U(L, t) = G(t) \tag{3.3}$$

And a measurement at the boundary

$$Y(t) = R_1 U_x(x^*, t) + R_0 U(x^*, t) \tag{3.4}$$

With $x^* = 0$ or L

The problem is to estimate the state $U(x, t)$ with the measurements $Y(t)$ and the inputs $G(t)$

3.2   Derivation of the Auxiliary Systems

For the derivation of the auxiliary system, we apply the modulation functional to the state. First we apply the modulation functional to the second spatial derivative of the state. Using the properties of the Theorem 2.2.4

$$\langle \varphi, u_{n_{xx}} \rangle_{\Omega, I} = \int_{t-T}^{t} \varphi(x, \tau - t + T) u_{n_x}(x, \tau) d\tau \Big|_{x=0}^{x=L}$$
$$- \int_{t-T}^{t} \varphi_x(x, \tau - t + T) u_n(x, \tau) d\tau \Big|_{x=0}^{x=L} + \langle \varphi_{xx}, u_n \rangle_{\Omega, I}$$
$$= \int_{t-T}^{t} (M_L^2 + M_0^2)[\varphi, u_n] d\tau + \langle \varphi_{xx}, u_n \rangle_{\Omega, I} \tag{3.5}$$

where:

$$M_L^2[\varphi, u_n] = \varphi(L, \tau - t + T) u_{n_x}(L, \tau) - \varphi_x(L, \tau - t + T) u_n(L, \tau)$$
$$M_0^2[\varphi, u_n] = -\varphi(0, \tau - t + T) u_{n_x}(0, \tau) + \varphi_x(0, \tau - t + T) u_n(0, \tau) \tag{3.6}$$

Now we apply the modulation functional to the spatial derivative of the state. Using the properties of the Theorem 2.2.4

$$\langle \varphi, u_{n_x} \rangle_{\Omega, I} = \int_{t-T}^{t} \varphi(x, \tau - t + T) u_n(x, \tau) \Big|_{x=0}^{x=L} + \langle \varphi_x, u_n \rangle_{\Omega, I}$$

$$\langle \varphi, u_{n_x} \rangle_{\Omega, I} = \int_{t-T}^{t} (M_L^1 + M_0^1)(\varphi, u_n) d\tau + \langle \varphi_x, u_n \rangle_{\Omega, I} \tag{3.7}$$

Where:

$$M_L^1(\varphi, u_n) = \varphi(L, \tau - t + T) u_n(L, \tau)$$
$$M_0^1(\varphi, u_n) = -\varphi(0, \tau - t + T) u_n(0, \tau) \tag{3.8}$$

The next step is to apply the Modulation functional to the time derivative of the state.Using the properties of the Theorem 2.2.3:

$$\langle \varphi, u_{n_t} \rangle_{\Omega, I} = \int_0^L \varphi(x, \tau - t + T) u_n(x, \tau) dx \Big|_{\tau=t-T}^{\tau=t} - \langle \varphi_t, u_n \rangle_{\Omega, I}$$

Selecting the following conditions for the modulating function, and using a function basis $\{\psi^m, m \in 0, 1, ..., N\}$ for estimation:

$$\begin{cases} \varphi^m(x, 0) = 0 \\ \varphi^m(x, T) = v(x)\psi^m(x) \end{cases} \tag{3.9}$$

Then, the spatial integration terms becomes:

$$\int_0^L \varphi^m(x, \tau - t + T) u_n(x, \tau) dx \Big|_{\tau=t-T}^{\tau=t} = \int_0^L \varphi^m(x, T) u_n(x, t) dx$$

Using the basis expansion from Equation (2.16) in Chapter 2

$$\int_0^L \varphi^m(x, T) u_n(x, t) dx = \sum_{i=0}^{\infty} c^i(t) \langle \psi^m, \psi^i \rangle_v = c^m(t)$$

Finally:

$$\langle \varphi^m, u_{n_t} \rangle_{\Omega, I} = c^m(t) - \langle \varphi_t^m, u_n \rangle_{\Omega, I} \tag{3.10}$$

Applying the modulation functional to the Equation (3.1):

$$\langle \varphi_i^m, u_{i_t} \rangle_{\Omega, I} = \sum_{j=1}^n \langle \varphi_i^m, \epsilon_{ij}(x) u_{j_{xx}} \rangle + \sum_{j=1}^n \langle \varphi_i^m, \phi_{ij}(x) u_{j_x} \rangle + \sum_{j=1}^n \langle \varphi_i^m, \lambda_{ij}(x) u_j \rangle, i = 1, ..., n$$

$$\tag{3.11}$$

Using MF associative properties

$$\langle \varphi_i^m, u_{i_t} \rangle_{\Omega, I} = \sum_{j=1}^n \langle \epsilon_{ij}(x) \varphi_i^m, u_{j_{xx}} \rangle + \sum_{j=1}^n \langle \phi_{ij}(x) \varphi_i^m, u_{j_x} \rangle + \sum_{j=1}^n \langle \lambda_{ij}(x) \varphi_i^m, u_j \rangle, i = 1, ..., n$$

From the previous results, Equation (3.2), (3.7) and (3.10):

$$c_i^m(t) = \langle \varphi_{i_t}^m, u_i \rangle_{\Omega, I} + \sum_{j=1}^n \int_{t-T}^t (M_L^2 + M_0^2)[\epsilon_{ij}(x) \varphi_i^m, u_j] + (M_L^1 + M_0^1)[\phi_{ij}(x) \varphi_i^m, u_j] d\tau$$

$$+ \sum_{j=1}^n \langle (\epsilon_{ij} \varphi_i^m)_{xx} - (\phi_{ij} \varphi_i^m)_x + \lambda_{ij} \varphi_i^m, u_j \rangle_{\Omega, I}, i = 1, ..., n$$

Expanding the spatial derivations in the left part:

$$c_i^m(t) = \langle \varphi_{i_t}^m, u_i \rangle_{\Omega,I} + \sum_{j=1}^n \int_{t-T}^t (M_L^2 + M_0^2)[\epsilon_{ij}(x)\varphi_i^m, u_j] + (M_L^1 + M_0^1)[\phi_{ij}(x)\varphi_i^m, u_j] d\tau$$

$$+ \sum_{j=1}^n \langle \epsilon_{ij}\varphi_{i_{xx}}^m + (2\epsilon_{ij} - \phi_{ij})\varphi_{i_x}^m + (\epsilon_{ij_{xx}} - \phi_{ij_x} + \lambda_{ij})\varphi_i^m, u_j \rangle_{\Omega,I}, i = 1, ..., n$$

$$(3.12)$$

Up to this part, the procedure is straightforward similar to [12], but it is worth noticing that to eliminate the part in brackets will imply to solve a coupled PDE with only 1 equation, making it an ill posed problem. In order to solve this, the idea is to generate more equations. Multiplying by k_i every Equation (3.12) and adding together every equation we have:

$$\sum_{i=1}^n k_i c_i^m(t) = \sum_{i=1}^n \sum_{j=1}^n k_i \int_{t-T}^t (M_L^2 + M_0^2)[\epsilon_{ij}(x)\varphi_i^m, u_j] + (M_L^1 + M_0^1)[\phi_{ij}(x)\varphi_i^m, u_j] d\tau$$

$$+ \sum_{i=1}^n k_i \langle \varphi_{i_t}^m, u_i \rangle_{\Omega,I} + \sum_{i=1}^n k_i \sum_{j=1}^n \langle \epsilon_{ij}\varphi_{i_{xx}}^m + (2\epsilon_{ij} - \phi_{ij})\varphi_{i_x}^m + (\epsilon_{ij_{xx}} + \phi_{ij_x} + \lambda_{ij})\varphi_i^m, u_j \rangle_{\Omega,I}$$

$$(3.13)$$

Putting k_i into the brackets and changing index i with j

$$\sum_{i=1}^n k_i c_i^m(t) = \sum_{i=1}^n \sum_{j=1}^n k_i \int_{t-T}^t (M_L^2 + M_0^2)[\epsilon_{ij}(x)\varphi_i^m, u_j] + (M_L^1 + M_0^1)[\phi_{ij}(x)\varphi_i^m, u_j] d\tau$$

$$+ \sum_{i=1}^n k_i \langle \varphi_{i_t}^m, u_i \rangle_{\Omega,I} + \sum_{i=1}^n \sum_{j=1}^n \langle k_j\epsilon_{ji}\varphi_{j_{xx}}^m + k_j(2\epsilon_{ji_x} - \phi_{ji})\varphi_{j_x}^m + k_j(\epsilon_{ji_{xx}} + \phi_{ji_x} + \lambda_{ji})\varphi_i^m, u_i \rangle_{\Omega,I}$$

$$(3.14)$$

Then interchanging the summations:

$$\sum_{i=1}^n k_i c_i^m(t) = \sum_{i=1}^n \sum_{j=1}^n k_i \int_{t-T}^t (M_L^2 + M_0^2)[\epsilon_{ij}(x)\varphi_i^m, u_j] + (M_L^1 + M_0^1)[\phi_{ij}(x)\varphi_i^m, u_j] d\tau$$

$$+ \sum_{i=1}^n \langle k_i\varphi_{i_{m_t}}^m + \sum_{j=1}^n (k_j\epsilon_{ji}\varphi_{j_{xx}}^m + k_j(2\epsilon_{ji} - \phi_{ji})\varphi_{j_x}^m + k_j(\epsilon_{ji_{xx}} + \phi_{ji_x} + \lambda_{ji})\varphi_i^m), u_i \rangle_{\Omega,I}$$

$$(3.15)$$

Finally dividing and multiplying by k_i the term in brackets, we have

$$\sum_{i=1}^n k_i c_i^m(t) = \sum_{i=1}^n \sum_{j=1}^n k_i \int_{t-T}^t (M_L^2 + M_0^2)[\epsilon_{ij}(x)\varphi_i^m, u_j] + (M_L^1 + M_0^1)[\phi_{ij}(x)\varphi_i^m, u_j] d\tau$$

$$+ \sum_{i=1}^n k_i \langle \varphi_{i_t}^m + \sum_{j=1}^n (\frac{k_j}{k_i}\epsilon_{ji}\varphi_{j_{xx}}^m + \frac{k_j}{k_i}(2\epsilon_{ji} - \phi_{ji})\varphi_{j_x}^m + \frac{k_j}{k_i}(\epsilon_{ji_{xx}} + \phi_{ji_x} + \lambda_{ji})\varphi_i^m), u_i \rangle_{\Omega,I}$$

$$(3.16)$$

For now, we will assume that the terms $M_L^2, M_0^2, M_L^1, M_0^1$ can be calculated with known terms. That will be demonstrated in the next section. In order to vanish the term in brackets and leaving the left part of Equation (3.16) only with known

terms, we have the following condition:

$$-\varphi_{i_t}^m = \sum_{j=1}^{n} \frac{k_j}{k_i} \epsilon_{ji} \varphi_{j_{xx}}^m + \sum_{j=1}^{n} \frac{k_j}{k_i} (2\epsilon_{ji} - \phi_{ji}) \varphi_{j_x}^m + \sum_{j=1}^{n} \frac{k_j}{k_i} (\epsilon_{ji_{xx}} + \phi_{ji_x}^m + \lambda_{ji}) \varphi_i^m, i = 1, \ldots, n$$

(3.17)

The following coupled PDE is implied for the determination of the modulating functions:

$$\begin{cases} -\varphi_t^m(x,t) = \bar{\Sigma}(x)\varphi_{xx}^m(x,t) + \bar{\Phi}(x)\varphi_x^m(x,t) + \bar{\Lambda}(x)\varphi^m(x,t) \\ \qquad\qquad \bar{\Sigma}(x) = \begin{bmatrix} \frac{k_1}{k_1}\epsilon_{11}(x) & \cdots & \frac{k_n}{k_1}\epsilon_{n1}(x) \\ \vdots & \ddots & \vdots \\ \frac{k_1}{k_n}\epsilon_{1n}(x) & \cdots & \frac{k_n}{k_n}\epsilon_{nn}(x) \end{bmatrix} \\ \quad \bar{\Phi}(x) = \begin{bmatrix} \frac{k_1}{k_1}(2\epsilon_{11_x} - \phi_{11})(x) & \cdots & \frac{k_n}{k_1}(2\epsilon_{n1_x} - \phi_{n1})(x) \\ \vdots & \ddots & \vdots \\ \frac{k_1}{k_n}(2\epsilon_{1n_x} - \phi_{1n})(x) & \cdots & \frac{k_n}{k_n}(2\epsilon_{nn_x} - \phi_{nn})(x) \end{bmatrix} \\ \bar{\Lambda}(x) = \begin{bmatrix} \frac{k_1}{k_1}(\epsilon_{11_{xx}} + \phi_{11_x} + \lambda_{11})(x) & \cdots & \frac{k_n}{k_1}(\epsilon_{n1_{xx}} + \phi_{n1_x} + \lambda_{n1})(x) \\ \vdots & \ddots & \vdots \\ \frac{k_1}{k_n}(\epsilon_{1n_{xx}} + \phi_{1n_x} + \lambda_{1n})(x) & \cdots & \frac{k_n}{k_n}(\epsilon_{nn_{xx}} + \phi_{nn_x} + \lambda_{nn})(x) \end{bmatrix} \end{cases}$$

(3.18)

With the initial and final condition given by Equation (3.9)

$$\varphi^m(x,0) = 0$$
$$\varphi^m(x,T) = v(x)\psi^m(x)$$

(3.19)

The boundary conditions are free at the moment, but the main problem is that the final condition needs to be met. For that reason, we add the following boundary condition:

$$\varphi^m(0,\tau) = \eta^m(\tau)$$

(3.20)

The main problem in this system is the negative sign in the spatial derivative implying a non-causal nature in the distributed dynamics. For that reason, we made a transformation to forward time:

$$\xi^m(x,\sigma) := \varphi^m(x, T - \sigma)$$

(3.21)

Resulting in the transformed auxiliary problem with an added boundary condition for the signal model control to fulfil the specifications

$$
\begin{cases}
\zeta_\sigma^m(x,\sigma) = \bar{\Sigma}(x)\zeta_{xx}^m(x,\sigma) + \bar{\Phi}(x)\zeta_x^m(x,\sigma) + \bar{\Lambda}(x)\zeta^m(x,\sigma) \\[2mm]
\bar{\Sigma}(x) = \begin{bmatrix} \frac{k_1}{k_1}\epsilon_{11}(x) & \dots & \frac{k_n}{k_1}\epsilon_{n1}(x) \\ \vdots & \ddots & \vdots \\ \frac{k_1}{k_n}\epsilon_{n1}(x) & \dots & \frac{k_n}{k_n}\epsilon_{nn}(x) \end{bmatrix} \\[6mm]
\bar{\Phi}(x) = \begin{bmatrix} \frac{k_1}{k_1}2\epsilon_{11_x} - \phi_{11}(x) & \dots & \frac{k_n}{k_1}2\epsilon_{1n_x} - \phi_{1n}(x) \\ \vdots & \ddots & \vdots \\ \frac{k_1}{k_n}2\epsilon_{n1_x} - \phi_{n1}(x) & \dots & \frac{k_n}{k_n}2\epsilon_{nn_x} - \phi_{nn}(x) \end{bmatrix} \\[6mm]
\bar{\Lambda}(x) = \begin{bmatrix} \frac{k_1}{k_1}\epsilon_{11_{xx}} + \phi_{11_x} + \lambda_{11}(x) & \dots & \frac{k_n}{k_1}\epsilon_{1n_{xx}} + \phi_{1n_x} + \lambda_{1n}(x) \\ \vdots & \ddots & \vdots \\ \frac{k_1}{k_n}\epsilon_{n1_{xx}} + \phi_{n1_x} + \lambda_{n1}(x) & \dots & \frac{k_n}{k_n}\epsilon_{nn_{xx}} + \phi_{nn_x} + \lambda_{nn}(x) \end{bmatrix} \\[4mm]
\zeta^m(x,0) = v(x)\psi^m(x) \\[1mm]
\zeta^m(x,T) = 0 \\[1mm]
\zeta^m(0,\sigma) = \tilde{\eta}^m(\sigma)
\end{cases} \tag{3.22}
$$

The specification: $\zeta^m(x,T) = 0$ is main reason of the added boundary condition for the auxiliary model. This specification implies that the auxiliary model has to stabilize in the time window T. If not, the approximation of the coefficient c^m will have an error introduced and in consequence, the estimation will have an error induced.

If Equation (3.22) holds true, then Equation (3.16) becomes:

$$
\sum_{i=1}^{n} k_i c_i^m(t) = \sum_{i=1}^{n}\sum_{j=1}^{n} k_i \int_{t-T}^{t} (M_L^2 + M_0^2)[\epsilon_{ij}(x)\varphi_i^m, u_j] + (M_L^1 + M_0^1)[\phi_{ij}(x)\varphi_i^m, u_j] d\tau
$$
$$\tag{3.23}$$

In order to determine each one of c_i^m, we can form other $(n-1)$ more equations similar to Equation (3.23), with different k_i to form a system of n equations that have the following form: And if Equation (3.16) holds true for every one of these equations, then:

$$
\sum_{i=1}^{n} k_{hi} c_i^m(t) = \sum_{i=1}^{n}\sum_{j=1}^{n} k_{hi} \int_{t-T}^{t} (M_L^2 + M_0^2)[\epsilon_{ij}(x)\varphi_i^m, u_j] + (M_L^1 + M_0^1)[\phi_{ij}(x)\varphi_i^m, u_j] d\tau
$$
$$h = 1,\dots,n$$
$$\tag{3.24}$$

If the function basis approximation order is N, then we will have $N+1$ systems with the form of Equation (3.22). In total, it will make $n(N+1)$ auxiliary systems to solve and $n(N+1)^2$ modulating functions in total. It is also worth noticing, that after solving Equation (3.22), an inverse transformation in time has to be made in order

to obtain the modulation functions. This transformation has the following form:

$$\varphi^m(x, \sigma) := \xi^m(x, T - \sigma) \tag{3.25}$$

The main idea for the procedure is to use a different modulating function for every equation of the system. Then to overcome the coupling that exists int the system, we add together all the equations to get the coupling into the modulating function equation. Finally we can construct more coupled systems adding together the equations but with different constants.

3.3   Calculation of the Modulation Operators

Now we will proceed to demonstrate that M_L^2, M_L^1, M_0^2 and M_0^1 can be calculated with known terms. Without loss of generality, we will assume $x^* = 0$. We have the following system of equations:

$$P_1 U_x(0, t) + P_0 U(0, t) = F(t)$$
$$R_1 U_x(0, t) + R_0 U(0, t) = Y(t)$$

If P_1 and R_1 or P_0 and R_0 are linearly independent , then $U(0, t)$ and $U_x(0, t)$ can be determined:

$$\begin{bmatrix} U_x(0, t) \\ U(0, t) \end{bmatrix} = \begin{bmatrix} P_1 & P_0 \\ R_1 & R_0 \end{bmatrix}^{-1} \begin{bmatrix} F(t) \\ Y(t) \end{bmatrix} \tag{3.26}$$

With also knowledge of the Modulation Function φ, then M_0^2 and M_0^1 can be known and calculated.

$$\sum_{i=1}^{n} \sum_{j=1}^{n} k_{hi} \int_{t-T}^{t} (M_0^2[\epsilon_{ij}(x)\varphi_{hi}^m, u_j] + M_0^1[\phi_{ij}(x)\varphi_{hi}^m, u_j)])d\tau =$$

$$\sum_{i=1}^{n} \sum_{j=1}^{n} k_{hi} \int_{t-T}^{t} (-(\epsilon_{ij}\varphi_{hi}^m)(0, \tau - t + T)u_{j_x}(0, \tau) \tag{3.27}$$

$$+ ((\epsilon_{ij}\varphi_{hi}^m)_x - \phi_{ij}\varphi_{hi}^m)(0, \tau - t + T)u_j(0, \tau))d\tau$$

Putting the equation in a vectorial form:

$$= \int_{t-T}^{t} \begin{bmatrix} -\tilde{\Sigma}_h(0, \tau - t + T) & (\tilde{\Sigma}_{h_x} - \tilde{\Phi}_h)(0, \tau - t + T) \end{bmatrix} \begin{bmatrix} U_x(0, \tau) \\ U(0, \tau) \end{bmatrix} d\tau \tag{3.28}$$

Where:

$$\tilde{\Sigma}_h(x, t) = \{k_{hi}(\varphi_{hi}\epsilon_{ij})(x, t)\}_{1 \le i, j \le n}$$
$$\tilde{\Phi}_h(x, t) = \{k_{hi}(\phi_{ij}\varphi_{hi})(x, t)\}_{1 \le i, j \le n} \tag{3.29}$$

Using the relation in Equation (3.26), we have:

$$= \int_{t-T}^{t} \begin{bmatrix} -\tilde{\Sigma}_h(0, \tau - t + T) & (\tilde{\Sigma}_{h_x} - \tilde{\Phi}_h)(0, \tau - t + T) \end{bmatrix} \begin{bmatrix} P_1 & P_0 \\ R_1 & R_0 \end{bmatrix}^{-1} \begin{bmatrix} F(\tau) \\ Y(\tau) \end{bmatrix} d\tau \tag{3.30}$$

Now for M_L^2, M_L^1, we can rewrite the equation similarly:

$$\sum_{i=1}^{n} \sum_{j=1}^{n} k_{hi} \int_{t-T}^{t} (M_L^2[\epsilon_{ij}(x)\varphi_{hi}^m, u_j] + M_L^1[\phi_{ij}(x)\varphi_{hi}^m, u_j]) d\tau$$

$$= \sum_{i=1}^{n} \sum_{j=1}^{n} k_{hi} \int_{t-T}^{t} ((\epsilon_{ij}\varphi_{hi}^m)(L)u_{j_x}(L) - ((\epsilon_{ij}\varphi_{hi}^m)_x + \phi_{ij}\varphi_{hi}^m)(L)u_j(L)) d\tau \tag{3.31}$$

$$= \int_{t-T}^{t} (\tilde{\Sigma}_h(L)U_x(L) - (\tilde{\Sigma}_{h_x}(L) + \tilde{\Phi}_h(L))U(L)) d\tau$$

From here, we can use the relation from Equation (4.7) to only use known terms.

- If Q_1 is invertible, then $U_x(L,t) = Q_1^{-1}(G(t) - Q_0 U(L,t))$

$$\sum_{i=1}^{n} \sum_{j=1}^{n} k_{hi} \int_{t-T}^{t} [M_L^2(\epsilon_{ij}(x)\varphi_{hi}^m, u_j] + M_L^1[\phi_{ij}(x)\varphi_{hi}^m, u_j]] d\tau$$

$$= \int_{t-T}^{t} (\tilde{\Sigma}_h(L)Q_1^{-1}G - ((\tilde{\Sigma}_{h_x} + \tilde{\Phi}_h)(L) + \tilde{\Sigma}_h(L)Q_1^{-1}Q_0)U(L)) d\tau \tag{3.32}$$

And imposing

$$(\tilde{\Sigma}_{h_x} + \tilde{\Phi}_h)(L, \tau - t + T) + \tilde{\Sigma}_h(L, \tau - t + T)Q_1^{-1}Q_0 = 0 \tag{3.33}$$

Then we have:

$$\sum_{i=1}^{n} \sum_{j=1}^{n} k_{hi} \int_{t-T}^{t} (M_L^2[\epsilon_{ij}(x)\varphi_{hi}^m, u_j] + M_L^1[\phi_{ij}(x)\varphi_{hi}^m, u_j]) d\tau$$

$$= \int_{t-T}^{t} (\tilde{\Sigma}_h(L, \tau - t + T)Q_1^{-1}G(\tau)) d\tau \tag{3.34}$$

Finally in addition with Equation (3.30):

$$\sum_{i=1}^{n} \sum_{j=1}^{n} k_{hi} \int_{t-T}^{t} (M_L^2 + M_L^1)[\epsilon_{ij}(x)\varphi_{hi}^m, u_j] + (M_0^2 + M_0^1)[\phi_{ij}(x)\varphi_{hi}^m, u_j]] d\tau$$

$$= \int_{t-T}^{t} \begin{bmatrix} -\tilde{\Sigma}_h(0, \tau - t + T) & (\tilde{\Sigma}_{h_x} - \tilde{\Phi}_h)(0, \tau - t + T) \end{bmatrix} \begin{bmatrix} P_1 & P_0 \\ R_1 & R_0 \end{bmatrix}^{-1} \begin{bmatrix} F(\tau) \\ Y(\tau) \end{bmatrix} d\tau$$

$$+ \int_{t-T}^{t} (\tilde{\Sigma}_h(L, \tau - t + T)Q_1^{-1}G(\tau)) d\tau \tag{3.35}$$

- If Q_0 is invertible, then $U(L,t) = Q_0^{-1}(G(t) - Q_1 U_x(L,t))$

$$\sum_{i=1}^{n}\sum_{j=1}^{n} k_{hi} \int_{t-T}^{t} M_L^2[\epsilon_{ij}(x)\varphi_{hi]^m,u_j} + M_L^1[\phi_{ij}(x)\varphi_{hi}^m, u_j]d\tau$$

$$= \int_{t-T}^{t}((\tilde{\Sigma}_h(L) + (\tilde{\Sigma}_{h_x} + \tilde{\Phi}_h)(L)Q_0^{-1}Q_1)U_x(L) - ((\tilde{\Sigma}_{h_x} + \tilde{\Phi}_h)(L)Q_0^{-1}G))d\tau \tag{3.36}$$

And imposing

$$\tilde{\Sigma}_h(L, \tau - t + T) + (\tilde{\Sigma}_{h_x} + \tilde{\Phi}_h)(L, \tau - t + T)Q_0^{-1}Q_1 = 0 \tag{3.37}$$

Then we have:

$$\sum_{i=1}^{n}\sum_{j=1}^{n} k_{hi} \int_{t-T}^{t} (M_L^2[\epsilon_{ij}(x)\varphi_{hi}^m, u_j] + M_L^1[\phi_{ij}(x)\varphi_{hi}^m, u_j])d\tau$$

$$= - \int_{t-T}^{t}((\tilde{\Sigma}_{h_x} + \tilde{\Phi}_h)(L, \tau - t + T)Q_0^{-1}G(\tau))d\tau \tag{3.38}$$

Finally in addition with Equation (3.30):

$$\sum_{i=1}^{n}\sum_{j=1}^{n} k_{hi} \int_{t-T}^{t} (M_L^2 + M_L^1)[\epsilon_{ij}(x)\varphi_{hi}^m, u_j] + (M_0^2 + M_0^1)[\phi_{ij}(x)\varphi_{hi^m}, u_j)]d\tau$$

$$= \int_{t-T}^{t}\left[-\tilde{\Sigma}_h(0, \tau - t + T) \quad (\tilde{\Sigma}_{h_x} - \tilde{\Phi}_h)(0, \tau - t + T)\right]\begin{bmatrix} P_1 & P_0 \\ R_1 & R_0 \end{bmatrix}^{-1}\begin{bmatrix} F(\tau) \\ Y(\tau) \end{bmatrix}d\tau$$

$$- \int_{t-T}^{t}((\tilde{\Sigma}_{h_x} + \tilde{\Phi}_h)(L, \tau - t + T)Q_0^{-1}G(\tau))d\tau \tag{3.39}$$

We can see here that in both of the cases, we can express M_L^2, M_L^1, M_0^2 and M_0^1 in the known terms from the problem statement and also with the modulation functions obtained from the auxiliary models. Also it is worth noticing that Equation (3.33) and (3.37) adds a boundary condition to the auxiliary systems.

3.4   Reconstruction of the states

For the reconstruction of the states, we will have to ensure first that the auxiliary systems requirements are fulfilled. Once we solved the auxiliary system problem, after an inverse time transformation with the Equation (3.25) then we will have as outcome the modulating functions φ_{ij}^m for $1 \leq i, j \leq n$ and $0 \leq m \leq N$. Then we can rewrote Equation (3.24) in a linear system of equations form:

$$K \begin{bmatrix} c_1^m(t) \\ \vdots \\ c_n^m(t) \end{bmatrix} = \mathcal{M}_m(t) \tag{3.40}$$

Where:

$$\mathcal{M}_m(t) = \begin{bmatrix} \sum_{i=1}^{n} \sum_{j=1}^{n} k_{1i} \int_{t-T}^{t} (M_L^2 + M_L^1)[\epsilon_{ij}(x)\varphi_{1i}^m, u_j] + (M_0^2 + M_0^1)[\phi_{ij}(x)\varphi_{1i}^m, u_j)]d\tau \\ \vdots \\ \sum_{i=1}^{n} \sum_{j=1}^{n} k_{ni} \int_{t-T}^{t} (M_L^2 + M_L^1)[\epsilon_{ij}(x)\varphi_{ni}^m, u_j] + (M_0^2 + M_0^1)[\phi_{ij}(x)\varphi_{ni}^m, u_j)]d\tau \end{bmatrix}$$
(3.41)

and using:

$$K = \begin{bmatrix} k_{11} & \dots & k_{1n} \\ \vdots & \ddots & \vdots \\ k_{n1} & \dots & k_{nn} \end{bmatrix}, C(t) = \begin{bmatrix} C_0(t) & \dots & C_N(t) \end{bmatrix} = \begin{bmatrix} c_{1_0}(t) & \dots & c_{1_N}(t) \\ \vdots & \ddots & \vdots \\ c_{n_0}(t) & \dots & c_{n_N}(t) \end{bmatrix}$$
(3.42)

If K is invertible or non-singular, then we can have the coefficients uncoupled:

$$C(t) = K^{-1} \begin{bmatrix} \mathcal{M}_0(t) & \dots & \mathcal{M}_N(t) \end{bmatrix}$$
(3.43)

With these coefficients we can reconstruct the state using the function expansion representation showed in Chapter 2:

$$U(x,t) = \begin{bmatrix} \sum_{k=0}^{\infty} c_1^k(t)\psi^k(x) \\ \vdots \\ \sum_{k=0}^{\infty} c_n^k(t)\psi^k(x) \end{bmatrix} \approx \begin{bmatrix} \sum_{k=0}^{N} c_1^k(t)\psi^k(x) \\ \vdots \\ \sum_{k=0}^{N} c_n^k(t)\psi^k(x) \end{bmatrix} = C(t)\Psi(x)$$
(3.44)

With this expression we can reconstruct the state and solve the problem of the state estimation.

It can be observed that for the reconstruction of the state we require first the calculation of the coefficients of the basis expansion. This calculation notated in Equation (3.43) depends on the matrix K and $\mathcal{M}_m$

3.5 Implementation

For the implementation of the method, we can divide the procedure in two parts: Offline and online, because there are some steps in the procedure that do not need to be iterated. The offline part starts with the calculation of the orthonormal basis of functions. This step is done using the Gram-Schmidt procedure described in Chapter 2 and it will require to specify the approximation order N beforehand, a function basis and a weight function $v(x)$. The outcome of the Gram-Schmidt procedure will be the elements of the orthonormal basis $\Psi(x) = [\psi^0(x), ..., \psi^N(x)]$. After the orthonormal basis calculation, the auxiliary models can be solved since now the boundary conditions of the models are defined. This solution will require the design of a boundary control in order to fulfil the constraints on the modulating functions. All of these steps can be made offline since there is no update to be done.

The next steps are from the online part, illustrated in Figure 3.1. After the calculation of the modulating functions, with every time step the measuring of the system has to be done. With the modulating functions, measurement and inputs of the system, the modulation kernels can be calculated and therefore the modulation kernel vector. Then, the decoupling of the coefficients can be made with Equation (3.43) and finally the reconstruction of the states can be done with Equation (3.44). The procedure can be resumed in the following steps:

- Offline part

    1. Define parameters for orthonormal basis calculation:
       Approximation order N, Function Basis, Weight function $v(x)$
    2. Gram-Schmidt procedure to obtain the Orthonormal Basis $\Psi(x) = [\psi^0(x), ..., \psi^N(x)]$
    3. Create and solve auxiliary models with initial condition $v(x)\Psi(x)$ and control scheme η to achieve $\xi(x, T) = 0$. Solution will be $\xi(x, \sigma)$
    4. Inverse time transformation (3.21) to obtain modulating functions $\varphi(x, t)$

- Online part

    1. Measurement of the system
    2. Calculation of the modulation kernels
    3. Decoupling of the coefficients with (3.43)
    4. Calculation of the states with (3.44)

The most heavy computational part in the whole process is the solution of the auxiliary models since it is a coupled PDE solution , but the main advantage is that it can be made offline, therefore there is no burden onto the online computation. In the online part, the decoupling and calculation of the states are matrix multiplication without further complications and also the matrices K^{-1} and $\Psi(x)$ can be calculated offline and there is no need for an actualization in the online section. The modulation part implies a numerical integration that it is the more heavy computational part in the online part. This integration can be done with numerical methods such as the trapezoidal rule or Newton-Cotes formulas for further improvement.

The present chapter has explained the application of the modulating function method for the state estimation of n-Coupled Reaction-Advection-Diffusion PDE. Using the theoretical framework from the last chapter, the method implementation is not complicated and as explained in the last subsection, the separation into offline and online parts makes the implementation easier.
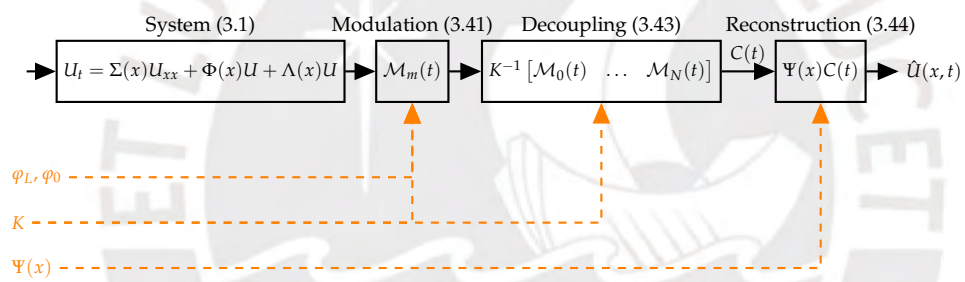
FIGURE 3.1: Diagram of the online implementation part

Chapter 4

Comparative Simulations

This chapter presents simulations that show the performance of the observer developed in the last chapter for three different type of systems in order to demonstrate the feasibility of the use of the modulation function observer. The first one is a stable Coupled Reaction Diffusion PDE that represents a linearised Chemical Tubular Reactor for which a backstepping observer has also been developed. Here, the effect of the different parameters such as the time window T, time sample T_s and control strategy are explored; furthermore, the performance of the observer with noise in the measurement is tested. Additionally, a comparison with the aforementioned backstepping observer is done. The second system is an unstable Coupled Reaction Diffusion PDE, which is used to demonstrate the performance of the observer on an unstable system and also the same parameters are explored. Finally, a coupled Reaction Diffusion PDE with spatially varying coefficients is used to showcase the use of the observer for such systems and its performance.

4.1 Stable 2-Coupled Reaction-Diffusion PDE

4.1.1 Problem Definition

In order to exemplify the use and efficiency of the method, a linearized Chemical Tubular Reactor model is used for the simulation. The coupled temperature-concentration system of Chemical Tubular Reactors is given by [4]:

$$
\begin{aligned}
u_{1_t}(x,t) &= D_1 u_{1_{xx}}(x,t) + k_0 \delta (1 - u_2(x,t))e^{-\frac{\mu}{1+u_1(x,t)}} \\
u_{2_t}(x,t) &= D_2 u_{2_{xx}}(x,t) + k_0 (1 - u_2(x,t))e^{-\frac{\mu}{1+u_1(x,t)}} \\
u_{1_x}(0,t) &= 0 \\
u_{2_x}(0,t) &= 0 \\
u_1(1,t) &= u_{1_c}(t) \\
u_2(1,t) &= u_{2_c}(t)
\end{aligned}
\tag{4.1}
$$

with the physical parameters:

$$
D_1 = 0.14, D_2 = 0.16, k_0 = 2.426x10^7, \delta = 0.5, \mu = 20. \tag{4.2}
$$

The system is linearized around u_1^s and u_2^s, which are the steady-state variables and by setting $v_i(x,t) = u_i(x,t) - u_i^s(x)$ the steady state can be obtained as follows:

$$v_{1_t}(x,t) = D_1 v_{1_{xx}}(x,t) + a_{11}v_1(x,t) + a_{12}(x)v_2(x,t)$$
$$v_{2_t}(x,t) = D_2 v_{2_{xx}}(x,t) + a_{21}v_1(x,t) + a_{22}(x)v_2(x,t)$$

(4.3)

where:

$$a_{11}(x) = k_0\delta \frac{1 - u_2^s(x)}{(1 + u_1^s(x))^2}e^{-\frac{\mu}{1+u_1^s(x)}}$$

$$a_{21}(x) = \frac{1}{\delta}a_{11}(x)$$

$$a_{12}(x) = -k_0\delta u_2^s(x)e^{-\frac{\mu}{1+u_1^s(x)}}$$

$$a_{22}(x) = \frac{1}{\delta}a_{12}(x).$$

(4.4)

Finally, by taking the average values of the coefficients $a_{ij}(x)$, the following linear 2-Coupled Reaction-Diffusion PDE is obtained:

$$\begin{cases} U = \Sigma U_{xx} + \Lambda U \\ \Sigma = \begin{bmatrix} 0.14 & 0 \\ 0 & 0.16 \end{bmatrix}, \Lambda = \begin{bmatrix} -0.065 & -0.146 \\ -0.130 & -0.293 \end{bmatrix} \\ U(x,t) = \begin{bmatrix} u_1(x,t) & u_2(x,t) \end{bmatrix}^T \end{cases}$$

(4.5)

with a Neumann boundary condition:

$$U_x(0,t) = 0$$

(4.6)

a known actuation at the boundary:

$$U(L,t) = G(t)$$

(4.7)

and a measurement at the boundary

$$Y(t) = U_x(L,t).$$

(4.8)

The problem is to estimate the state $U(x,t)$ based on the knowledge of the actuation $G(t)$ and the measurement $Y(t)$.

4.1.2 Solution of the problem

For the solution of this problem the same argument explored in the Chapter 3 is used, but with $x^* = L$. In this case, the auxiliary systems are similar to Equation

(3.22):

$$
\begin{cases}
\xi_\sigma^m(x,\sigma) = \bar{\Sigma}\xi_{xx}^m(x,\sigma) + \bar{\Lambda}\xi^m(x,\sigma) \\[2mm]
\qquad \bar{\Sigma} = \begin{bmatrix} \frac{k_1}{k_1}\epsilon_{11} & \frac{k_2}{k_1}\epsilon_{21} \\ \frac{k_1}{k_2}\epsilon_{21} & \frac{k_2}{k_2}\epsilon_{22} \end{bmatrix} = \begin{bmatrix} \epsilon_{11} & 0 \\ 0 & \epsilon_{22} \end{bmatrix} \\[4mm]
\qquad \bar{\Lambda} = \begin{bmatrix} \frac{k_1}{k_1}(\epsilon_{11_{xx}} + \lambda_{11}) & \frac{k_2}{k_1}(\epsilon_{12_{xx}} + \lambda_{12}) \\ \frac{k_1}{k_2}(\epsilon_{21_{xx}} + \lambda_{21}) & \frac{k_2}{k_2}(\epsilon_{22_{xx}} + \lambda_{22}) \end{bmatrix} = \begin{bmatrix} \lambda_{11} & \frac{k_2}{k_1}\lambda_{12} \\ \frac{k_1}{k_2}\lambda_{21} & \lambda_{22} \end{bmatrix} \\[4mm]
\xi^m(x,0) = v(x)\psi^m(x) \\[1mm]
\xi^m(x,T) = 0 \\[1mm]
\xi^m(0,\sigma) = \eta^m(\sigma)
\end{cases}
\tag{4.9}
$$

For the present problem since $x^* = L$, the modulation kernel can be reformulated as:

$$
\sum_{i=1}^{n}\sum_{j=1}^{n} k_{hi} \int_{t-T}^{t} (M_L^2 + M_0^2)[\epsilon_{ij}(x)\varphi_{hi}^m, u_j] + (M_L^1 + M_0^1)[\phi_{ij}(x)\varphi_{hi}^m, u_j]d\tau
$$

$$
= \int_{t-T}^{t} \begin{bmatrix} -\tilde{\Sigma}_h(0,\tau - t + T) & (\tilde{\Sigma}_{h_x} - \tilde{\Phi}_h)(0,\tau - t + T) \end{bmatrix} \begin{bmatrix} U_x(0,\tau) \\ U(0,\tau) \end{bmatrix} d\tau \tag{4.10}
$$

$$
+ \int_{t-T}^{t} \begin{bmatrix} \tilde{\Sigma}_h(L,\tau - t + T) & -(\tilde{\Sigma}_{h_x} + \tilde{\Phi}_h)(L,\tau - t + T) \end{bmatrix} \begin{bmatrix} U_x(L,\tau) \\ U(L,\tau) \end{bmatrix} d\tau
$$

and using the problem conditions from Equation (4.6), (4.7) and (4.8):

$$
\sum_{i=1}^{n}\sum_{j=1}^{n} k_{hi} \int_{t-T}^{t} (M_L^2 + M_0^2)[\epsilon_{ij}(x)\varphi_{hi}^m, u_j] + (M_L^1 + M_0^1)[\phi_{ij}(x)\varphi_{hi}^m, u_j]d\tau
$$

$$
= \int_{t-T}^{t} \begin{bmatrix} -\tilde{\Sigma}_h(0,\tau - t + T) & \tilde{\Sigma}_{h_x}(0,\tau - t + T) \end{bmatrix} \begin{bmatrix} 0 \\ U(0,\tau) \end{bmatrix} d\tau \tag{4.11}
$$

$$
+ \int_{t-T}^{t} \begin{bmatrix} \tilde{\Sigma}_h(L,\tau - t + T) & -\tilde{\Sigma}_{h_x}(L,\tau - t + T) \end{bmatrix} \begin{bmatrix} Y(\tau) \\ G(\tau) \end{bmatrix} d\tau.
$$

If we impose the following boundary condition on the modulation functions:

$$
\varphi_{hi_x}^m(0,t) = 0, 1 \leq (h,i) \leq 2 \tag{4.12}
$$

Then $\tilde{\Sigma}_{h_x} = 0$ is valid, and consequently the modulation kernel can be reduced to:

$$
\sum_{i=1}^{n}\sum_{j=1}^{n} k_{hi} \int_{t-T}^{t} (M_L^2 + M_0^2)[\epsilon_{ij}(x)\varphi_{hi}^m, u_j] + (M_L^1 + M_0^1)[\phi_{ij}(x)\varphi_{hi}^m, u_j]d\tau
$$

$$
= \int_{t-T}^{t} \begin{bmatrix} \tilde{\Sigma}_h(L,\tau - t + T) & -\tilde{\Sigma}_{h_x}(L,\tau - t + T) \end{bmatrix} \begin{bmatrix} Y(\tau) \\ G(\tau) \end{bmatrix} d\tau. \tag{4.13}
$$

Using the added boundary condition in Equation (4.12), the auxiliary system from Equation (4.9) becomes:

$$
\begin{cases}
\xi_\sigma^m(x,\sigma) = \bar{\Sigma}\xi_{xx}^m(x,\sigma) + \bar{\Lambda}\xi^m(x,\sigma) \\[6pt]
\qquad \bar{\Sigma} = \begin{bmatrix} \epsilon_{11} & 0 \\ 0 & \epsilon_{22} \end{bmatrix}, \bar{\Lambda} = \begin{bmatrix} \lambda_{11} & \frac{k_2}{k_1}\lambda_{12} \\ \frac{k_1}{k_2}\lambda_{21} & \lambda_{22} \end{bmatrix} \\[10pt]
\xi^m(x,0) = v(x)\psi^m(x) \\[4pt]
\xi_x^m(0,\sigma) = 0 \\[4pt]
\xi^m(L,\sigma) = \eta^m(\sigma) \\[4pt]
\xi^m(x,T) = 0
\end{cases}
\tag{4.14}
$$

If Equation (4.14) is fulfilled and the backwards time transformation from Equation (3.25) is applied, then the modulation functions φ_{hi_m} can be obtained and therefore $\tilde{\Sigma}_h$ and $\tilde{\Sigma}_{h_x}$. Finally, the coefficients uncoupled can be obtained in a similar form to Equation (3.43):

$$
C(t) = K^{-1}\begin{bmatrix} \mathcal{M}_0(t) & \dots & \mathcal{M}_N(t) \end{bmatrix}
\tag{4.15}
$$

where:

$$
\mathcal{M}_m(t) = \begin{bmatrix} \int_{t-T}^t \begin{bmatrix} \tilde{\Sigma}_1(L,\tau-t+T) & -\tilde{\Sigma}_{1_x}(L,\tau-t+T) \end{bmatrix} \begin{bmatrix} Y(\tau) \\ G(\tau) \end{bmatrix} d\tau \\ \vdots \\ \int_{t-T}^t \begin{bmatrix} \tilde{\Sigma}_n(L,\tau-t+T) & -\tilde{\Sigma}_{n_x}(L,\tau-t+T) \end{bmatrix} \begin{bmatrix} Y(\tau) \\ G(\tau) \end{bmatrix} d\tau \end{bmatrix}
\tag{4.16}
$$

With these coefficients we can reconstruct the state using the function expansion representation showed in Chapter 3 with Equation (3.44):

$$
U(x,t) \approx C(t)\Psi(x)
\tag{4.17}
$$

The whole procedure is straightforward similar to the one presented in Chapter 3. Finally, the state can be reconstructed using the coefficients, that are obtained with the modulation operators that are the result of a integration that needs only the modulation functions obtained from the auxiliary systems in Equation (4.14), the actuation $G(t)$ and the measurement $Y(t)$ solving the problem stated.

4.1.3 Simulations

After the solution of the problem, explained in the last subchapter, a simulation of the problem with different scenarios regarding to the boundary conditions and noise presence are explored and also compared to the observer presented in [29]. The programming and graphical representations have been developed in MATLAB®.

Preliminaries

This part is devoted to explain the offline procedure realized for the state estimation of the process described. In the following, the simulations and plots for the system have been done using the following actuation and initial condition, similar to [29] in order to keep the comparison fair:

$$U(1,t) = G(t) = \begin{bmatrix} 5\sin(t) \\ 10\sin(2t) \end{bmatrix}$$

$$U(x,0) = \begin{bmatrix} \sin(\pi x) + \sin(3\pi x) \\ \sin(\pi x) + \sin(3\pi x) \end{bmatrix} \tag{4.18}$$

The first step is to determine the function basis and order to work with. For this case, a polynomial basis $\{1, x, \ldots, x^N\}$ and the weight function $v(x) = x(L - x)^2$ are used in the Gram-Schmidt procedure to obtain the orthonormal basis. Although a higher basis order naturally will lead to a better approximation, there is an inconvenience with this choice. The exactitude of the basis expansion approximation is not always better as the order increases if the step size in the dimension x does not increase also. With a higher order basis, the higher order terms tend to have a faster dynamic at the boundaries and in consequence, the numerical integration done for the coefficients calculation is less accurate. An illustration of this phenomena is shown in the Figure 4.1 where using a step size X_S of 2×10^{-2} in x, the best performing basis order is $N = 5$, and increasing the basis order results in a worse approximation; although, using a smaller step size of 10^{-3} in x, the best performing basis order is $N = 16$ with a smaller error on the projection. This shows that for a better approximation, a smaller step size has to be chosen in order to select a higher basis order.

After the selection of the orthonormal basis for the approximation, the terms $v(x)\psi_m(x)$ can be calculated in order to create and solve the auxiliary models described in Equation (3.22). For this purpose we select the following matrix K:

$$K = \begin{bmatrix} 1 & 1 \\ 1 & -1 \end{bmatrix}. \tag{4.19}$$

It is worth noticing that another value of K can be chosen, but every element cannot be zero to avoid indetermination in Equation (3.22) and the matrix must be invertible in order to make possible the decoupling from Equation (3.43). The other choice that has to be done is the control $\tilde{\eta}_m(\sigma)$ from Equation (3.22) in order to stabilize the system in the time window T and fulfill the condition $\xi(x, T) = 0$. In order to demonstrate the effect of this variable, three cases are considered: No control, a more aggressive control(Control 1 called Cont1) and a more conservative control(Control 2 called Cont2). For this, the backstepping control explained in the Chapter 2 and defined by Equation (2.23) is used with different $\tilde{k}$ values. The plot of the modulating functions is shown in Figure 4.4, and their L_2-norm in the 4.5. It can be seen that

(A) ISE of u_1 with $X_s = 2 \times 10^{-2}$

(B) ISE of u_2 with $X_s = 2 \times 10^{-2}$

(C) ISE of u_1 with $X_s = 10^{-3}$
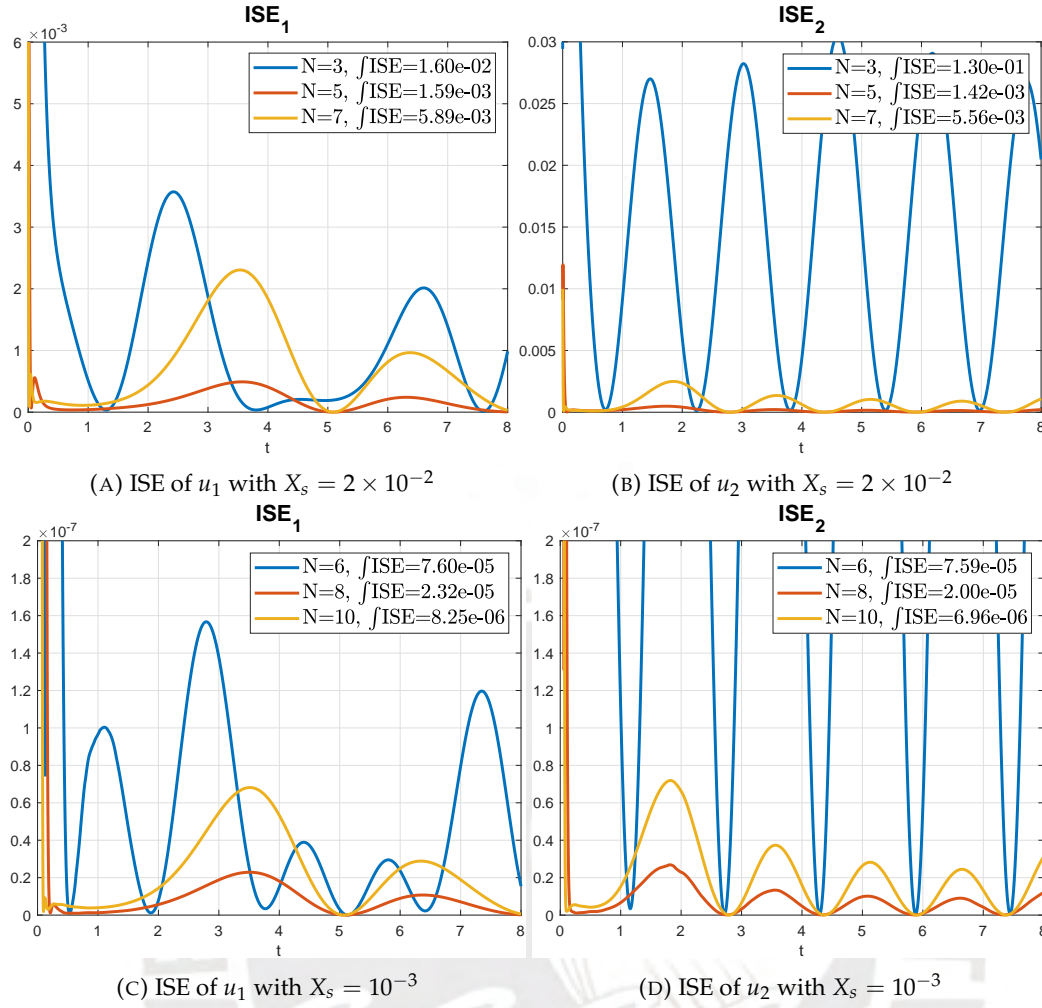
(D) ISE of u_2 with $X_s = 10^{-3}$

FIGURE 4.1: Projection errors for different function expansion order

in both cases the control strategies make possible a faster stabilization of every modulation function as Table 4.1 shows, where a reduction on the L_2-norm of the modulation functions exists with the ones obtained with control strategies in comparison to the modulation functions obtained without a control strategy. On the other hand, it is worth noticing that the modulation functions constructed with a signal model controller have faster dynamics, especially if the control is more aggressive as in the comparison can be seen where the MF obtained with Cont1 is much oscillating than the MF obtained with Cont2. This is important for the modulation kernel calculation, since the dynamics of the modulation function have an impact on the precision of the numeric integration and thus, on the state estimation.

Simulation Scenarios

The first comparison to be explored is the use of different control strategies for the signal model control on the auxiliary systems solution from Equation (3.22). For the present example, three different control strategies are used, the same ones used in the last subsection. For the specifications of the simulation, a time grid resolution of
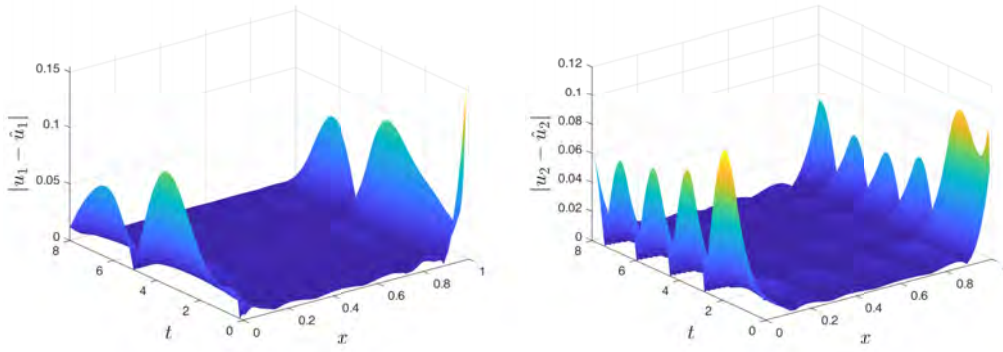
FIGURE 4.2: Absolute error of the basis expansion for $N = 5$ and $X_s = 2 \times 10^{-2}$
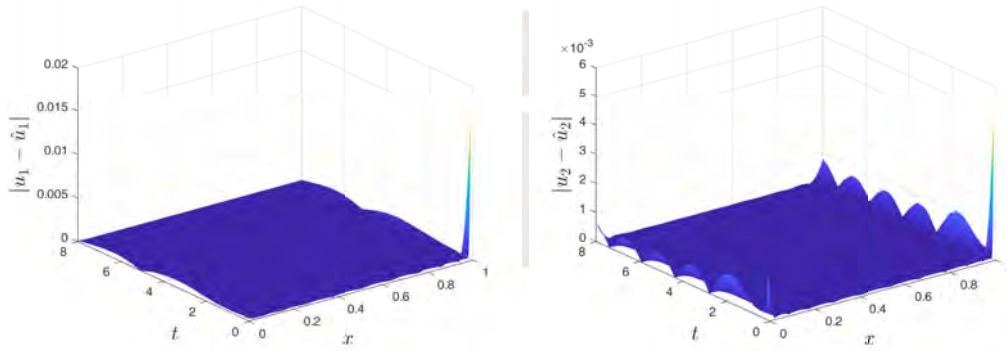

FIGURE 4.3: Absolute error of the basis expansion for $N = 8$ and $X_s = 10^{-3}$

MF	Original	Control 1	Control 2
$log_{10}\|\|\varphi_{11}^{0}(x,T)\|\|$	-2.64	-7.82	-5.92
$log_{10}\|\|\varphi_{12}^{0}(x,T)\|\|$	-5.30	-9.82	-8.24
$log_{10}\|\|\varphi_{21}^{0}(x,T)\|\|$	-2.11	-7.44	-5.49
$log_{10}\|\|\varphi_{21}^{0}(x,T)\|\|$	-2.66	-8.41	-6.30
$log_{10}\|\|\varphi_{11}^{1}(x,T)\|\|$	-3.89	-9.44	-7.25
$log_{10}\|\|\varphi_{12}^{1}(x,T)\|\|$	-6.54	-11.34	-9.40
$log_{10}\|\|\varphi_{21}^{1}(x,T)\|\|$	-3.34	-9.09	-6.85
$log_{10}\|\|\varphi_{21}^{1}(x,T)\|\|$	-3.89	-10.14	-7.74
$log_{10}\|\|\varphi_{11}^{2}(x,T)\|\|$	-5.16	-10.48	-8.92
$log_{10}\|\|\varphi_{12}^{2}(x,T)\|\|$	-6.82	-12.41	-11.09
$log_{10}\|\|\varphi_{21}^{2}(x,T)\|\|$	-9.49	-10.13	-8.52
$log_{10}\|\|\varphi_{21}^{2}(x,T)\|\|$	-6.31	-11.17	-9.39

TABLE 4.1: L_2-norms of the modulating function at the end of the time window

$T_s = 10^{-3}$ has been used and a space grid resolution $X_s = 2 \times 10^{-2}$ with a horizon time window $T = 4$. The results are illustrated in Figure 4.6.

As distinguished in the figure, the error can be analyzed in 2 sections, before and after the time window T. In the plots before the time window, it can be seen that
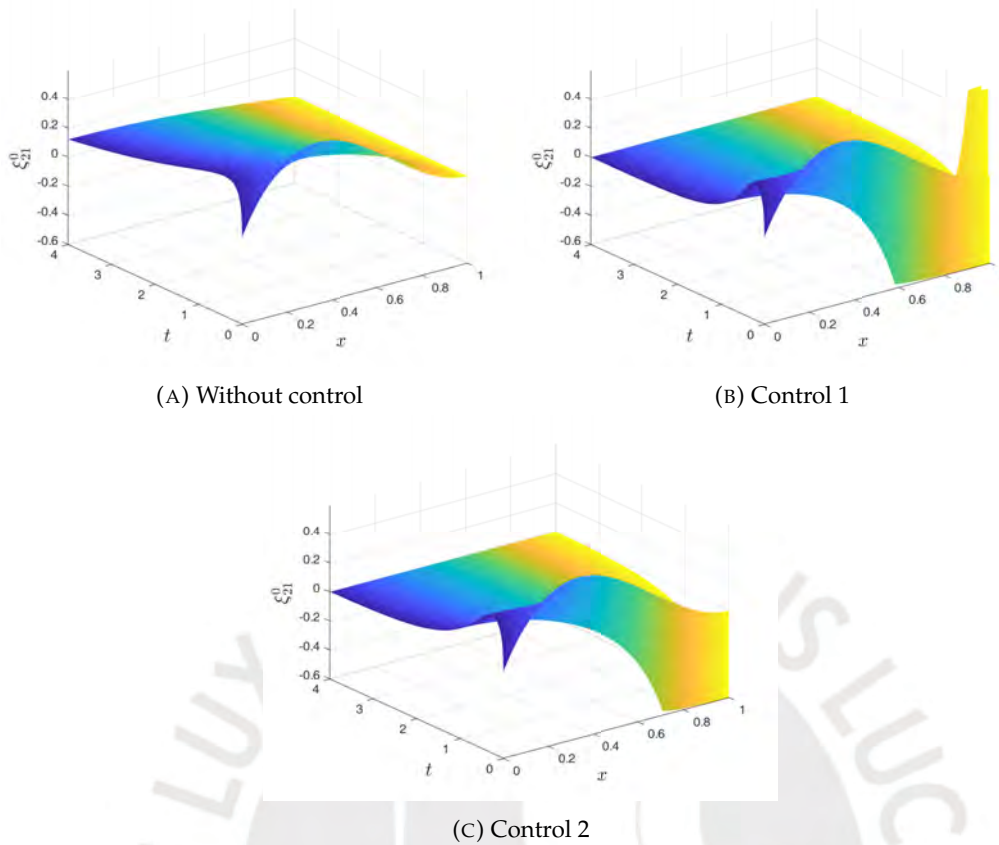
(A) Without control

(B) Control 1

(C) Control 2

FIGURE 4.4: Plots of the MF ξ_{21}^0 with different control strategies

the faster converging strategy is Cont1, the more aggressive controller, as expected. Then Cont2, a less aggresive controller and finally Orig, the solution without any control strategy. This is explained by Figure 4.5, where the more aggressive controllers have a faster convergence time.

After the time window, the two control strategies perform better than the solution without any control strategy as expected, since as described in Table 4.1 the final values of the modulating function at the end of the time window is smaller. Furthermore, the condition $\xi(x, T) = 0$ from Equation (3.22) is not fulfilled by any of the control strategies but is more closely approximated by Cont2 and Cont1 as Table 4.1 shows. A strange phenomenon is the better performance of Cont2 despite the greater value of the modulation function norm at the end of the time window. This can be explained from a numerical point of view. The more aggressive control strategy has faster dynamics and more oscillations in the control and the modulation function solution. Despite the faster convergence, this also results in a less accurate numerical integration with the same time sample. A better method for the numerical integration and the use of a smaller sampling time can enhance the performance.

The next comparison concerns the effect of the time window T in the performance of the estimation. The results are illustrated in Figure 4.7.

The effect of the time window T can be observed in the ISE values for the different T values. As T increases, the estimation error decreases, since the MF final value
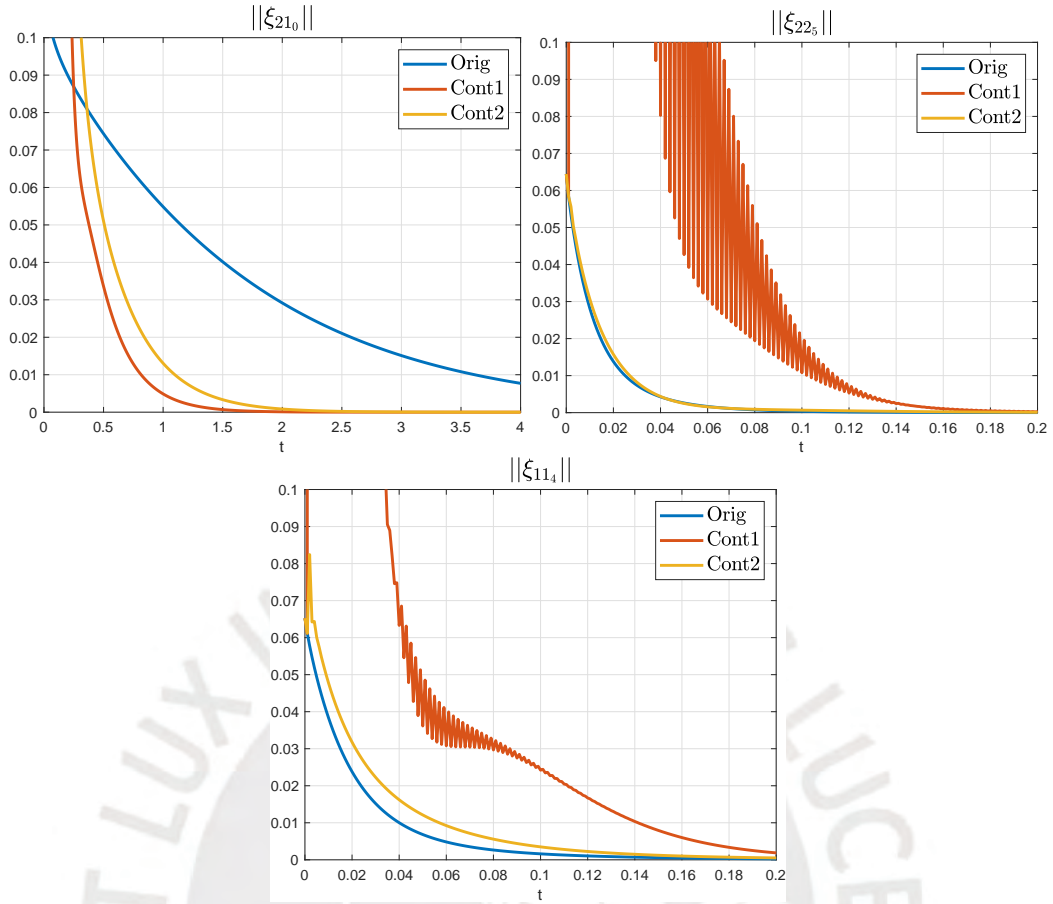
FIGURE 4.5: L2-Norms of the functions ξ_{21}^0, ξ_{22}^5 and ξ_{11}^4 with different control strategies

at the time window T is smaller and results in a smaller error in the coefficients estimation as described by Equation (3.22). A drawback in using a higher time window T, is that the size of the modulation kernel is greater and it results in a higher computational burden since the number of operations needed in the modulation is increasing.

The next comparison explored is the effect of the sampling time T_s on the state estimation. Every plot has the same control strategy(Cont2). Its results are illustrated in Figure 4.8

Time sample has an impact in the numerical integration of the modulation kernels. This can be seen in the plots of each ISE, where with smaller time sample, the error is smaller despite the equal conditions. A solution for this, is the use of different numerical integration such as Newton-Cotes methods that normally perform better than the trapezoidal rule that is used for the current implementation.

Another important factor to take into account is the effect of noise in the measurement in the state estimation. For this purpose, white noise with different SNR was induced onto the measurement signal for the state estimation and the results are presented in Figure 4.9.

Naturally, the noise has an impact on the error as shown in the plots. This effect

(A) ISE of u_1 (B) ISE of u_2

(C) Before T (D) After T
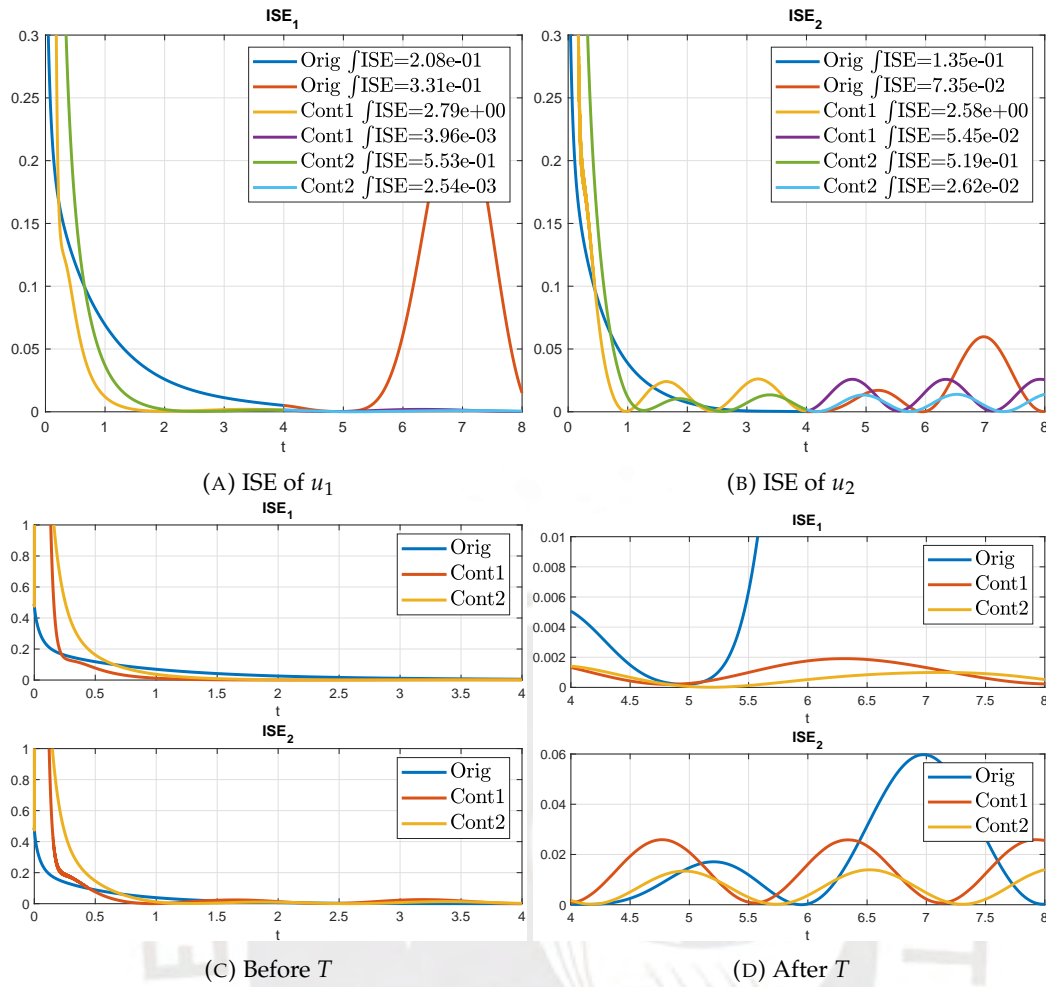
FIGURE 4.6: ISE with different control strategies for MF solving on a
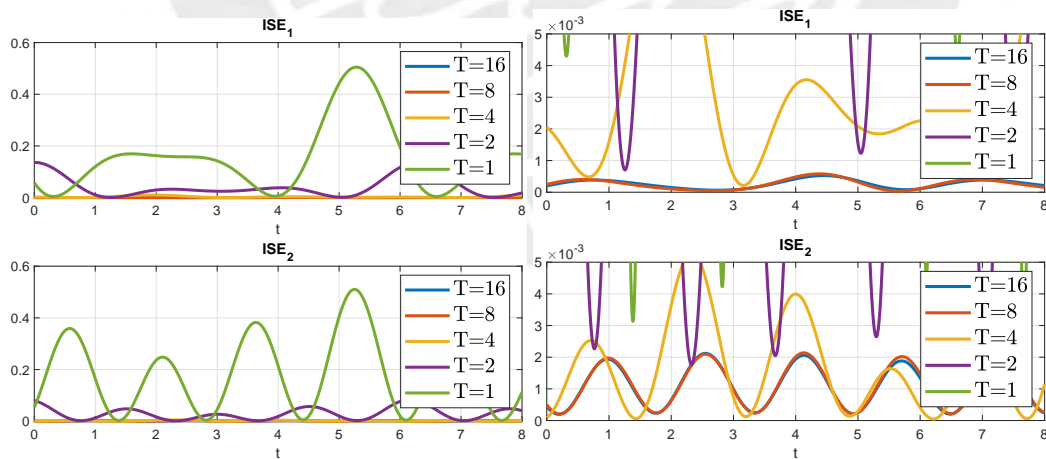Stable Coupled Reaction Diffusion system

FIGURE 4.7: ISE with different time window T for the modulation
operation on a Stable Coupled Reaction Diffusion system

is also a deviation from the ISE with an induced noise that increases as the SNR increases. The effect of the noise is more visible on Figure 4.10 where the row above is the absolute error for each state with a sampling time of 1e-3 and the row below
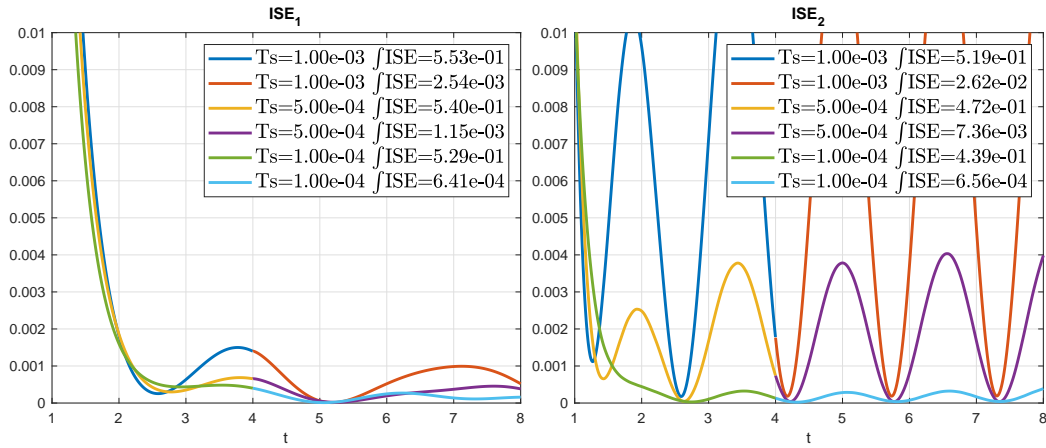
FIGURE 4.8: ISE with different time sample T_s for the modulation operation on a Stable Coupled Reaction Diffusion system
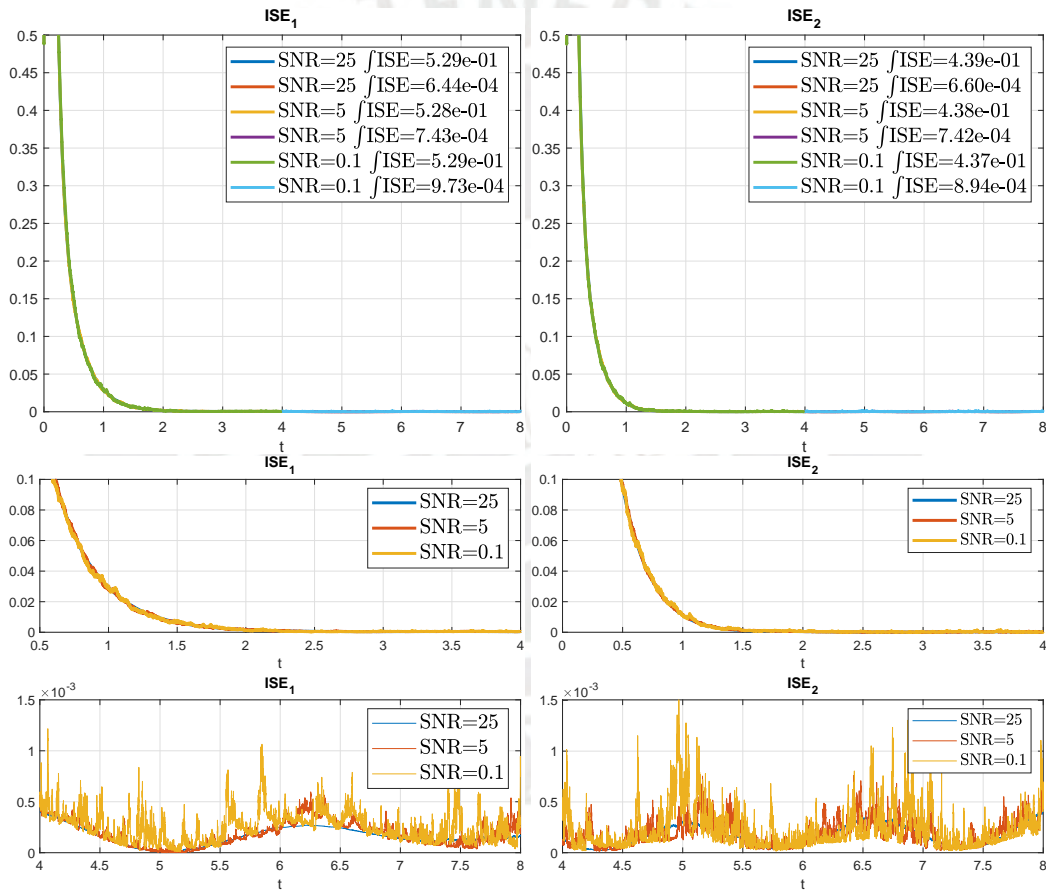
FIGURE 4.9: ISE with different SNR on the measurement for the State Estimation on a Stable Coupled Reaction Diffusion system

is the absolute error with a sampling time of 1e-4 with an SNR of 0.1 in the measurement for each case. It can be seen that as the sampling time increases the error decreases in the middle of the space axis while the error at the boundary practically not, where also the noise impact is much clearer.

Finally, the backstepping observer described in Chapter 2 is compared in same conditions with the modulation function based state estimation presented in this
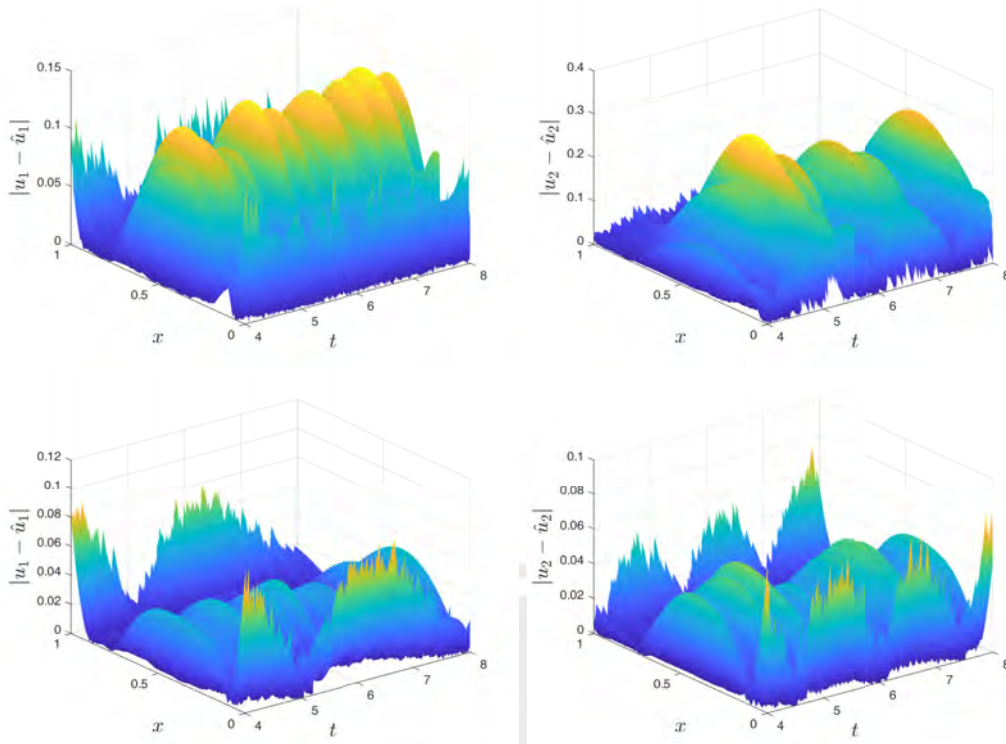
FIGURE 4.10: Absolute error for the estimation with SNR=0.1 and $T_s = 10^{-3}$(above) and $T_s = 10^{-4}$(below) on a Stable Coupled Reaction Diffusion system

thesis. The same observer was applied and tested in [29]. For the sake of a fair comparison, the simulations are run with the same boundary conditions on the systems described in the former subsection with Equation (4.18). For the backstepping observer, the parameter $\tilde{k}$ has been chosen according to [29] to 8, according to Condition 1 in [29]; 0.5, according to Algorithm 2 in [29] and 1, in order to achieve a better performance of the observer. The MF observer uses a time sample of 10^{-4}, a time window of 4 seconds and the control strategy Cont2 described before. The results of the comparison are shown in Figure 4.11.

In the comparison can be observed that the MF observer converges in the first 4 seconds faster as can be seen on Table 4.2, with the ISE error for the first state and the second being smaller than the other observers. In the other hand, in the section before the time window, the backstepping observer keeps converging whereas the MF observer stops converging as it is by design. This is explained by the ISE error at $t = 8$ for the MF observer being greater than the backstepping observers. The plot of the ISE error in Figure 4.11 shows this behaviour and the influence of the values of the state at the boundary in the error of the MF observer after the time window T . This comparison shows the main differences between each approach and how the MF observer behaves with its non-asymptotic nature.
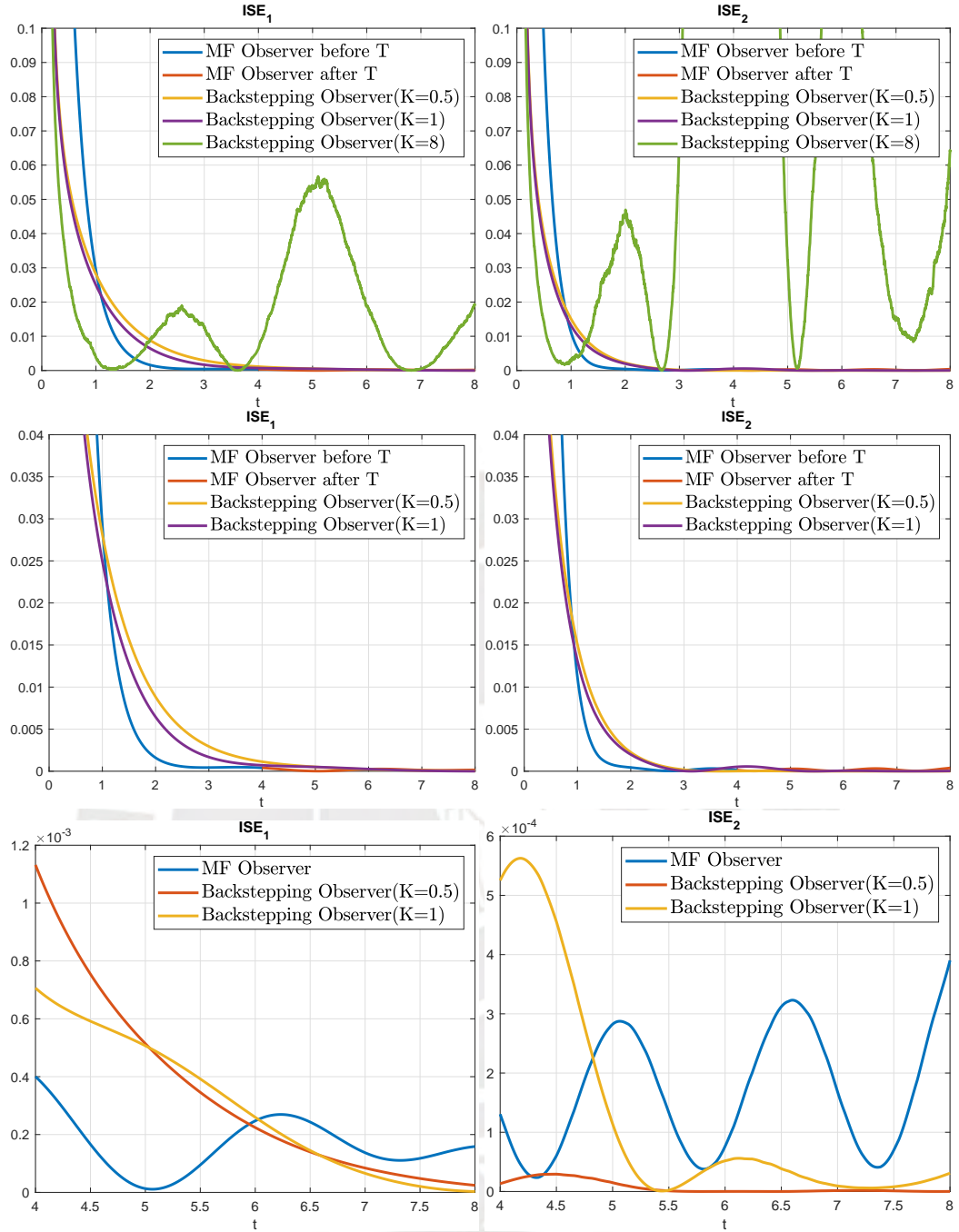
FIGURE 4.11: ISE comparison of the backstepping and MF observer for the State Estimation on a Stable Coupled Reaction Diffusion system

4.2   Unstable Coupled Reaction-Diffusion PDE

The following linear 2-Coupled Reaction-Diffusion PDE is used to demonstrate the performance of the MF observer in an unstable system:

$$\begin{cases} U = \Sigma U_{xx} + \Lambda U \\[2mm] \Sigma = \begin{bmatrix} 2 & 0 \\ 0 & 2 \end{bmatrix}, \Lambda = \begin{bmatrix} 1 & 2 \\ 4 & 5 \end{bmatrix} \\[2mm] U(x,t) = \begin{bmatrix} u_1(x,t) & u_2(x,t) \end{bmatrix}^T \end{cases} \quad (4.20)$$

Observer	$ISE_1(t=2)$	$ISE_1(t=T=4)$	$ISE_1(t=8)$
MF Observer	1.60×10^{-3}	4.00×10^{-4}	1.59×10^{-4}
Backstepping Observer$(K=1)$	6.45×10^{-3}	7.06×10^{-4}	2.96×10^{-6}
Backstepping Observer$(K=0.5)$	8.83×10^{-3}	1.13×10^{-3}	2.45×10^{-5}

TABLE 4.2: ISE of u_1 at different times for the stable Coupled Reaction
Diffusion PDE

With a Neumann boundary condition:

$$U_x(0,t) = 0 \tag{4.21}$$

A known actuation at the boundary:

$$U(L,t) = G(t) \tag{4.22}$$

And a measurement at the boundary

$$Y(t) = U_x(L,t) \tag{4.23}$$

The problem is to estimate the state $U(x,t)$ with the known actuation $G(t)$ and the measurement $Y(t)$.

The solution to the problem is straightforward similar to the prior system, since the only difference are the values in the parameters of the system and in consequence, the Equations (4.15), (4.16) and (3.44) can also be used without any modifications and the simulations can run with only the modification of the parameters values.

For the simulation, the same boundary conditions as the former systems has been used. Additionally, it is worth noticing that the system is unstable as can be noted in Figure 4.13, thus making necessary the use of a control strategy for the auxiliary systems. This can be observed in Figure 4.12

The error for the estimation without a control strategy is much greater than the one that uses a control strategy for each state, due to the necessity to fulfil the condition $\xi(x,T) = 0$. The results of the estimation can also be seen in Figure 4.13 where the original states are in the row above and the estimated states in the row below, showing the similitude between both.

The effect of noise was also tested and the results are shown in Figure 4.14.

The absolute error is shown in Figure 4.15, where the major error is presented in the spatial boundaries, similar to the former system. It is also worth noticing that the error seems to increase as time increases, since the state values also increases as the Figure 4.13 shows and according to the error induced by the approximation of the condition $\xi(x,T) = 0$, resulting by the Equations (3.9) and (3.10) in an error induced in the coefficients calculation and therefore an error in the state estimation. The
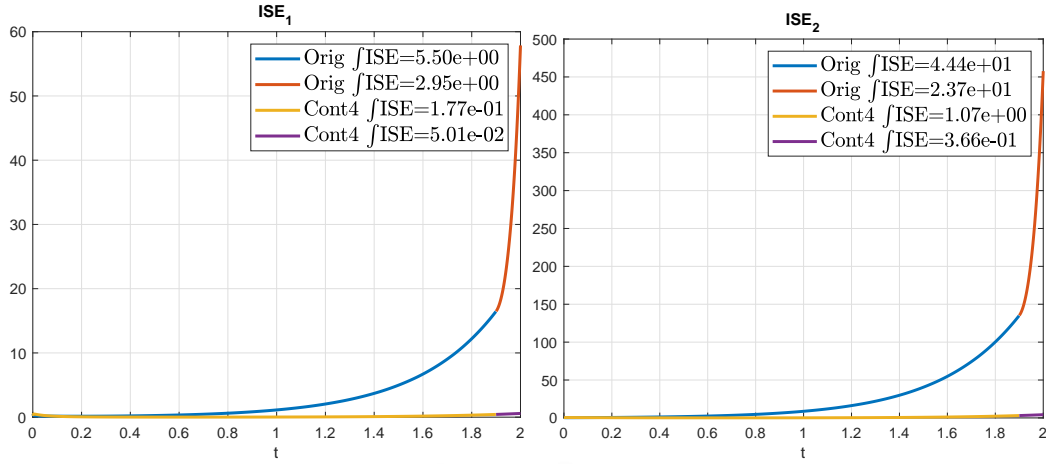
FIGURE 4.12: ISE with different control strategy for the MF solution
for the State Estimation on an Unstable Coupled Reaction Diffusion
system

distribution of the absolute error in the time and spatial axis can be seen in Figure
4.15.

4.3 Coupled Reaction-Diffusion with spatially varying coefficients PDE

The following linear 2-Coupled Reaction-Diffusion PDE with spatially varying coefficients is used to demonstrate the performance of the MF observer in an unstable
system:

$$
\begin{cases}
U = \Sigma U_{xx} + \Lambda U \\
\Sigma = \begin{bmatrix} 1 & 0 \\ 0 & 3 \end{bmatrix}, \Lambda = \begin{bmatrix} 1 & x \\ x & 1 \end{bmatrix} \\
U(x,t) = \begin{bmatrix} u_1(x,t) & u_2(x,t) \end{bmatrix}^T
\end{cases}
\tag{4.24}
$$

With a Neumann boundary condition:

$$U_x(0,t) = 0 \tag{4.25}$$

A known actuation at the boundary:

$$U(L,t) = G(t) \tag{4.26}$$

And a measurement at the boundary

$$Y(t) = U_x(L,t) \tag{4.27}$$

The problem is to estimate the state $U(x,t)$ with the known actuation $G(t)$ and the
measurement $Y(t)$.
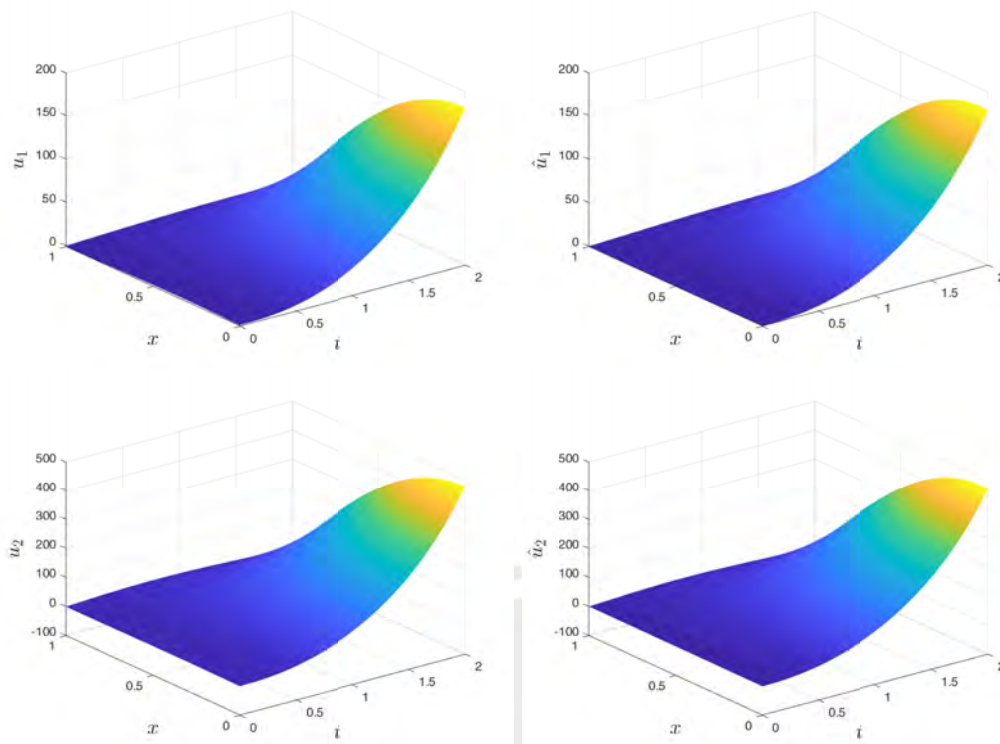
FIGURE 4.13: Original states(above) and estimated states(below) of an Unstable Coupled Reaction Diffusion system

The present system has been used in [11] with the use a backstepping observer. For the simulation, the same boundary conditions as the former systems has been used.

The solution to the problem is straightforward similar to the prior system, since the only difference are the values in the parameters of the system and even the spatially varying coefficients do not have any change in the formulation of the problem and in consequence, the Equations (4.15), (4.16) and (3.44) can also be used without any modifications and the simulations can run with only the modification of the parameters values.

The results with a time sample of 1e-3 and 1e-4 are shown on Figure 4.16.

Performance of the observer also improves with a smaller time sample such as the other systems, especially notable in the ISE of the second state.

The absolute error of the estimation is shown in 4.17 and the comparison of the original and estimated state are shown in Figure 4.18

The influence of noise shown in Figure 4.19, where the noise seems to have a smaller impact compared to the former systems, even increasing the SNR value as the plots indicate.

This chapter has shown the performance of the observer in three different systems that are coupled reaction-diffusion PDE. The first system tested demonstrates the use of the MF observer in a reaction-diffusion PDE with constant coefficients, where also the different effect of the parameters such as sampling time, time window
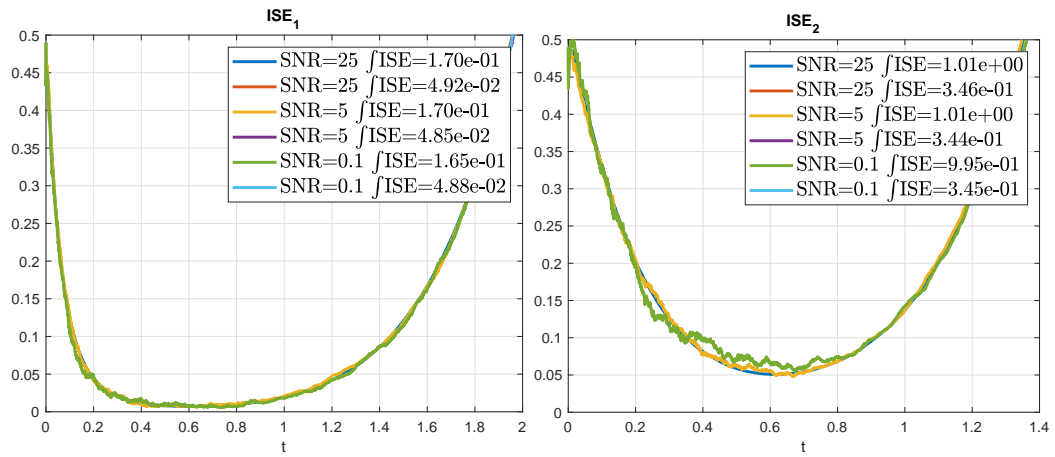
FIGURE 4.14: ISE for the state estimation for the State Estimation on an Unstable Coupled Reaction Diffusion system
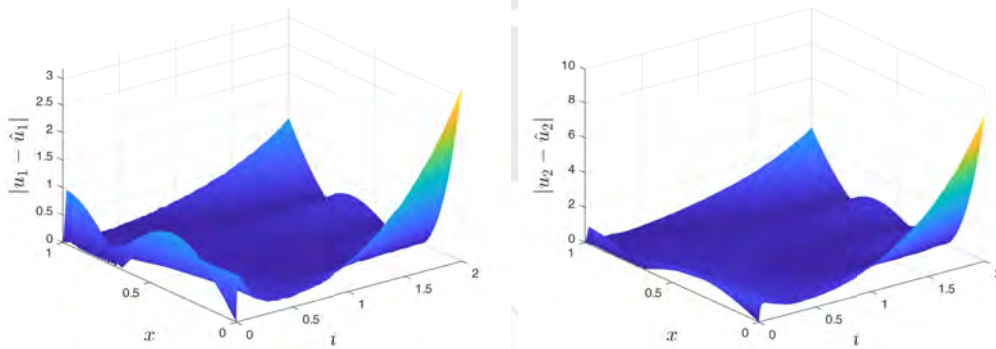

FIGURE 4.15: Comparison of the original and estimated state of an Unstable Coupled Reaction Diffusion system

and control strategy on the estimation. Noise influence also has been investigated. Other two systems change the original problem introducing unstable dynamics and spatially varying coefficients respectively. The chapter demonstrates how the MF observer can be applied and the effect of the different parameters.
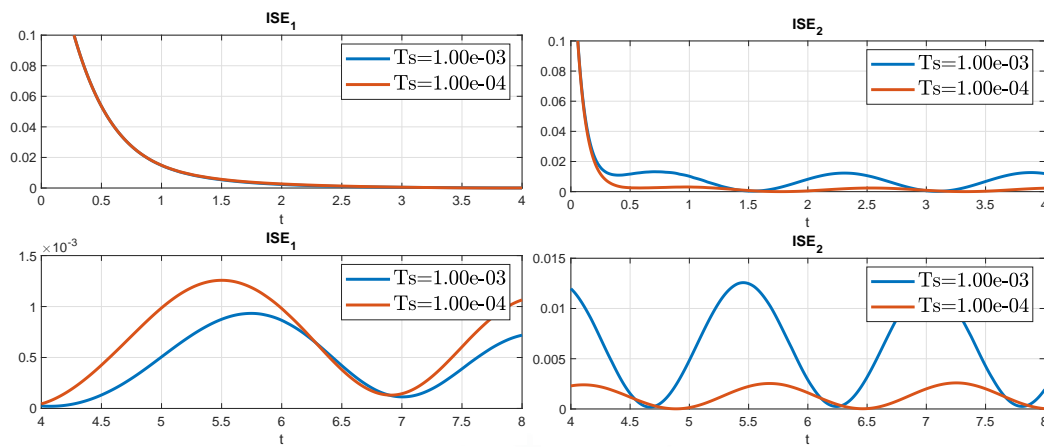
FIGURE 4.16: Effect of time sample *Ts* on the ISE for a Coupled Reaction Diffusion system with Spatially Varying coefficients
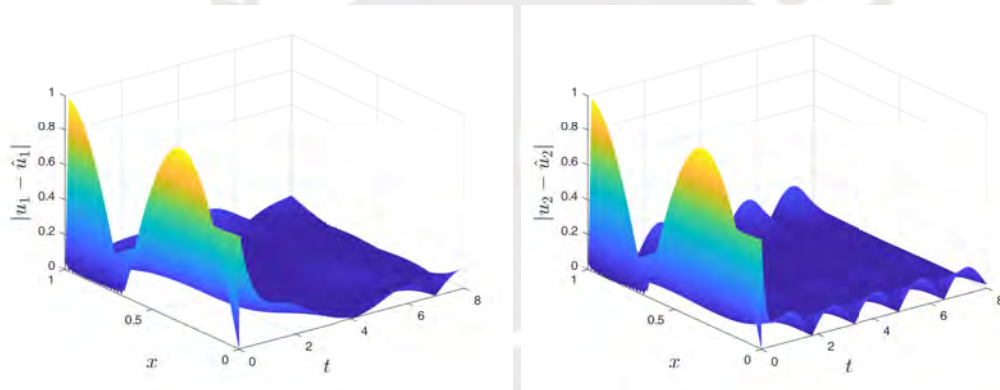
FIGURE 4.17: Absolute error of the estimation for each state on a Coupled Reaction Diffusion system with Spatially Varying coefficients
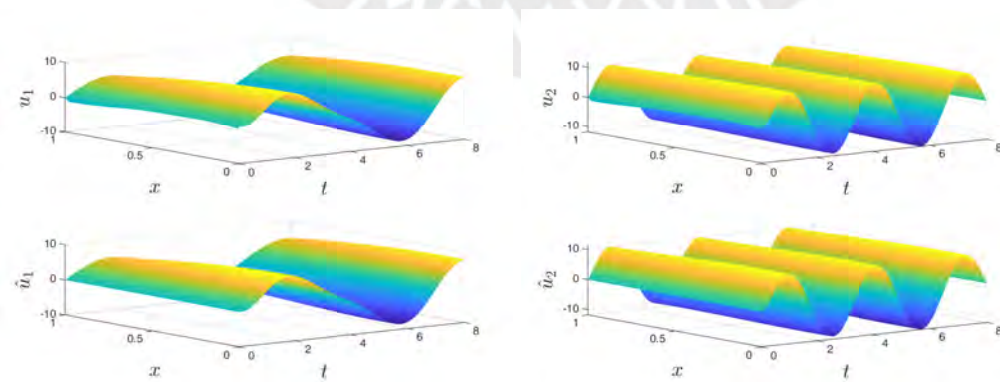
FIGURE 4.18: Comparison of the original and estimated state for the State Estimation on a Coupled Reaction Diffusion system with Spatially Varying coefficients
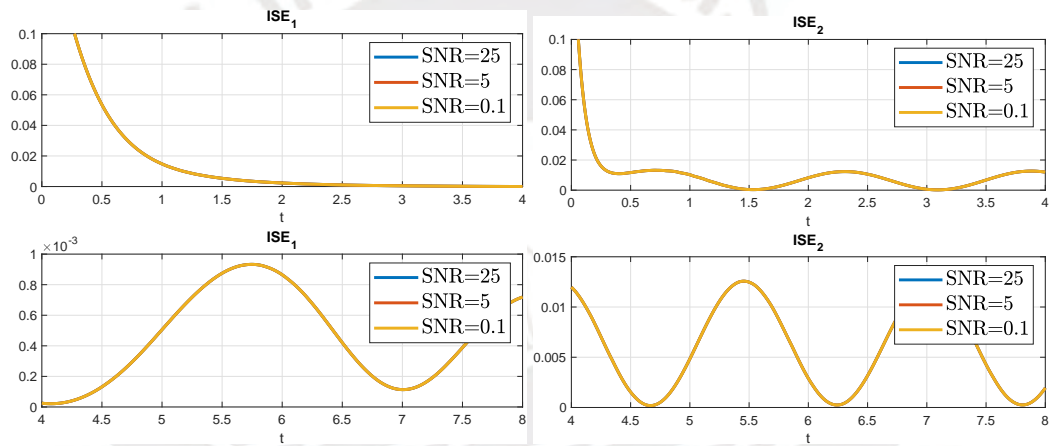
FIGURE 4.19: Effect of the noise on the ISE for each state on a Coupled
Reaction Diffusion system with Spatially Varying coefficients

Chapter 5

Conclusions

The presented modulation function based observer for Coupled Reaction-Diffusion PDEs demonstrates a sufficiently satisfying state estimation for different systems tested in the last chapter. The mentioned observer, requires a measurement on the boundary, knowledge of the actuation and the modulation functions resulting from solving auxiliary systems.

The observer approximates the original states using their basis expansion formulation. In order to achieve this, the coefficients of the respective basis expansion need to be calculated. This calculation cannot be done straightforward applying the modulation operator as in [12] due to the coupling between states. To overcome this problem, a linear combination of every equation can be performed and then, the modulation operator is applied. In order to simplify this operation, auxiliary systems need to be solved. The auxiliary systems are similar to the original system with a modification in the coefficients that is related to a matrix K that can be freely chosen, creating a new system. The solution of the auxiliary system, including the signal modelling control, requires for the modulation functions to be zero at the end of the time window, transforming the problem into a stabilization problem. If the system is stable, there is no strict need for a controller but its use can enhance the performance making the stabilization faster and thus, the estimation more accurate as the results of the last chapter have shown. For this purpose, backstepping controllers have been developed for different types of systems and their solution with the signal modelling control problem can be done offline, without the necessity of new calculations.

As the results from the last chapter shows, the MF Observer is capable of dealing with the three kind of systems tested. The more important parameters for the observer are the sampling time T_s, used for the time integration and the sampling of the different signals; the time window T, used for the solution of the signal modelling control; the approximation order N, that determines the number of modulation functions. The results shows that the time sample has an impact in the estimation, since the numerical integration uses a trapezoidal rule. A better suited numerical integration method can improve the estimation. The length of the time window also plays an important role in the estimation. A longer time window gives more time to the modulation function to stabilize as Table 4.1 shows and in consequence, a smaller

error in the estimation. The approximation order has to be chosen in relation with the chosen grid resolution in x, since increasing the approximation order does not always result in a more accurate estimation. This is caused by the dynamics at the boundaries that are very oscillating, resulting in a bad approximation due to the numerical integration. The choice of these parameters has to be made carefully in order to achieve a better state estimation. Fortunately, this tuning section can be made offline and the solutions of the auxiliary systems can be compared and improved.

The estimation error can be attributed to three different parts. Numerical errors, that are related to the numerical integration. The integration depends on the value of the sampling time T_s and its error can be reduced using smaller values of T_s. The error from the basis expansion approximation can be reduced by increasing the basis order and the grid resolution in x. This allows to increment the approximation order of the basis. Finally, the error in estimating the coefficients attributed to the non fulfillment of the condition from Equation (3.9). If the condition is not fullfilled, then Equation (3.10) becomes:

$$\int_0^L \varphi^m(x, \tau - t + T) u_n(x, \tau) dx \Big|_{\tau=t-T}^{\tau=t} = c^m(t) - \int_0^L \varphi^m(x, 0) u_n(x, t-T) dx = \hat{c}^m(t)$$

where $\hat{c}^m(t)$ are the coefficients approximated with the method and if $\varphi^m(x, 0) = \xi^m(x, T) = 0$, then $c^m(t) = \hat{c}^m(t)$ and the estimation is faithful to the basis expansion coefficients. However, if it does not fulfill, the error on the coefficients can be calculated with:

$$c^m(t) - \hat{c}^m(t) = \int_0^L \varphi^m(x, 0) u_n(x, t-T) dx$$

and using:

$$\bar{\varphi}^m(t) = \sup_x \varphi^m(x, t)$$

$$\bar{\xi}^m(t) = \sup_x \xi^m(x, t)$$

$$\bar{u}^m(t) = \sup_x u(x, t)$$

an upper boundary of the coefficients error can be calculated:

$$c^m(t) - \hat{c}^m(t) = \int_0^L \varphi^m(x, 0) u_n(x, t-T) dx \le L \bar{\varphi}^m(0) \bar{u}_n(t-T) = L \bar{\xi}^m(T) \bar{u}_n(t-T).$$
$$(5.1)$$

The values of L and $\bar{\xi}^m(T)$ are fixed and known from the signal modelling control problem, making the error dependant on $\bar{u}_n(t-T)$ and thus on the maximum value of $u_n(x, t-T)$ that changes with time. This explains the tendency of the errors shown in the last chapter and in A. The errors are mostly proportional to the boundary values as the results from A shows. In order to reduce this error, a better control strategy can be used to reduce the value $\xi^m(x, T)$ and the value of the time window T can be increased in order to give more time for the system to stabilize and achieve a reduced value of $\xi^m(x, T)$.

The method explained in the thesis presents some advantages with respect to

other observers such as the backstepping observers as described in Table 5.1. Such advantages are the easy calculation for the state estimation, since it only requires numerical integrations and matrix multiplications in comparison to the backstepping observer that requires the solution of a coupled PDE for each time step. This advantage also makes possible a real-time implementation of the method, especially considering the operations needed and the possibility of the implementation with FIR filters as described in [12]. From the results on the last chapters, the robustness against noise is also demonstrated.

The main issue with regard to the method is the dependency on the sampling time for the performance of the observer. The results show that smaller values of sampling time T_s are needed in order to achieve better results due to the numerical integration, increasing the number of values stored and operations. Another drawback is the state values dependency of the error from Equation (5.1), since backstepping controllers with their convergence does not have this issue.

Advantages	Issues
• Easy calculation for state estimation • Good response to noise • Real-time implementation	• Dependency on sampling time • Error depending on state values
Inaccuracies	Future Ideas
• Basis expansion approximation • Error at the boundaries	• Better suited control method • Combination with non-linear terms

TABLE 5.1: Advantages, issues, inaccuracies and future ideas for the method

Further works could consider the use and development of better control methods for each system in order to reduce the error on the coefficients and the window time T. Backstepping controllers could be further explored and their tuning in order to achieve this purpose. The influence and election of the matrix K is another topic to look into, since their values affect the coefficients for the auxiliary systems thus, modifying the dynamics of the systems. The possibility of stabilizing unstable systems and achieving faster stabilization could be achieved by using different values of K. Another area of interest, is the use of more equations in order to form an overdetermined system of equations and give more robustness to the coefficients calculation. Finally, an expansion of the method for the use with non linear coupling systems could be explored in addition to systems with time varying coefficients in order to develop the method in further systems.

Appendix A

Simulation Plots

The present appendix shows the results of the simulation for the state estimation of the system presented in Equation (4.5) with different boundary conditions in order to illustrate their effect.

A.1 Bell shaped Boundary Condition

Using:

$$U(1,t) = G(t) = \begin{bmatrix} 5\left(\frac{1}{1+e^{-0.5(t-2)}}\right)\left(1 - \frac{1}{1+e^{-(t-7)}}\right) \\ 3\left(\frac{1}{1+e^{-2(t-1)}}\right)\left(1 - \frac{1}{1+e^{-2(t-7.5)}}\right) \end{bmatrix} \tag{A.1}$$
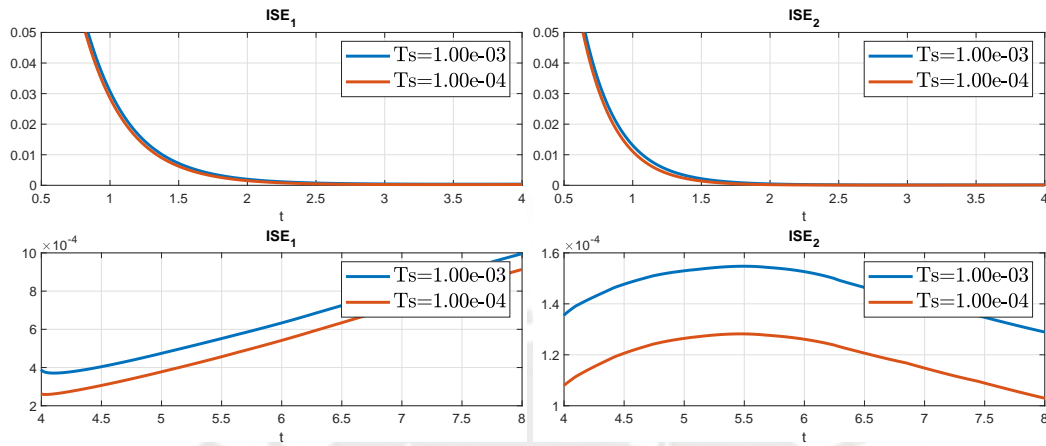
the results are:
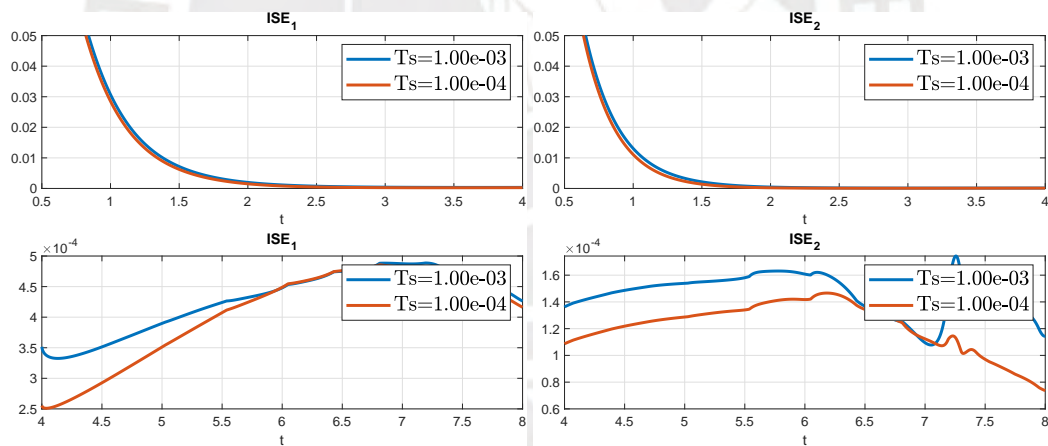
FIGURE A.1: ISE with different time sample T_s for the modulation operation on a Stable Coupled Reaction Diffusion system with a Bell shaped boundary condition
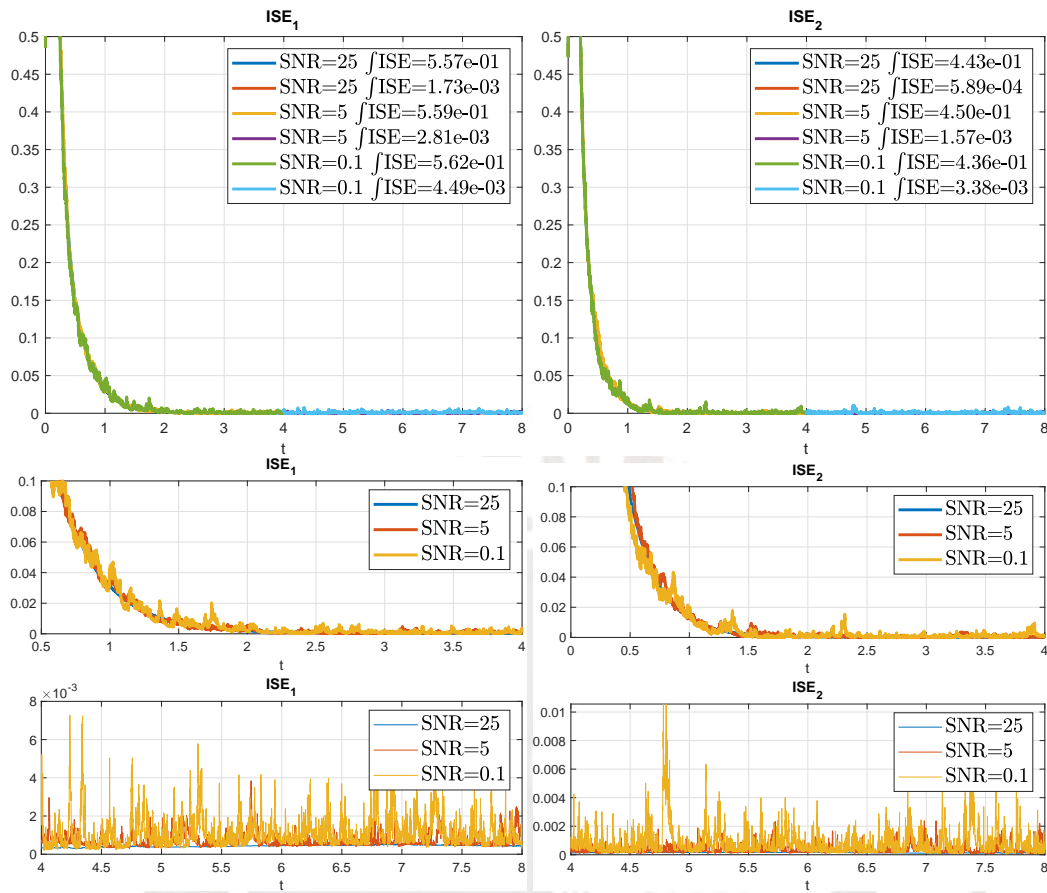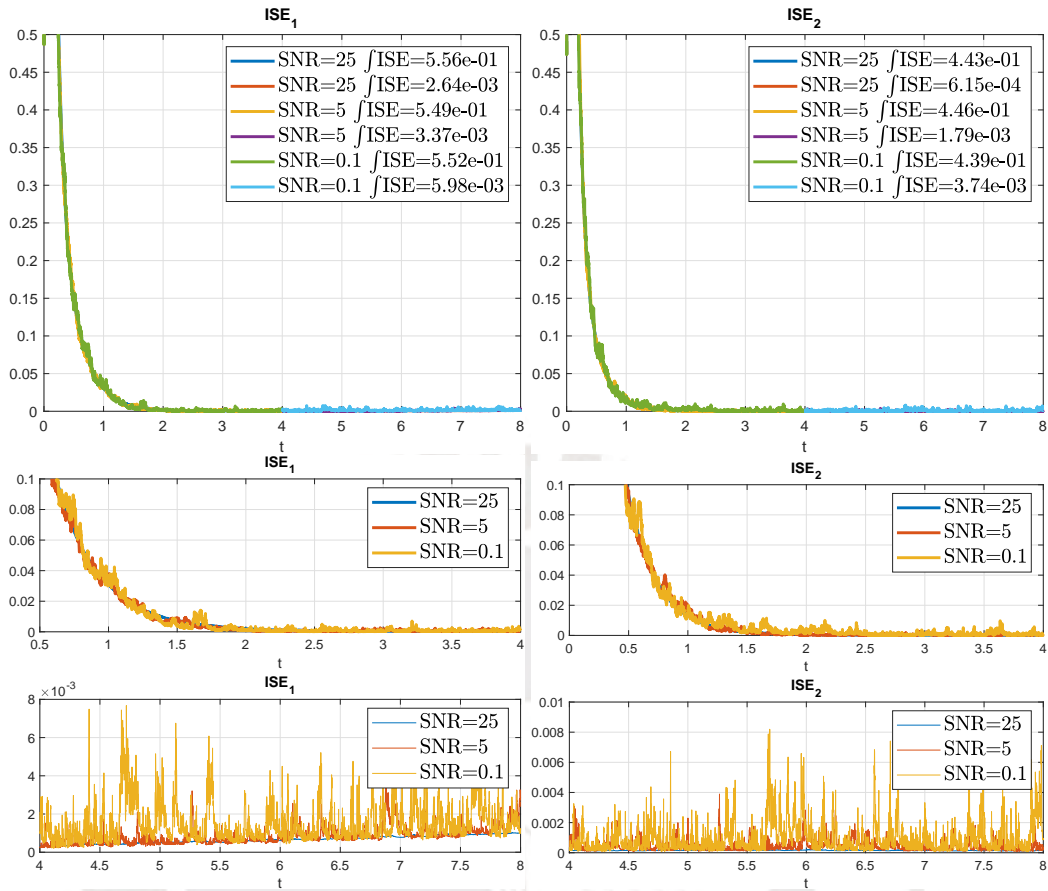
FIGURE A.2: ISE with different SNR on the measurement for the State Estimation on a Stable Coupled Reaction Diffusion system with a Bell shaped boundary condition
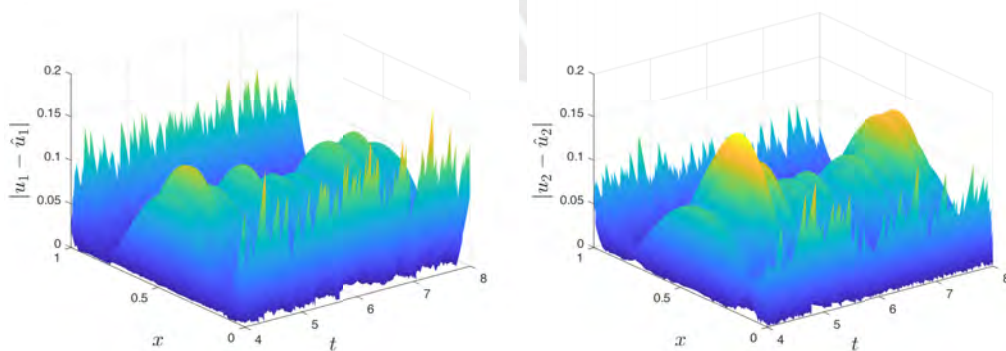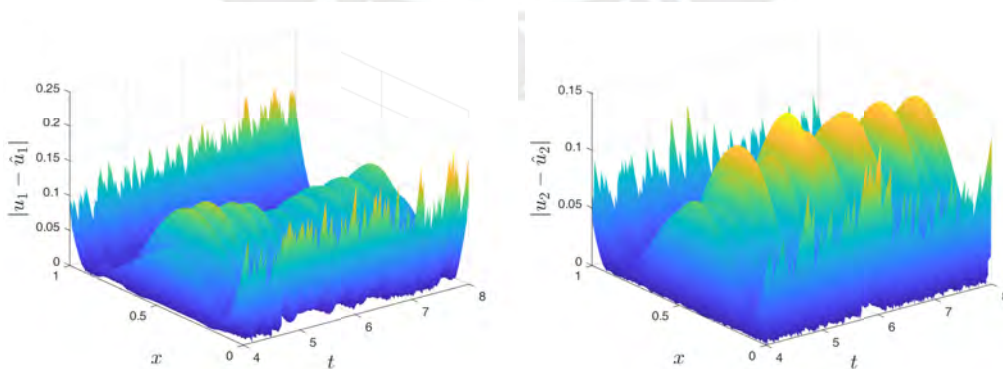

FIGURE A.3: Absolute error for the estimation with SNR=0.1 and $T_s = 10^{-3}$ on a Stable Coupled Reaction Diffusion system with a Bell shaped boundary condition
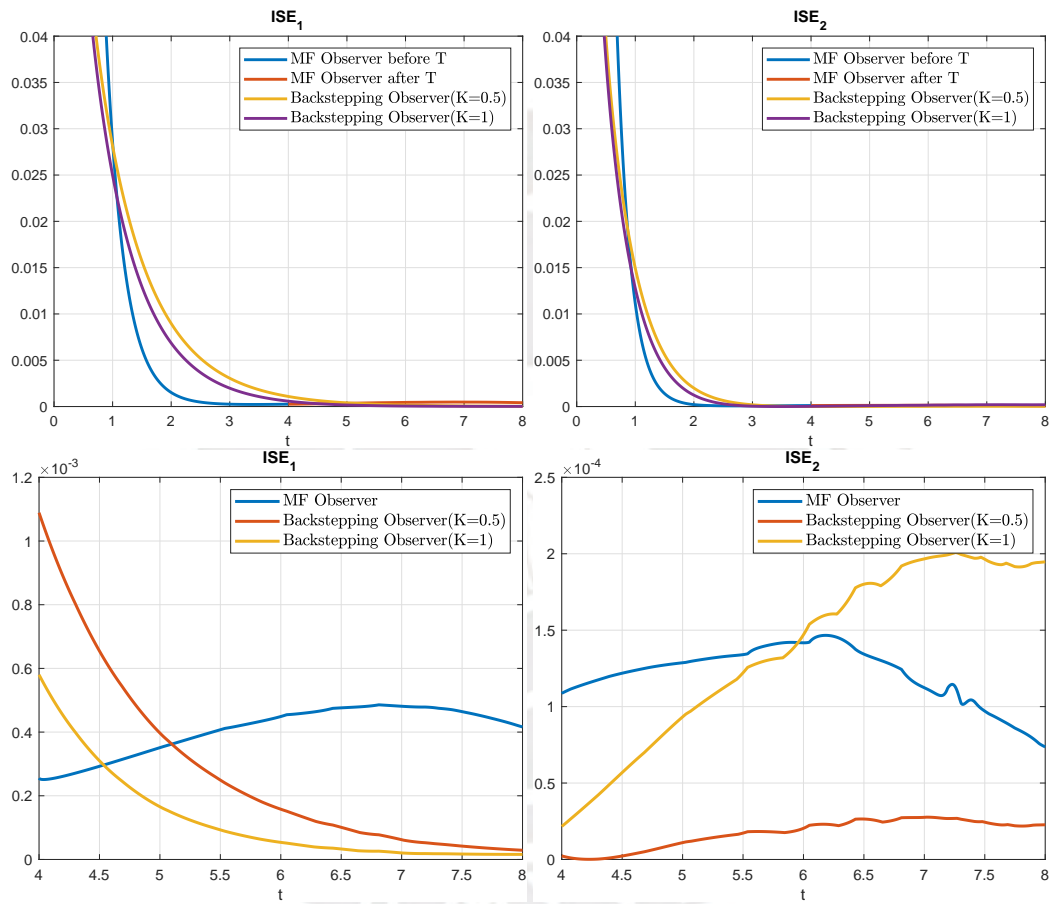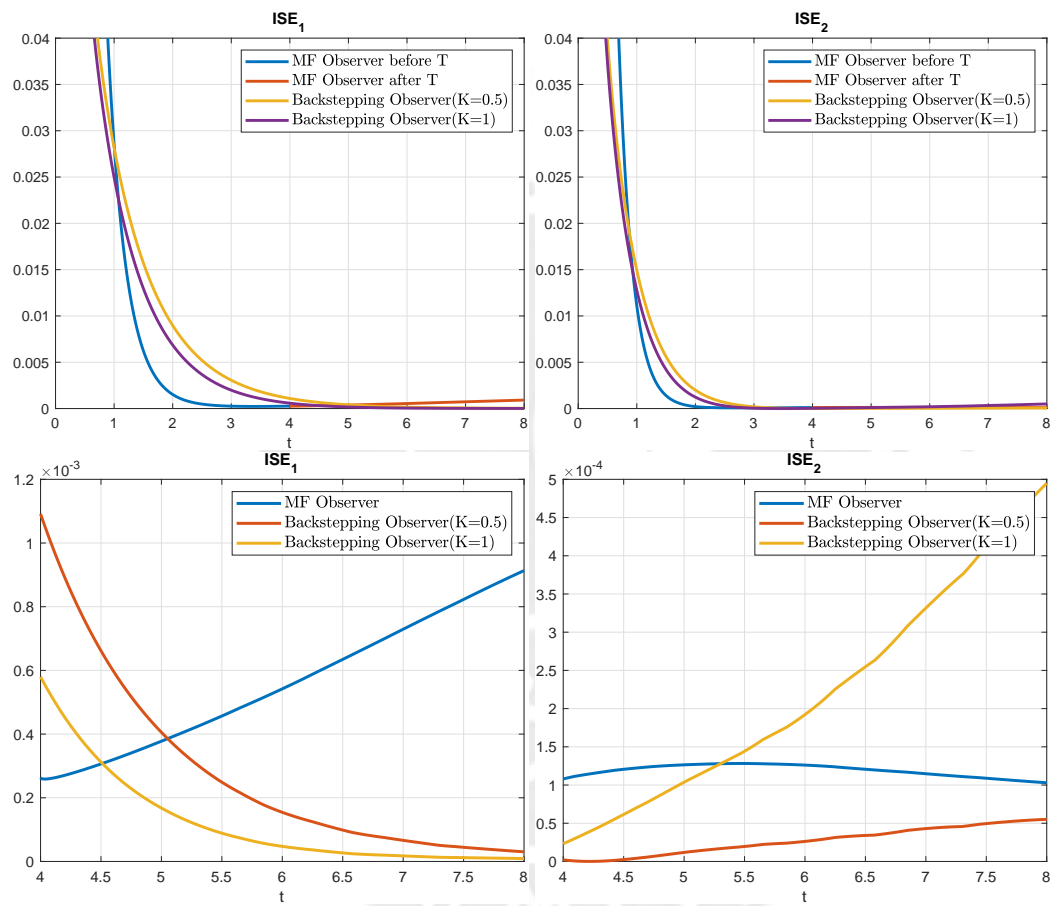
FIGURE A.4: ISE comparison of the backstepping and MF observer for the State Estimation on a Stable Coupled Reaction Diffusion system with a Bell shaped boundary condition

A.2   Sigmoid Boundary Condition

Using:

$$U(1,t) = G(t) = \begin{bmatrix} 5\left(\frac{1}{1+e^{-0.5(t-2)}}\right) \\ 3\left(\frac{1}{1+e^{-2(t-1)}}\right) \end{bmatrix} \tag{A.2}$$
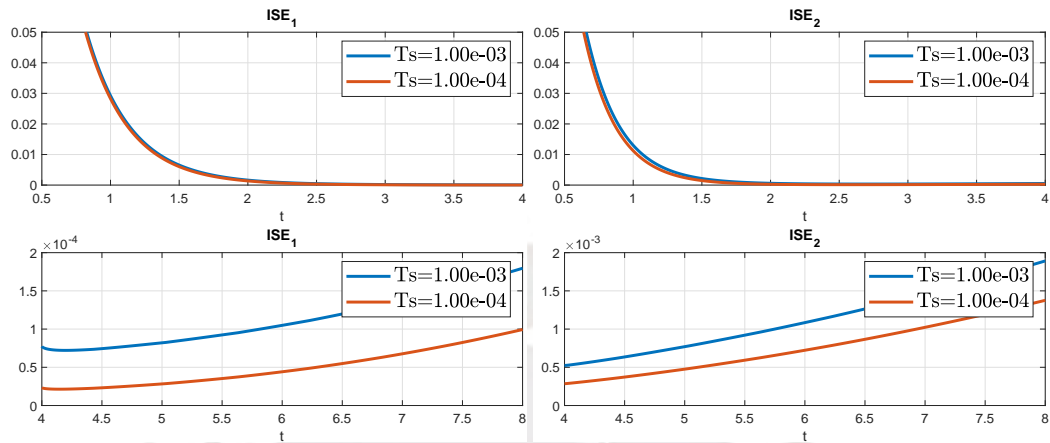
the results are:

FIGURE A.5: ISE with different time sample T_s for the modulation operation on a Stable Coupled Reaction Diffusion system with a Sigmoid boundary condition
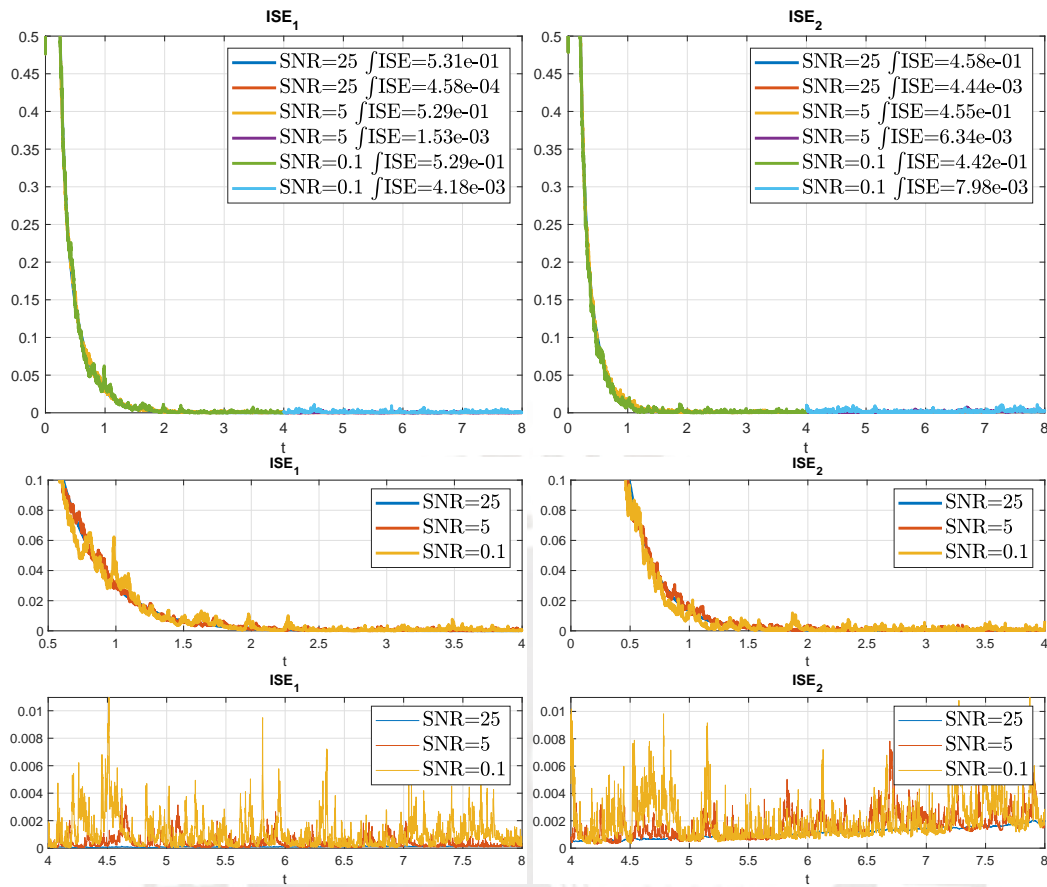
FIGURE A.6: ISE with different SNR on the measurement for the State Estimation on a Stable Coupled Reaction Diffusion system with a Sigmoid boundary condition

FIGURE A.7: Absolute error for the estimation with SNR=0.1 and $T_s = 10^{-3}$ on a Stable Coupled Reaction Diffusion system with a Sigmoid boundary condition

FIGURE A.8: ISE comparison of the backstepping and MF observer for the State Estimation on a Stable Coupled Reaction Diffusion system with a Sigmoid boundary condition

A.3   Linear Boundary Condition

Using:

$$U(1,t) = G(t) = \begin{bmatrix} 0.5t \\ 1+t \end{bmatrix} \tag{A.3}$$

the results are:

FIGURE A.9: ISE with different time sample T_s for the modulation operation on a Stable Coupled Reaction Diffusion system with a Linear boundary condition

FIGURE A.10: ISE with different SNR on the measurement for the State Estimation on a Stable Coupled Reaction Diffusion system with a Linear boundary condition
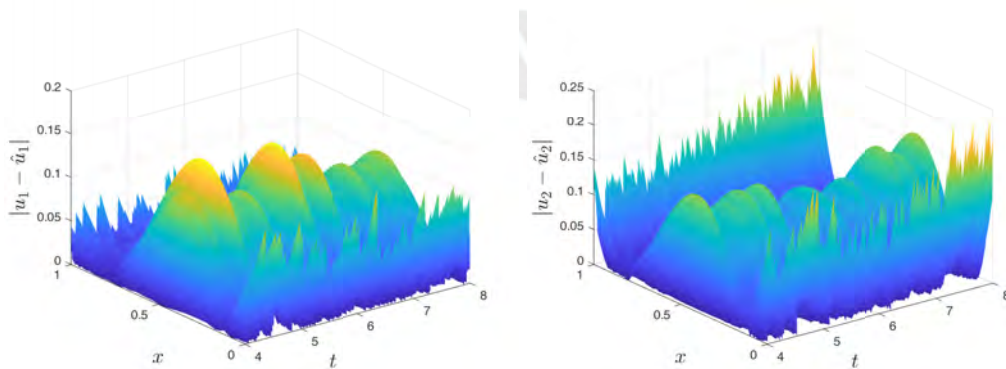

FIGURE A.11: Absolute error for the estimation with SNR=0.1 and $T_s = 10^{-3}$ on a Stable Coupled Reaction Diffusion system with a Linear boundary condition
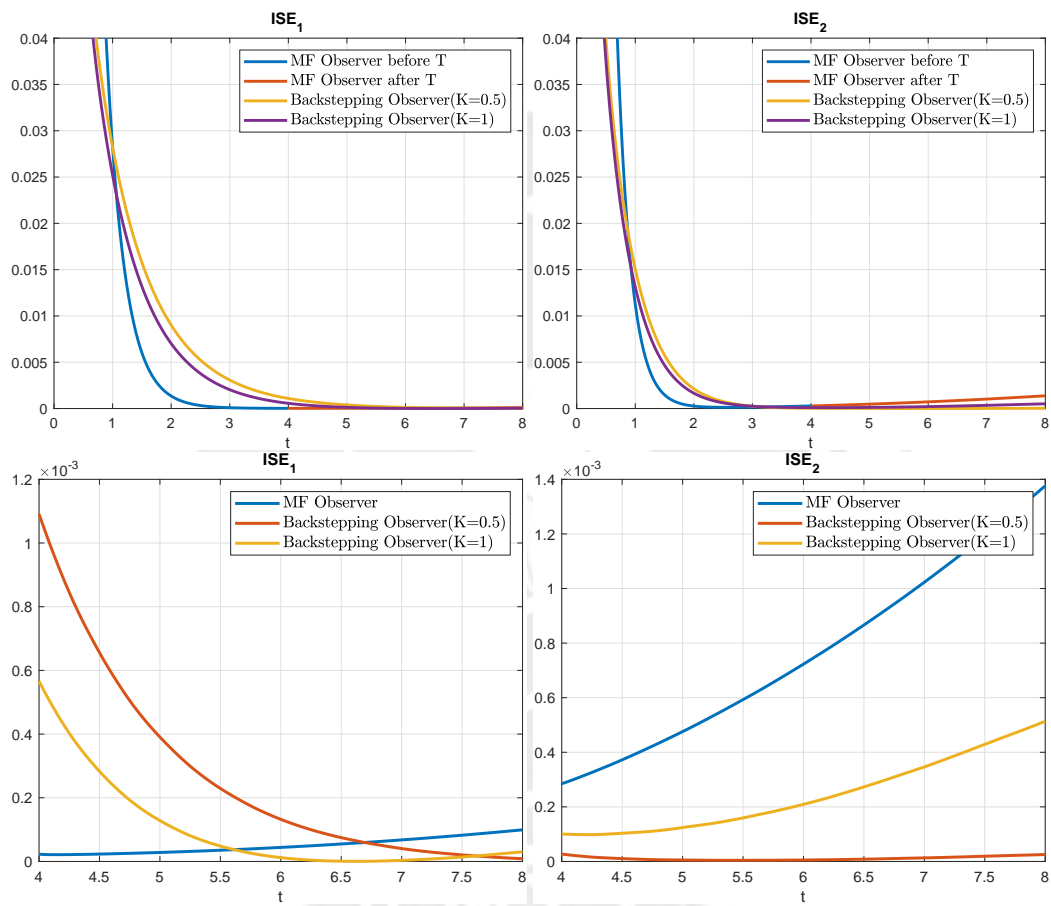
FIGURE A.12: ISE comparison of the backstepping and MF observer for the State Estimation on a Stable Coupled Reaction Diffusion system with a Linear boundary condition

A.4   Constant Boundary Condition

Using:

$$U(1,t) = G(t) = \begin{bmatrix} 6 \\ 4 \end{bmatrix} \tag{A.4}$$
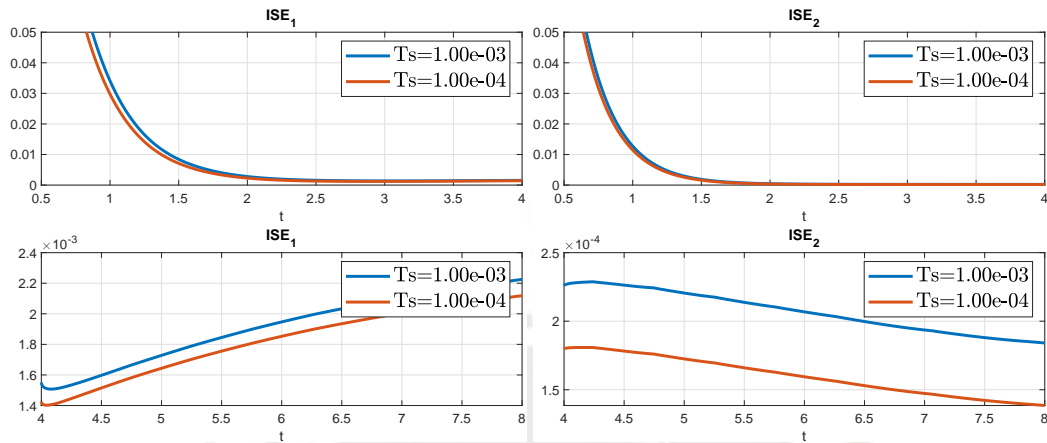
the results are:

FIGURE A.13: ISE with different time sample T_s for the modulation operation on a Stable Coupled Reaction Diffusion system with a Constant boundary condition
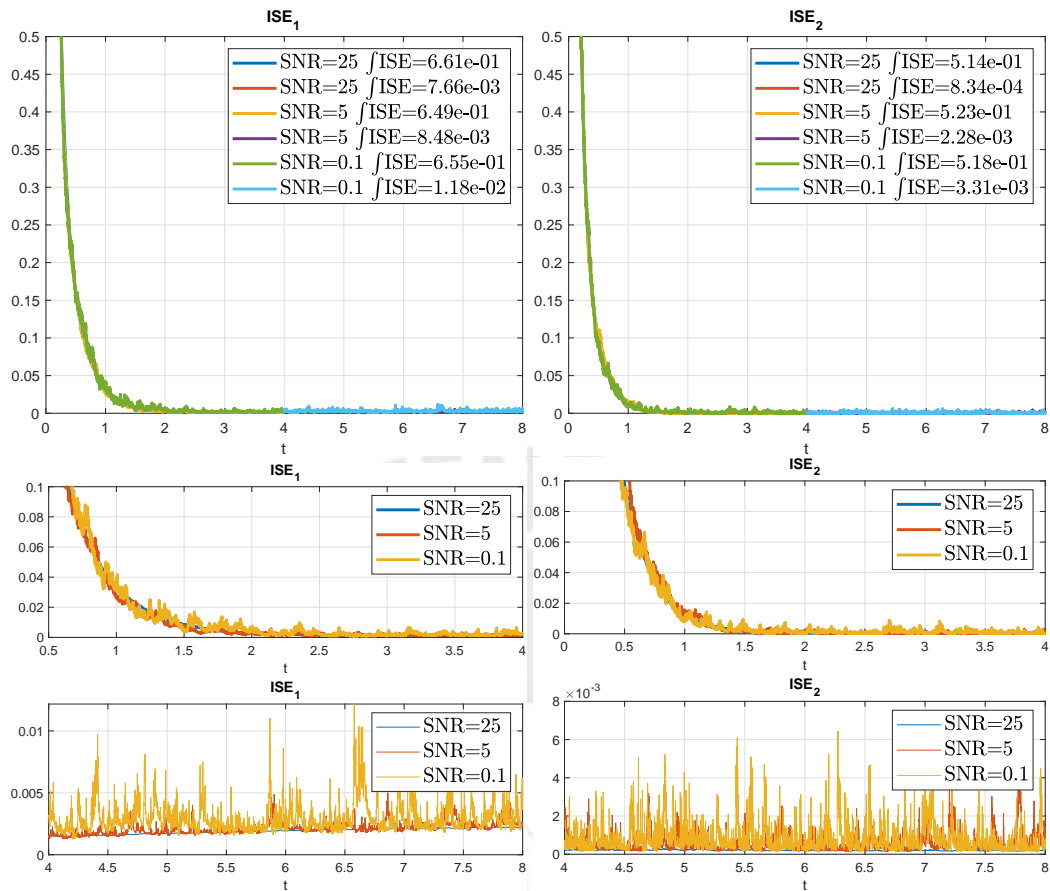
FIGURE A.14: ISE with different SNR on the measurement for the State Estimation on a Stable Coupled Reaction Diffusion system with a Constant boundary condition
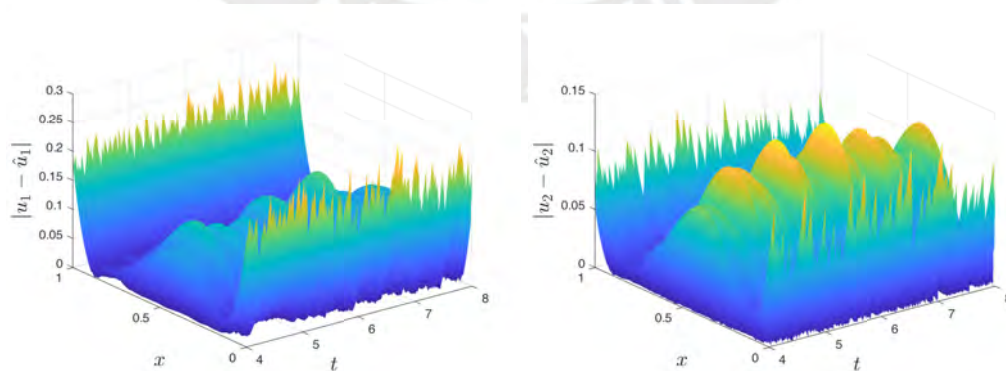

FIGURE A.15: Absolute error for the estimation with SNR=0.1 and $T_s = 10^{-3}$ on a Stable Coupled Reaction Diffusion system with a Constant boundary condition
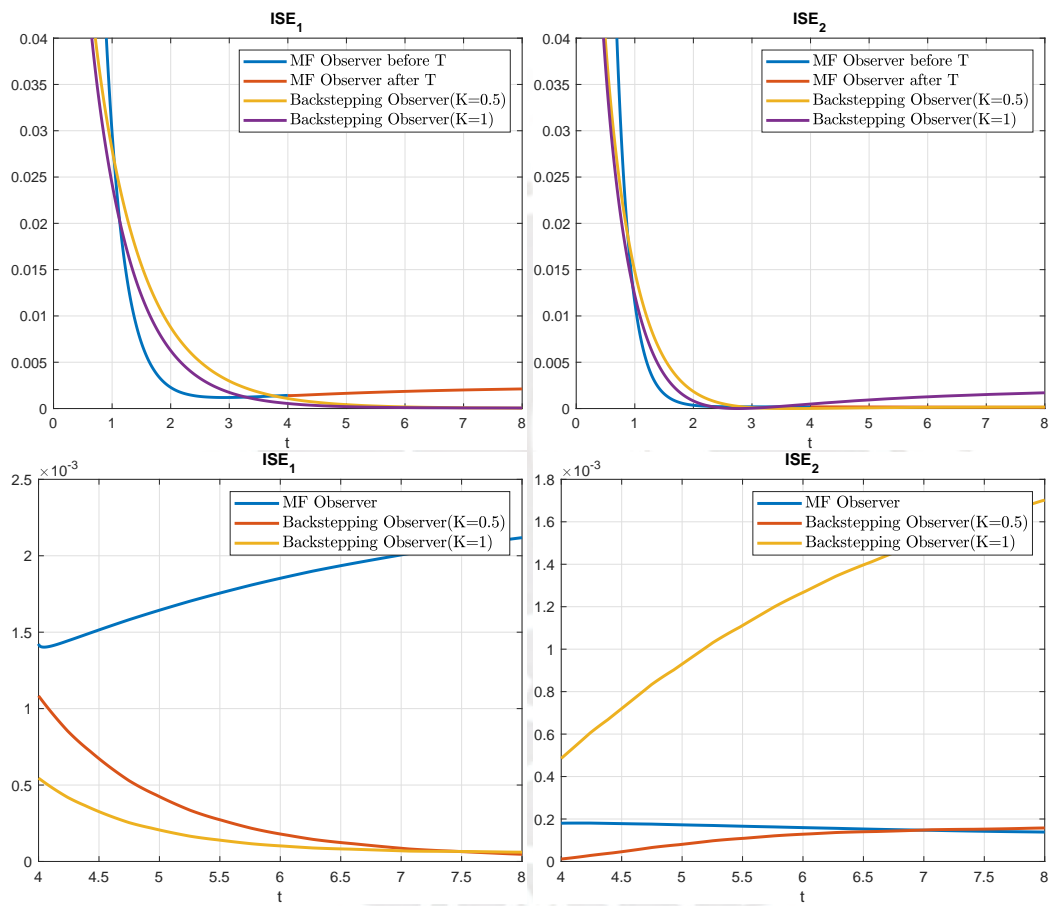
FIGURE A.16: ISE comparison of the backstepping and MF observer for the State Estimation on a Stable Coupled Reaction Diffusion system with a Constant boundary condition

A.5   Sinusoidal Boundary Condition

Using:

$$U(1,t) = G(t) = \begin{bmatrix} \sin(6\pi t) \\ \sin(8\pi t) \end{bmatrix} \qquad\qquad\text{(A.5)}$$
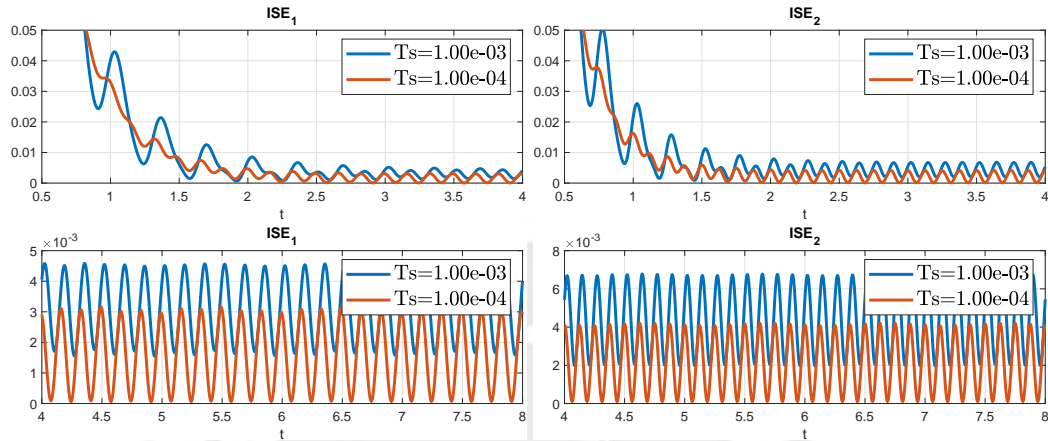
the results are:

FIGURE A.17: ISE with different time sample T_s for the modulation operation on a Stable Coupled Reaction Diffusion system with a Sinusoidal boundary condition
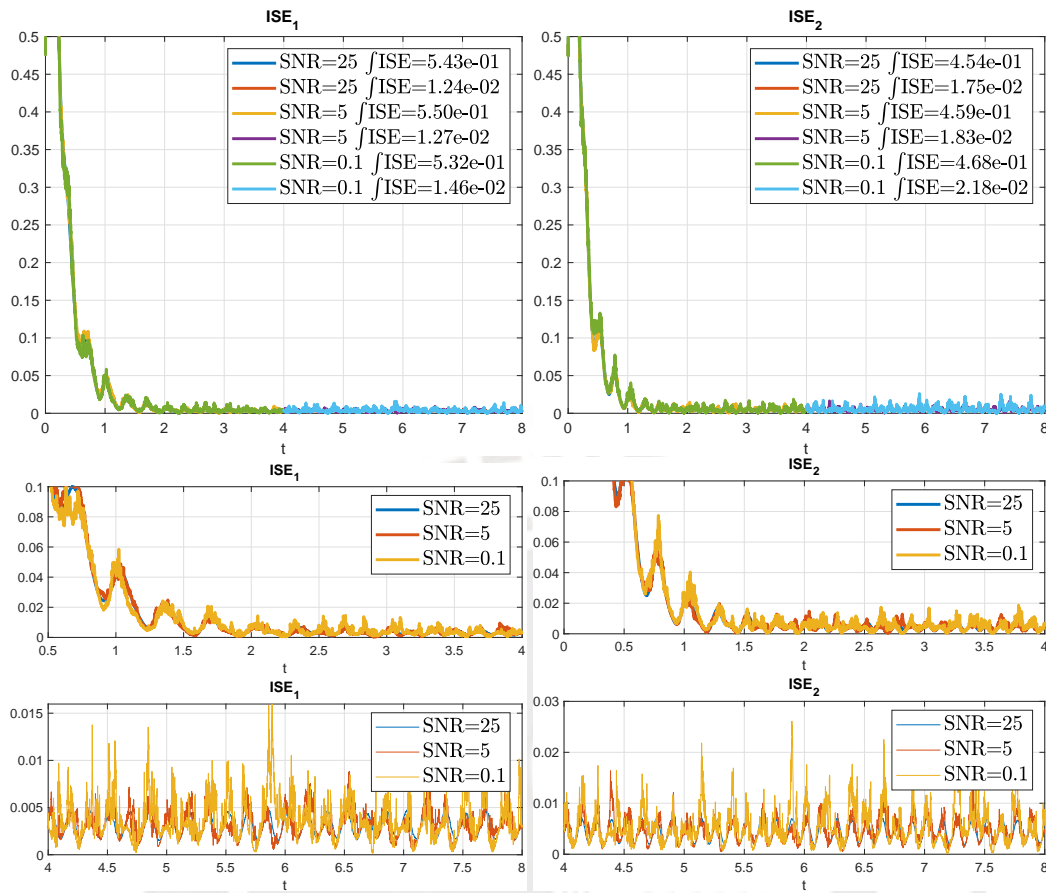
FIGURE A.18: ISE with different SNR on the measurement for the State Estimation on a Stable Coupled Reaction Diffusion system with a Sinusoidal boundary condition

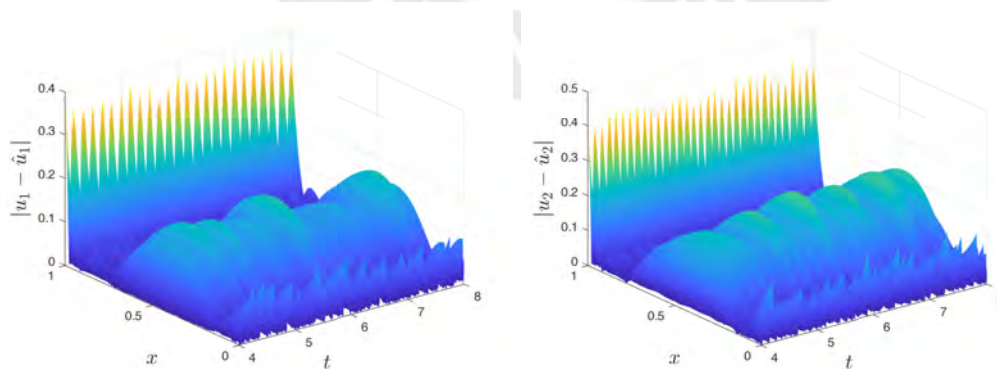

FIGURE A.19: Absolute error for the estimation with SNR=0.1 and $T_s = 10^{-3}$ on a Stable Coupled Reaction Diffusion system with a Sinusoidal boundary condition
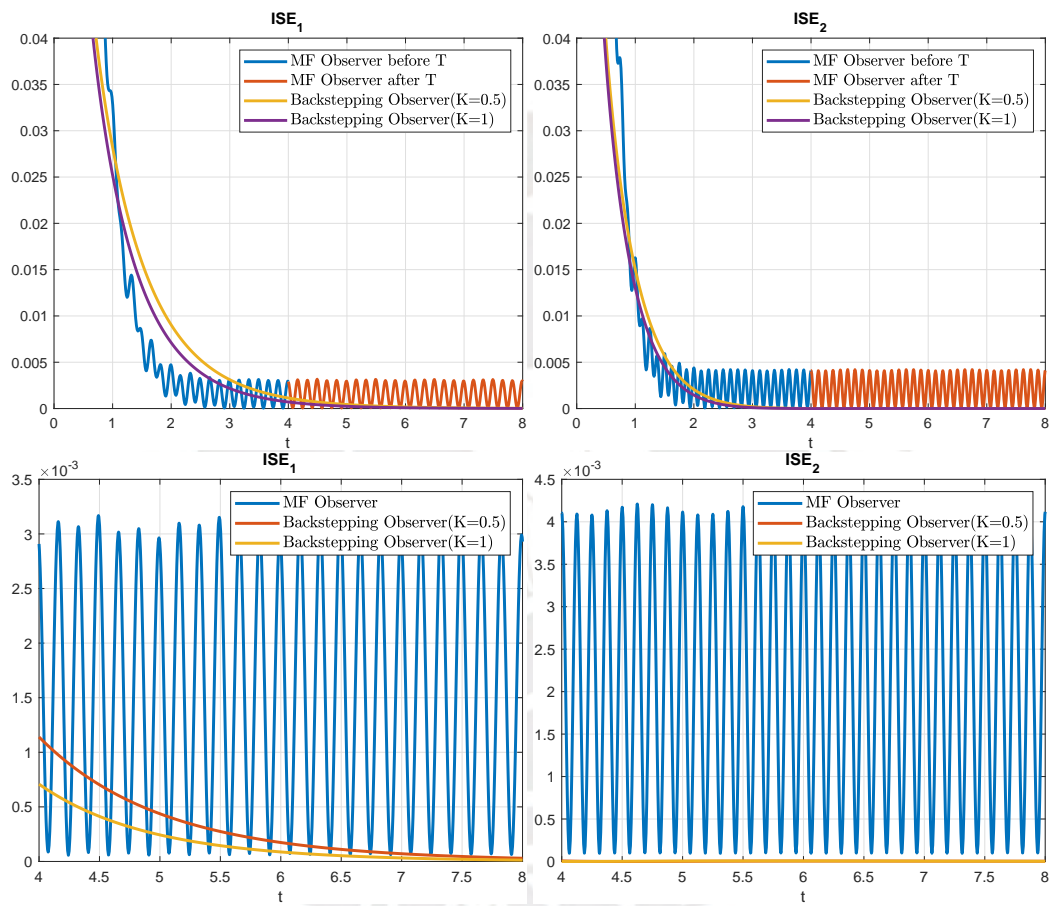
FIGURE A.20: ISE comparison of the backstepping and MF observer for the State Estimation on a Stable Coupled Reaction Diffusion system with a Sinusoidal boundary condition

Bibliography

[1] Alessandro Pisano et al. "Boundary control of coupled reaction-advection-diffusion equations having the same diffusivity parameter". In: *IFAC-PapersOnLine* 49.8 (2016), pp. 86–91.

[2] Antonello Baccoli et al. "Anticollocated Backstepping Observer Design for a Class of Coupled Reaction-Diffusion PDEs". In: *Journal of Control Science and Engineering* 2015 (2015), pp. 1–10.

[3] Antonello Baccoli et al. "On the boundary control of coupled reaction-diffusion equations having the same diffusivity parameters". In: *53rd IEEE Conference on Decision and Control*. IEEE, Dec. 2014.

[4] Bai-Nan Liu et al. "Backstepping observer-based output feedback control for a class of coupled parabolic PDEs with different diffusions". In: *Systems & Control Letters* 97 (Nov. 2016), pp. 61–69.

[5] Cai Li et al. "Diffusive gradients in thin films: devices, materials and applications". In: *Environmental Chemistry Letters* 17.2 (Dec. 2018), pp. 801–831.

[6] Delphine Bresch-Pietri et al. "Output-feedback adaptive control of a wave PDE with boundary anti-damping". In: *Automatica* 50.5 (May 2014), pp. 1407–1415.

[7] F. Fischer et al. "Algebraic fault detection and isolation for parabolic distributed-parameter systems using modulation functions". In: *IFAC-PapersOnLine* 49.8 (2016), pp. 162–167.

[8] F. Fischer et al. "Source estimation for first order time-varying hyperbolic systems". In: *Mathematical Theory of Networks and Systems* (2018), pp. 78–84.

[9] Krstic M. et al. *Boundary Control of PDEs: A Course on Backstepping Designs*. Philadelphia: SIAM, 2008.

[10] Leobardo Camacho-Solorio et al. "Boundary observer design for coupled reaction-diffusion systems with spatially-varying reaction". In: *2017 American Control Conference (ACC)*. IEEE, May 2017.

[11] Leobardo Camacho-Solorio et al. "Boundary observers for coupled diffusion–reaction systems with prescribed convergence rate". In: *Systems & Control Letters* 135 (Jan. 2020), p. 104586.

[12] Lilia Ghaffour et al. "Non-asymptotic State Estimation of Linear Reaction Diffusion Equation using Modulating Functions". In: *IFAC-PapersOnLine* 53.2 (2020), pp. 4196–4201.

[13]   Long Hu et al. "Control of Homodirectional and General Heterodirectional Linear Coupled Hyperbolic PDEs". In: *IEEE Transactions on Automatic Control* 61.11 (Nov. 2016), pp. 3301–3314.

[14]   M. Laabissi et al. "Trajectory analysis of nonisothermal tubular reactor nonlinear models". In: *Systems & Control Letters* 42.3 (Mar. 2001), pp. 169–184.

[15]   Maria Cameron et al. "Inverse problem in seismic imaging". In: *Proceedings in Applied Mathemathics and Mechanics* 7.1 (Dec. 2007), pp. 1024803–1024804.

[16]   Paul Albertus et al. "Experiments on and Modeling of Positive Electrodes with Multiple Active Materials for Lithium-Ion Batteries". In: *Journal of The Electrochemical Society* 156.7 (2009), A606.

[17]   Philippe Moireau et al. "Joint state and parameter estimation for distributed mechanical systems". In: *Computer Methods in Applied Mechanics and Engineering* 197.6-8 (Jan. 2008), pp. 659–677.

[18]   Rafael Vazquez et al. "Boundary control of coupled reaction-diffusion systems with spatially-varying reaction". In: *IFAC-PapersOnLine* 49.8 (2016), pp. 222–227.

[19]   S. Elmetennani et al. "Bilinear reduced order approximate model of parabolic distributed solar collectors". In: *Solar Energy* 131 (June 2016), pp. 71–80.

[20]   Satishkumar B. Chikkannanavar et al. "A review of blended cathode materials for use in Li-ion batteries". In: *Journal of Power Sources* 248 (Feb. 2014), pp. 91–100.

[21]   Sharefa Asiri et al. "Modulating functions-based method for parameters and source estimation in one-dimensional partial differential equations". In: *Inverse Problems in Science and Engineering* 25.8 (Oct. 2016), pp. 1191–1215.

[22]   Shuxia Tang et al. "Stabilization for a coupled PDE–ODE control system". In: *Journal of the Franklin Institute* 348.8 (Oct. 2011), pp. 2142–2155.

[23]   Ulf Jakob F. Aarsnes et al. "Avoiding stick slip vibrations in drilling through startup trajectory design". In: *Journal of Process Control* 70 (Oct. 2018), pp. 24–35.

[24]   Y. Orlov et al. "Adaptive distributed parameter systems identification with enforceable identifiability conditions and reduced-order spatial differentiation". In: *IEEE Transactions on Automatic Control* 45.2 (2000), pp. 203–216.

[25]   Y. Orlov et al. "Discontinuous feedback stabilization of minimum-phase semilinear infinite-dimensional systems with application to chemical tubular reactor". In: *IEEE Transactions on Automatic Control* 47.8 (Aug. 2002), pp. 1293–1304.

[26]   Y. Orlov et al. "Output Feedback Stabilization of Coupled Reaction-Diffusion Processes with Constant Parameters". In: *SIAM Journal on Control and Optimization* 55.6 (Jan. 2017), pp. 4112–4155.

[27]   Yinchuan Yang et al. "Tubular reactor-enhanced ecological floating bed achieves high nitrogen removal from secondary effluents of wastewater treatment". In: *Environmental Chemistry Letters* 18.4 (Apr. 2020), pp. 1361–1368.

[28]   Ying Cui et al. "Diffusive gradients in thin films using molecularly imprinted polymer binding gels for in situ measurements of antibiotics in urban wastewaters". In: *Frontiers of Environmental Science & Engineering* 14.6 (July 2020).

[29]   Bainan Liu. "Boundary Observer-based Output Feedback Control of Coupled Parabolic PDEs". Institut National des Sciences Appliquées - Centre Val de Loire, 2018.

[30]   M. Shinbrot. "On the analysis of linear and nonlinear dynamical systems from transient-response data". In: *NACA Technical Notes* (1954).

[31]   M. Shinbrot. "On the analysis of linear and nonlinear systems". In: *Trans. ASME* (1957).